UAlg FCT
UNIVERSIDADE DO ALGARVE
FACULDADE DE CIÊNCIAS E TECNOLOGIA

Universidade do Algarve

Effects of light quality supplied by light emitting diodes (LEDs) on microalgal production

Peter Simon Claus Schulze

Dissertação
Mestrado em Aquacultura

Trabalho efectuado sob a orientação de:

Prof. Dr. João Carlos Serafim Varela

&

Prof. Dr. José Antonio Perales Vargas-Machuca

2014

Universidade do Algarve
Faculdade de Ciências e Tecnologia

Effects of light quality supplied by light emitting diodes (LEDs) on microalgal production

by

Peter Simon Claus Schulze

Supervised by

Prof. Dr. João Varela

Universidade do Algarve, Faro, Portugal

&

Prof. Dr. José Antonio Perales Vargas-Machuca

Universidad de Cádiz, Spain

performed at

Departamento de Tecnologías del Medio Ambiente, Universidad de Cádiz, Spain

Centro de Ciências do Mar Universidade do Algarve, Campus de Gambelas Portugal, Faro

2014

Declaração de autoria de trabalho

Declaro ser o autor deste trabalho, que é original e inédito. Autores de trabalhos consultados estão devidamente citados no texto e constam da listagem de referências incluídas.

_____	_____	_____
Peter Schulze	Location	Date

Acknowledgements

First and foremost, I would like to express my very best thanks to my supervisors Prof. José Antonio Perales from the University of Cádiz (UCA), Centro Andaluz de Ciencia y Tecnología Marinas (Cacytmar) and Prof. João Varela from the University of Algarve (UAlg), Centre of Marine Science (CCMar) for their constant support and encouragement for the implementation of this project, the allocation of funds as well as for critically reading this thesis. Special thanks again to Prof. João Varela without whose help I would never have been able to publish a huge part of this work. Also I would like to thank Hugo Pereira from CCMar for his help with certain analyses, microscopy, his receptivity for any kind of questions I had as well his help with illustrations. Furthermore, I wish to thank Prof. Rui Guerra from the Physics Department of the UAlg for his support in providing information needed for part of the work and reviewing the manuscript. Moreover, I would like to thank Gloria Peralta Gonzáles from the Facultad de Ciencias del Mar y Ambientales, UCA for supplying a radiospectrometer and Edward P. Morris form the department of Ecology and Coastal Management for his technical support. Altogether I give special thanks to those people from the Cacytmar and CCMar who helped me solve all the problems I had. Very special thanks to my whole family for their acceptance and their aid to my studying abroad. Last but not least, I want to thank all my fellow students from the aquaculture study programme, who better than anyone else helped me with their support or rather kindly distracted me from this work, whenever that was necessary.

Abstract

Light-emitting diodes (LEDs) will become one of the world´s most important light sources and their integration in microalgal production systems (photobioreactors) needs to be considered. Microalgae need a balanced mix of wavelengths for normal growth, responding to light differently according to the pigments acquired or lost during their evolutionary history. In the present study, *Nannochloropsis oculata* and *Tetraselmis chuii* were exposed to different light qualities, and their effects on growth, biochemical components (carbohydrate, protein, total lipid and fatty acids) and morphologic traits (cell shape, size, growth phase, absorption spectrum, N-P-C elemental composition in biomass) were investigated. An additional experiment employed different LEDs in order to obtain di- and multichromatic tailored light to increase biomass production. Both *N. oculata* and *T. chuii* showed a higher maximal volumetric ash free dry weight content in the culture when exposed to blue (465 nm) and red (660 nm) light, respectively. However, balanced light quality, provided via fluorescent light (FL) and dichromatic blue and red light treatment, was found to be beneficial for biomass growth rates of both algae. Significant changes in the biochemical composition were observed among treatments. Furthermore, algae treated with monochromatic blue light (λ_e = 405 and 465 nm) often displayed higher nutrient uptake and different morphological traits as compared to algae exposed to red light (λ_e = 630 and 660 nm). It is suggested that differential response to light quality is partially influenced by observed changes in nutrient consumption and biomass productivity. In terms of biomass per input energy, the most efficient light sources were those with photon output peaks at 660 nm (e.g. LED 660 and FL for plant growth). Research and the application of LED technology to microalgal production is often hindered by inadequate light quantity measurements as well as by inadequate LED manufacture and engineering, leading to the use of inefficient LED modules, which, in turn, may affect microalgal growth and biochemistry.

Key words: *Tetraselmis chuii*, *Nannochloropsis oculata*, Light emitting diodes (LEDs), light requirements, Morphologic effects

Resumo

A biomassa de microalgas é usada como alimentação em aquacultura para animais, suplementos alimentares, nutracêuticos e na cosmética, sendo também considerada como uma promissora matéria-prima para produção de biocombustíveis. Isto deve-se ao fato da biomassa de microalgas possuir um alto conteúdo de produtos de valor acrescentado como os glícidos, proteínas, lípidos ou ácidos gordos insaturados. Para a produção destes componentes a luz, natural ou artificial, desempenha um papel essencial. Muito embora a luz solar seja o recurso mais eficiente em termos energéticos para produção de microalgas, a luz artificial é economicamente mais fiável quando a biomassa tem por finalidade a manufatura de produtos de valor acrescentado. As microalgas precisam de uma combinação equilibrada de luz com diferentes comprimentos de onda para um crescimento normal, reagindo à qualidade de luz de diferentes modos, de acordo com os pigmentos adquiridos, retidos ou perdidos durante a sua história evolutiva. Os díodos emissores de luz (*eng*. *Light emitting diodes*; LEDs) serão uma das mais importantes fontes de luz artificial do mundo, e a sua integração em sistemas de produção de microalgas (fotobiorreactores) precisa de ser reconsiderada.

Neste estudo, as microalgas *Nannochloropsis oculata* e *Tetraselmis chuii,* que são espécies utilizadas em aquacultura e na indústria nutracêutica, foram investigadas no que diz respeito aos efeitos de diferentes gamas de luz mono- (λ_e = 405, 465, 630 e 660 nm) e multicromática (luz branca fria e quente e também luz fluorescente usada para o crescimento de plantas e algas fotossintéticas) no crescimento, na composição bioquímica (glícidos, proteínas, lípidos e ácidos gordos) e características morfológicas (forma e tamanho celular, maturidade da cultura, espectro de absorção, elementos de composição de N-F-C em biomassa).

Foi realizada uma outra experiencia, com uso de diferentes LEDs, para obter di- e multicromaticidade de banda emissora adaptada para aumentar a produção de biomassa. As microalgas *N. oculata* e *T. chuii* obtiveram o peso seco livre de cinzas máximo quando expostas a luz monocromática azul (λ_e = 465 nm) e vermelha (λ_e = 660 nm), respetivamente. No entanto, verificou-se que o uso de gamas de luz monocromática suplementadas por tratamentos de luz fluorescente (FL), ou de gamas de luz dicromática obtida por LEDs azuis e vermelhas é benéfico para a produtividade em termos de biomassa sem cinzas (mg L^{-1} d^{-1}) em ambas as algas. Além disso, as algas expostas a luz fluorescente mostraram maior superfície celular quando comparadas com algas com outros tratamentos. Verificou-se também uma diferença cromática da alga *N. oculata* em tratamentos com LEDs 405 (λ_e = 405 nm) e luz

fluorescente, sendo observada uma maior acumulação de um conjunto pigmentar com tom verde e tom amarelo, respetivamente. Especificamente, as culturas de *N. oculata* expostas a LEDs 405 sofreram uma mudança significativa do espectro de absorção quando comparada com outros tratamentos. Em relação à composição bioquímica, as concentrações mais elevadas de lípidos e proteína em *N. oculata* foram obtidas, respetivamente, sob tratamento com FL e LED 405, sendo obtido o teor mais baixo em glícidos com o tratamento com LEDs 405.

A maior concentração de lípidos e proteínas em *T. chuii* foi obtida em tratamentos com LED 405 e CW LED, acompanhada por baixos teores de glícidos. Os fatores de conversão entre o teor de azoto na biomassa e teor de proteína obtida pelo método de Lowry (fatores N-prot) foram sempre mais elevados ou menores, quando as algas eram expostas a LEDs 405 e ou a FL, respetivamente. Em contraste, os rácios C:N eram menores sob LEDs 405 e maiores sob FL. Também a composição em ácidos gordos foi afetada pela luz, uma vez que os LEDs 405 e CW LEDs induziram os níveis mais elevados em termos de ácidos gordos polinsaturados *n*-3 (ómega-3) em *N. oculata* e *T. chuii,* respetivamente. As algas que foram tratadas com luz azul monocromática (λ_e= 405 e 465 nm) apresentaram uma maior absorção de nutrientes e várias características dissemelhantes quando comparadas com algas expostas a luz vermelha (λ_e= 630 e 660 nm). As alterações bioquímicas, morfológicas e fisiológicas acima mencionadas sugerem que as diferentes respostas das algas a distintas qualidades de luz são parcialmente influenciadas por mudanças na assimilação de nutrientes e crescimento celular.

Acerca da absorção de energia óptica por parte da biomassa, as fontes de luz que têm quantidades significativas de fotões com um comprimento de onda a 660 nm (por exemplo, LED 660 e FL adaptada ao crescimento de microalgas) são mais eficientes do que fontes com luz azul.

Por fim, podemos concluir que a aplicação da tecnologia LED na investigação e produção de microalgas é muitas vezes dificultada por um inadequado manuseamento da intensidade de luz, bem como por uma inadequada engenharia e fabricação de LEDs, levando ao uso de módulos de LEDs insuficientes, que por sua vez pode afetar o crescimento e a bioquímica das microalgas em estudo.

List of figures

Figure 1.2-1 Simplified diagram of how low-power (homostructured) LEDs work. To increase efficiency, however, most (high power) LED chips are built up in heterostructures, having a more complex internal structure with more than one semiconductor material, which can also include multiple quantum wells (see also refs. [27-30]).... 4

Figure 1.2-2 Emission spectra of different LEDs. The full-width-at-half-maximal (FWHM) corresponds to the difference of two wavelength values (usually ~20 nm) at which the LED attains 50% of its maximal intensity.... 5

Figure 1.2-3 Simplified diagram of how fluorescent lamps (FLs) work. 6

Figure 1.2-4 Emission spectra of different types of FLs, including grow-light, warm white, and cold daylight. 7

Figure 1.4-1 Approximate light requirements of microalgae based on results from Table 1.4-1, main pigments, and the evolutionary relationships among major microalgal megagroups. Pigment distribution was obtained from Takaichi [44] and evolutionary history is in accordance with Keeling [43]. Arrows denote the relative importance of different wavelengths: two upward green arrows, very important; one upward green arrow, important; one upward green arrow and one downward red arrow, important / accessory; one downward red arrow, accessory. Abbreviations: Chl: Chlorophyll, H: high pigment content, L: low pigment content, H L: variation between high and low pigment contents among species. 17

Figure 2.3-1 Photon distribution between 380 and 750 nm of the light sources under study. (A) single colour LEDs, peaking at λ_e = 405 nm (LED 405), 465 nm (LED 465), 630 nm (LED 630) and 660 nm (LED 660); (B) Mixed spectra light sources: Cool (CW LED) and warm (WW LED) white LED as well as a FL for plant growth (Sylvania Gro-Lux), (C) two-colour mix adapted spectra with high blue and low red (HBLR) and high red with low blue (HRLB) light emission; and (D) multi-colour mix spectra with high (HBmix) and low (HRmix) blue light content. 27

Figure 2.3-2 Design of the experiments. (A) represents a draft of the experimental setup for all experiments. (B) shows representative photographs of *T. chuii* under different light conditions, in which B.1 shows algae grown under LED 465, B.2 LED 405, B.3 LED 660, B.4 WW LED, B.5 FL, B.6 LED 630, B.7 CW LED, B.8 HRmix and B.9 HBLR.

Initial operating volume (V) was always 700 mL. Chambers indicated as B.0 were used as reserves and for controlling CO_2 and airflow..... 28

Figure 3.1-1 Verhulst model (eq. 4) applied to growth curves for *N. oculata* (A) and *T. chuii* (B) under FL treatment. Replicates of cell counts (n = 6) were sorted by size in three pairs and model (solid lines) was applied to the lowest (circles), medium (squares) and highest pairs (diamonds). Averaged results from the data modelling are given in Tables A.6-1 and A.6-2. Arrows indicate time points and number (n) of AFDW determinations. 39

Figure 3.1-2 Linear relationship between OD and AFDW (top) and OD and cell concentration (bottom) for *N. oculata* (A and C) and *T. chuii* (B and D). Equation for the correlation between OD and AFDW with confidence 95% band (dotted line) was for *N. oculata* and *T. chuii* AFDW = (0.3498±0.0099) OD + (0.0377±0.0111) (R^2 = 0.95 and r = 0.98) and AFDW = (0.8999±0.0317) OD - (0.0382±0.0201) (R^2 = 0.9414 and r = 0.97), respectively. Equation of the correlation between OD and cell counts was for *N. oculata* and *T. chuii* Cell conc.= (4.281 ± 0.136) × 10^6 OD + (5.124 ± 1.581) × 10^6 (R^2 = 0.90 r = 0.95) and Cell conc. = (2.299±0.062) × 10^6 OD + (3379±50397) (R^2 = 0.93 and r = 0.97). ... 40

Figure 3.1-3 Normalized AFDW-based growth parameters: productivity (P_{AFDW}), maximal concentration (X_{AFDW}) and growth rate (μ_{AFDW}) for *N. oculata* (A) and *T. chuii* (B). Reference data (red dashed line) was obtained with cells growing under FL. Statistical differences ($p < 0.05$) within AFDW productivity (black bar, left), maximal AFDW concentration (light grey bar, middle) and AFDW-based growth rate (dark grey bar, right) among light treatments are indicated by different letters. Statistically higher or lower values as compared to those of the reference (FL) cultures are given as + and - signed letters, respectively. Unsigned letters indicate no statistical differences were found between cells under a given light treatment and under FL (see also Table A.6-1 in Annex 6)..... 41

Figure 3.1-4 Normalized cell count-based growth parameters with data: productivity (P_{AFDW}), maximal concentration (X_{AFDW}) and growth rate (μ_{AFDW}) for *N. oculata* (A) and *T. chuii* (B). The reference data (red dashed line) was obtained with cells growing under FL. Statistical differences ($p < 0.05$) within cell productivity (black bar, left), maximal cell concentration (light grey bar, middle) and cell count-based growth rate (dark grey bar, right) among treatments are indicated by different letters. Statistically higher or

lower values as compared to those of the reference (FL) cultures are given as + and - signed letters, respectively. Unsigned letters indicate no statistical differences were found between cells under a given light treatment and under FL (See also and A.6-2 in Annex 6)..... 42

Figure 3.2-1 Illustration of cell length measurements. Left: N. oculata, right: T. chuii. 44

Figure 3.2-2 (A) *N. oculata* culture exposed to LED 660 treatment at t = 196 h. Inset image at the bottom right shows a more detailed cell aggregate. Cell walls of *N. oculata* can be observed within aggregates. (B) Colour difference between *N. oculata* cultures exposed to LED 405 (greenish colour; left test tube) and FL (yellowish colour; right test tube). (C) *T. chuii* cells under LED 405 assume often a coccoid shape, whereas cells exposed to LED 660 are usually more rod-like or cordiform (D)..... 45

Figure 3.2-3 Proposed cell cycle of *N. oculata*. Cell size increases and lipid bodies accumulate as the cell cycle progresses. It starts with (1) rod-shaped daughter cells, (2) rod-to-coccoid-shaped cells, (3) coccoid-shaped cells and (4) larger rod-to-coccoid-shaped "mother" cells. The photographs on the left were taken by differential interference contrast (DIC), whereas photographs on the right show DIC merged with BODIPY 505/515 fluorescence (green), which indicates lipid distribution. Red bar represents 5 µm and is applicable to all photographs. 47

Figure 3.2-4 Proposed cell cycle for *T. chuii,* starting with the release of elliptical daughter cells (1), which transit into matured cordiform cells (2). In stage (3), small flagellated cells appear, increasing in size towards the next stage (4). Thereafter cells lose flagella (5) and cell division is initiated. In the subsequent stage (6), cell division occurs and two coccoid daughter cells within the mother cell wall are formed. The left photographs of cells were taken by differential interference contrast (DIC), whereas photographs on the right hand side show DIC merged with BODIPY 505/515 fluorescence (green), which indicates lipid distribution. A remarkable lipid relocation could be observed starting from stage 1 and 2, during which lipids apparently move to the cytoplasm, co-localizing again with the U-shaped chloroplast by stage 4. In stages 5 and 6 the lipid bodies move back towards the cytoplasm and are equally partitioned between the two daughter cells. Red bar represents 10 µm and is applicable to all photographs. 48

Figure 3.3-1 Comparison of absorption spectra between *N. oculata* and *T. chuii* whole cells. Arrows with wavelengths indicating the peaks of major pigments. Absorption spectra represent the average of five different dilutions measured in duplicates for each alga as given in Annex 5. 49

Figure 3.3-2 Absorption spectra of *N. oculata* (A) and *T. chuii* (B) culture at the end of the experiment. Each curve represents the average of two absorption spectra of the same sample..... 51

Figure 3.4-1 Biochemical composition in % of AFDW for *N. oculata* (A) and *T. chuii* (B). Statistical differences ($p < 0.05$) within contents of total lipid (black bar), protein (light grey bar) and carbohydrates (dark grey bar) are indicated by different letters. 53

Figure 3.6-1 Photosynthetic efficiency $ø$ (PE) and CO_2 fixation rate F_{CO2} until day of harvest of *N. oculata* (black bar) and *T. chuii* (grey bar) exposed to different light qualities. Statistical differences among treatments are indicated by different letters for each alga. 62

Figure 4.1-1 Simplified growth patterns between light qualities observed by authors using (A) adequate [50, 57, 109] and (B) inadequate [14, 15, 25] devices to measure light intensity. TC indicates the threshold concentration above which algae continue to grow under light with an optimal wavelength range (red) as compared to cells under non-optimal light quality (blue). These differences usually lead to a well-defined TC (A), whereas faulty light intensity measurements often result in an undefined TC (B). 66

Figure 4.2-1 Suggested major interactions between light quality and cell productivity, cell size, nutrient assimilation and C:N ratios. See sections 4.1-4.6 for further discussion of the proposed model. Red light exposed algae (left pathway) show usually a high C:N ratio, indicating a reduced nutrient consumption but a higher Calvin cycle activity. The visible effect is many small cells in the culture. Blue light exposed algae (right pathway) show usually a low C:N ratio, indicating a high nutrient consumption (high enzyme activities; see 4.6). The visible effect is few big cells in the culture. Combining blue and red light (combined pathway, bottom) stimulates both, Calvin cycle and nutrient consumption. The result are many big cells and high C:N ratios. 69

Figure A.3-1 Spectral response curve of the used apogee MQ 100 quantum sensor (green line) with calibration light source (T5; cyan spectrum), optimum quantum response curve (black line; equal response among all wavelengths between 400 and 700 nm). Errors of

correction values were for LED 405, LED 465, LED 630, LED 660, CW LED, WW LED as well as FL 1.364, 1.032, 0.923, 1.490, 1.025, 1.042, and 1.135, respectively. T5 spectrum (top-left) was used to calibrate the quantum sensor data were kindly provided by Apogee Instruments Inc. 98

Figure A.3-2 Experimental setup for the estimation of approximate relative efficiency parameter (PPFD/W and W_{out_optic} m^{-2} / W_{input}) of light sources under study. 99

Figure A.3-3 Approximate efficiency parameter PPFD/W (A) and W_{out_optic} m^{-2}/W_{input} (B) of light sources at different distances. 100

Figure A.2-4 Calibration curve for Lowry [87] protein analysis. Concentration of bovine serum albumin (BSA) standard is plotted against optical density (OD) determined at 750 nm. Equation was: Y=897.76x- 8.964 (R^2 = 0.9991; r = 0.9995; p < 0.01). 101

Figure A.5-5 (A) represents the baseline noise of filter containing only filtered seawater for *N. oculata* and *T. chuii* absorption spectra analyses. (B) and (C) represent the deviations of absorption spectra due to changing biomass concentration on the filter and filter variations for *N. oculata* and *T. chuii*, respectively. Each curve represents the average of two absorption spectra of the same sample. Optical density (OD) shows the absorption of the original sample before data treatment at 680 nm. 103

Figure A.7-6 Original growth curves based on cell counts (top; daily counts with n = 6) and AFDW determinations (bottom) of *N. oculata* (A and C, respectively) as well as *T. chuii* (B and D, respectively). 107

Figure A.8-7 Absolut productivity of *N. oculata* in the first, second and third experiment (A and C) and *T. chuii* (B and D) under continuous conditions when μ is maximal, calculated according to eq. 7. (E) shows the data from A-D normalized (relative) for both algae. The reference data (red dashed line) was obtained with cells growing under FL. Statistical differences (p < 0.05) within *N. oculata* (black bar) and *T. chuii* (grey bar) among treatments are indicated by different letters. Statistical higher or lower values as compared to those of the reference (FL) cultures are given as + and - signed letters, respectively. Unsigned letters indicate no statistical differences were found between cells under a given light treatment and under also FL (See and A.6-2 in Annex 6). 108

Figure A.9-8 Photograph of preserved *N. oculata* cultures from the end of the experiment (t = 192 h), showing different colours among the treatments. Tube 1, containing LED 405-treated algae, shows a clear green colour; tubes 2, 3, 4, 5 and 6, containing LED 465,

LED 630, LED 660, CW LED and WW LED-treated algae, respectively, are more yellowish and less greenish; and finally tube 7, containing FL-treated algae, showed a clear yellow colour. 110

Figure A.10-9 Productivity of total lipids (black bar left), proteins (light grey bar middle) and carbohydrates (dark grey bar right) for *N. oculata* (A) and *T. chuii* (B) among light treatments. Different letters within each biochemical and among treatments indicate statistical differences. 112

Figure A.10-10 Energy demand for producing total lipids (black bar), proteins (light grey bar) and carbohydrates (dark grey bar) per litre of culture from *N. oculata* (A) and *T. chuii* (B). Different letters within each biochemical and among treatments indicate statistical differences. 114

List of Tables

Table 1.3-1 Comparison between LEDs and fluorescent lamps (FLs) largely based on data from US-DOE [13] and Kane *et al.* [31]. 8

Table 1.4-1 Impacts of light quality in microalgal growth parameters and preferred growth wavelengths (λmax) of several algae classified according to Keeling [43] and percentage of diminished biomass production under alternative wavelengths (λmin). 12

Table 1.5-1 Light quality effects on microalgal biochemical composition at specific wavelengths (λmax). 20

Table 3.2-1 Morphological cell parameter among all treatments from the first experiment. Different letters indicate statistical differences among treatments within each parameter. 45

Table 3.4-1 Nitrogen-protein (N-prot) factors and carbon:nitrogen (C:N) ratios among different algae and treatments. Statistical differences are given with different letters in the same column. 54

Table 3.4-2 Fatty acid profile of *N. oculata* exposed to different light qualities. Values are given as percentage of total FAME (n = 3). Different letters within each fatty acid indicates statistical differences. 56

Table 3.4-3 Fatty acid profile of *T. chuii* exposed to different light qualities. Values are given as percentage of total FAME (*n* = 3). Different letters within each fatty acid indicates statistical differences. 57

Table 3.5-1 Nitrate-based nitrogen (R_N; mg $N\text{-}NO_3^-$; *n* = 1) and phosphate-based phosphorous (R_P ; mg $P\text{-}PO_4^{3-}$; *n* = 4) consumption of *N. oculata* and nitrogen consumption of *T. chuii* during the experimental run. Nitrogen content in the medium at the harvesting time point is given as S(t). 60

Table 3.6-1 Optical energy supplied to photobioreactors in Experiment 1. 61

Table A.6-1 *N. oculata* and *T.* chuii growth parameters based on ash free dry weight (AFDW) determinations (*n* = 3). Statistical differences are indicated by different letters among each experiment and growth parameter. 104

Table A.6-2 *N. oculata* and *T. chuii* growth parameter based on cell counts. Statistical differences are indicated by different letters among each experiment and growth parameter. 105

List of abbreviations

AA	Arachidonic acid
AFDW	Ash free dry weight
ALA	α-linolenic acid
AlGaInP	Aluminium Gallium Indium Phosphorus
AM	Amplitude modulation
AW	Ash weight
c	Speed of light [299,792,458 m s^{-1}]
Cacytmar	Centro Andaluz de Ciencia y Tecnología Marinas
CCMar	Centre of Marine Science
Cm-LED	Colour mixed light emitting diode
CRI	Colour rendering índex
CW	Cool white
DHA	Docosapentaenoic acid

DW	Dry weight
E_{in}	Input optical energy [KJ]
E_{out}	Energy output of algal biomass [KJ]
EPA	Eicosapentaenoic acid
eV	Electron volt [1.60217657 10^{-19} J]
Exp.	Experiment
E_{λ}	Energy of one photon at a certain wavelength λ in joule [J]
$E_{\lambda,\mu mol}$	Energy of one µmol of photons at a wavelength λ in joule [J µmol^{-1}]
F_{CO_2}	CO_2 fixation of algae until time point of harvest [g CO_2]
$F_{\lambda 1,2}$	Variation-factor, between $PPFD_{\lambda 1}$ and $PPFD_{\lambda 2}$ measured via Luxmeter
FAME	Fatty acid methyl esters
FL	Fluorescent light
FWHM	The full-width-at-half-maximal
GaAlAs	Gallium Aluminium Arsenide
h	Max Planck constant [6.626 x 10^{-34}J s^{-1}]
HBLR	High blue low red light content (dichromatic)
HBmix	High blue content mixed with other wavelengths (multichromatic)
HHV	Higher energy value [KJ g^{-1}]
HRLB	High red low blue light content (dichromatic)
HRmix	High red light content mixed with other wavelengths (multichromatic)
HRT	Hydraulic retention time
IIN	Inorganic intracellular nutrients
InGaN	Indium Gallium Nitride
LA	Linoleic acid
LED	Light emitting diode
LED *nnn*	LED with a light emission peak with a wavelength of *nnn* nm
LHCP	Light harvesting complex protein
LHP	Light harvesting pigment
MUFA	Mono unsaturated fatty acid
N_A	Avogadro's number (6.02×10^{23} mol^{-1})
NPN	Non-proteinaceous nitrogen
NPQ	Non-photosynthetic quenching
OD	Optical density
OSE	Overall system efficiency

P_{AFDW}	Productivity of ash free dry weight (AFDW) under batch conditions [mg L^{-1} d^{-1}]
PAS	Photosynthetic active spectrum
PBR	Photobioreactor
PCE	Power conversion efficiency
P_{cell}	Productivity of cells under batch conditions [cell L^{-1} d^{-1}]
Pc-LED	Phosphor converted light emitting diode
$P_{cont,AFDW}$	Productivity under continuous culture conditions [mg L^{-1} d^{-1}]
PE	Photosynthetic efficiency
PN	Proteinaceous nitrogen
PPFD	Photosynthetically active photon flux density
PWM	Pulse width modulation
r	Pearson´s correlation
R_N	Nitrate-based nitrogen consumption rate [mg $N\text{-}NO_3^-$ L^{-1} d^{-1}]
ROS	Reactive oxygen species
R_P	Phosphate-based phosphorous consumption rate [mg $P\text{-}PO_4^{3-}$ L^{-1} d^{-1}]
$S(t)$	Nutrient content in the medium at time point of harvest [mg $N\text{-}NO_3^-$ L^{-1}] or [mg $P\text{-}PO_4^{3-}$ L^{-1}].
S_0	Initial nutrient concentration [mg $N\text{-}NO_3^-$ L^{-1}] or [mg $P\text{-}PO_4^{3-}$ L^{-1}]
SAR	Stramenopiles-Alveolata-Rhizaria algal megagroup
SFA	Saturated fatty acids
SMD	Surface mounted diodes
S_{na}	Unassimilated nutrient concentration, dissolved [mg $N\text{-}NO_3^-$ L^{-1}] or [mg $P\text{-}PO_4^{3-}$ L^{-1}]
$t_{(0.9\ xm)}$	Time point where 90% of maximal volumetric AFDW or cell concentration is reached [h]
$t_{(1.1\ xo)}$	Time point where initial AFDW or cell concentration increases by 10 % [h]
TFA	Total fatty acids
UAlg	University of Algarve
UCA	University of Cadiz
V_λ	Photopic luminous efficacy at a certain wavelength
WW	Warm white
X_{AFDW}	Maximal ash free dry weight (AFDW) concentration [mg L^{-1}]

X_{cell}	Maximal cell concentration [cell L^{-1}]
x_m	Maximal biomass concentration (AFDW or cell count based) [mg / Cell L^{-1}]
x_o	Initial biomass concentration (AFDW or cells count based) [AFDW / Cell L^{-1}]
Y_0	Nitrogen or Phosphorous content in biomass [mg N/ P mg DW^{-1}]
YPF	Yield photon flux
λ_a	Maximal absorption wavelength
λ_{a_blue}	Absorption peak within the blue spectral range
λ_{a_red}	Absorption peaks within the red spectral range
λ_e	Maximal emission wavelength
λ_{max}	Denotes the preferred wavelength for optimal growth or preferred wavelength for a metabolic effect.
λ_{min}	Alternative preferred wavelength that may be suboptimal.
μ_{AFDW}	Maximal growth rate based on ash free dry weight (AFDW) [d^{-1}]
μ_{cell}	Maximal growth rate based on cell counts [d^{-1}]
μ_n	Nitrogen based maximal specific growth rate
$\varnothing$	Photosynthetic efficiency until time point of harvest [%]
θ	Hydraulic retention time (HRT) [d]
λ	Wavelength of light [m; nm]
$\Phi_{\lambda,\Phi v}$	Spectral irradiance [J m^{-2} s^{-1}]
Φ_v	Luminous emittance [lux; lm m^{-2}]

Index

Declaração de autoria de trabalho I

Acknowledgements II

Abstract III

Resumo IV

List of figures VI

List of Tables XI

List of abbreviations XII

1 Introduction 1

1.1 Light for photosynthesis 2

1.2 Artificial light technologies for phototrophic growth 4

1.2.1 LEDs 4

1.2.2 FLs 6

1.3 Economics and efficiency 8

1.4 Effects of light quality on microalgal growth 11

1.4.1 Pigments and light requirements of microalgae 11

1.5 Effects of light quality on microalgal traits 19

1.6 Using LEDs for microalgal production 22

1.6.1 Estimation of preferred wavelengths 22

1.6.2 Tailored light sources 22

1.7 Justification of the dissertation 23

1.8 Objectives 24

2 Material and methods 26

2.1 Microalgae 26

2.2 Growth conditions 26

2.3 Light treatment 26

2.4 Sampling 29

2.5 Analytical methods 29
2.5.1 Proteins 29
2.5.2 Total lipids 30
2.5.3 Fatty acids 30
2.5.4 Biomass 31
2.5.5 Nutrients 31
2.5.6 Morphological traits 32
2.5.7 Absorption spectra 32
2.6 Data treatment 33
2.6.1 Growth model 33
2.6.2 Nitrogen consumption 35
2.6.3 Approximate photosynthetic efficiency 36
2.6.4 Statistical analysis 37
3 Results 38
3.1 Growth parameters and modelling 38
3.2 Cell morphology and cell cycle 44
3.3 Absorption spectra 49
3.4 Biochemical components 52
3.4.1 Fatty acids 55
3.5 Nutrients and growth parameters 59
3.6 Efficiency of light sources used 61
4 Discussion 63
4.1 Algal growth parameters 63
4.1.1 Complexity of light measurements 65
4.2 Cell morphology, cell cycle and culture maturity 67
4.3 Absorption spectra 71
4.4 Biochemical composition 72

4.5 Fatty acids 75
4.6 Nutrients 76
4.7 CO_2 chapter and photosynthetic efficiency 78
4.8 FL vs. LEDs 78
5 Conclusion 80
References 81
Annexes 94

1 Introduction

Parts of this section have already been published as Schulze *et al.* [1] (see Annex 1)

Microalgal biomass is used as feed in aquaculture, bulk food, and as feedstock for food / feed supplements, nutraceuticals and cosmetics and it has been considered as a promising feedstock for biofuel production [2-4]. For every purpose different biochemical attributes are necessary. For instance, in aquaculture high polyunsaturated fatty acids (PUFA) such as docosahexaenoic acid (DHA), arachidonic acid (AA) or eicosapentaenoic acid (EPA) and a species-specific protein / carbohydrate ratio are required [5-7], whereas triacylglycerols and hydrocarbons with fewer double bonds are important for biofuel production [8]. Therefore, manipulation of the biochemistry and growth properties of microalgae is often needed for a given purpose.

The composition of microalgae can change due to shifting environmental parameters, growth rates and/or phases of the algal lifecycle [9, 10]. Light quality and quantity supplied by sun- or artificial light is one of the most important parameters for phototrophic organisms as being required for photosynthesis as well as morphologic changes. In terrestrial plants, light quality and quantity have been recognized to be important for the development of several morphologic traits like stem, leaf and overall plant size, and events such as flowering [11, 12]. Even though sunlight is the most cost effective energy source to produce microalgae, artificial light is still economically feasible when biomass is used as feedstock for high value products, such as food/feed supplements (e.g. carotenoids and *n*-3 polyunsaturated fatty acids) and/or nutraceuticals [3]. Artificial light supplied to microalgal cultures also provides better regulation of photosynthetic photon flux density (PPFD), photoperiod and light spectra, which can result in gains of productivity and quality control of the biomass, two key factors for the success of any agricultural/industrial produce [4]. However, as the use of artificial light sources comes at a cost, their improvement in terms of photosynthetic and electric efficiency can provide a wider and cheaper array of products obtained from microalgal biomass [4]. This strategy has already been recognized as useful for horticulture [12]. Artificial lighting in microalgal research and production is usually carried out by means of fluorescence lamps (FLs), which have wide emission spectra, including wavelengths with low photosynthetic activity for certain microalgae [4]. Alternatively, light-emitting diodes (LEDs) can be used [3, 12, 13]. LEDs are long-lasting (~50,000 h), mercury-free and fast-responding (nanosecond scale) artificial light sources emitting nearly monochromatic light at different wavelengths

due to solid-state electronics [12, 13]. Hence, LEDs can provide not only a more sustainable control of supplemental light during microalgal growth, but also adjust the biochemical composition of the biomass by means of single wavelengths at different light intensities and/or pulse light frequencies [14-18].

1.1 Light for photosynthesis

The light (or radiance) is the main source of energy for photosynthesis. Light comes in discrete packets called photons or *quanta*. Each photon has a specific energy E_λ, which can be described as a function of its wavelength [19] (eq.1):

$$E_\lambda = \frac{h \times c}{\lambda} \quad (1)$$

where E_λ = energy of a photon (J), h = Max Planck constant (6.626 x 10^{-34}J s^{-1}), c = speed of light (299,792,458 m s^{-1}) and λ = wavelength of light (m).

Equation 1 indicates that photons with shorter wavelengths (e.g. λ = 400-500 nm, within the blue light range, have higher quantum energies than those with longer wavelengths (λ = 600-700 nm; red light). Plants and algae can use electromagnetic radiation with wavelengths between 380-750 nm for photosynthesis with variable efficiency. The energy from photons with λ ≥ 750 nm is not sufficient to induce chemical reactions, whereas photons with λ ≤ 380 nm can cause ionization [20]. Therefore, the energy or radiant flux measured in W that hits an area per time (W m^{-2} s^{-1}) is less useful to evaluate the light quantity for phototrophic organisms than the amount of photons with wavelengths between 400-700 nm that reach a surface per time unit defined as photosynthetically active photon flux density (PPFD) expressed in µmol photons s^{-1} m^{-2} or µE m^{-2} s^{-1} [21]. As PPFD is usually measured via quantum sensors and these do not respond equally to all wavelengths, the PPFD of light sources with narrow spectra are often significantly over- or underestimated at certain wavelengths if correction factors are not used [21, 22]. However, the amount of photons that can be effectively utilized by a prototroph for photosynthesis (yield photon flux; YPF) changes with their wavelength and thus the photon distribution through the photosynthetic active range remains as an important factor for efficient phototrophic growth [21].

LEDs can mimic the whole photosynthetic active spectrum from ultraviolet (λ < 390 nm) to infrared (λ > 720 nm) [23], allowing the emission of photons with high photosynthetic

efficiency at precise wavelengths, thus increasing YPF and lowering energy usage. Artificial light is often not evaluated in terms of photon release, but rather how it affects human vision via parameters such as colour temperature[1], colour rendering indexes[2] and/or luminous efficacies / emittance[3]. As absorption spectra of most light harvesting complexes used by photosynthetic organisms [24] differ from that of the human eye [13], these evaluation indexes are not suitable indicators of the quality of a light source for photoautotrophic cultivation. Unfortunately, some studies working with light quality effects on phototrophic organism use luminous emittance (lux; lm m^{-2}) to evaluate light intensities [15, 25, 26], which may result in uneven PPFD in different light quality treatments, making comparisons a difficult endeavour. For further details about converting luminous emittance to PPFD see Annex 2.

[1] The colour temperature of a light source is given in Kelvin (K) and denotes the trend of a light spectrum towards bluish or reddish wavelengths, being related to the irradiation spectrum of a heated Planck´s blackbody at a given temperature (K). The human eye perceives a blackbody heated up to 2000 K as having a reddish tint, whereas at 10,000 K a blackbody has a more bluish appearance.

[2] The colour rendering index (CRI) indicates how true the colour of an irradiated object is revealed to human eyes with a particular light source.

[3] The luminous efficacy (lm W^{-1}) is a measure of how efficient electrical power can be transformed to optical energy as perceived by the human eye, whereas luminous emittance (lux; lm m^{-2}) is the intensity of this optical energy striking a surface.

1.2 Artificial light technologies for phototrophic growth

1.2.1 LEDs

LEDs are semiconductors devices, consisting of a positive (p doped) layer and a negative (n doped) layer (Fig. 1.2-1). The p layer has an excess of electron holes in the valence band, due to the presence of acceptor dopant atoms, and the n layer has excess electrons in the conduction band due to the presence of donor dopant atoms. When n and p semiconductors are brought together, excess carriers diffuse to the opposite side, resulting in a depletion region without free carriers. By applying an opposite voltage the electrons from the n side and the holes from the p side enter the depletion region and recombine. This recombination corresponds to the de-excitation of an electron from the conduction band to the valence band, and a photon with the corresponding difference in energy (energy gap between the bands) can be released**.**

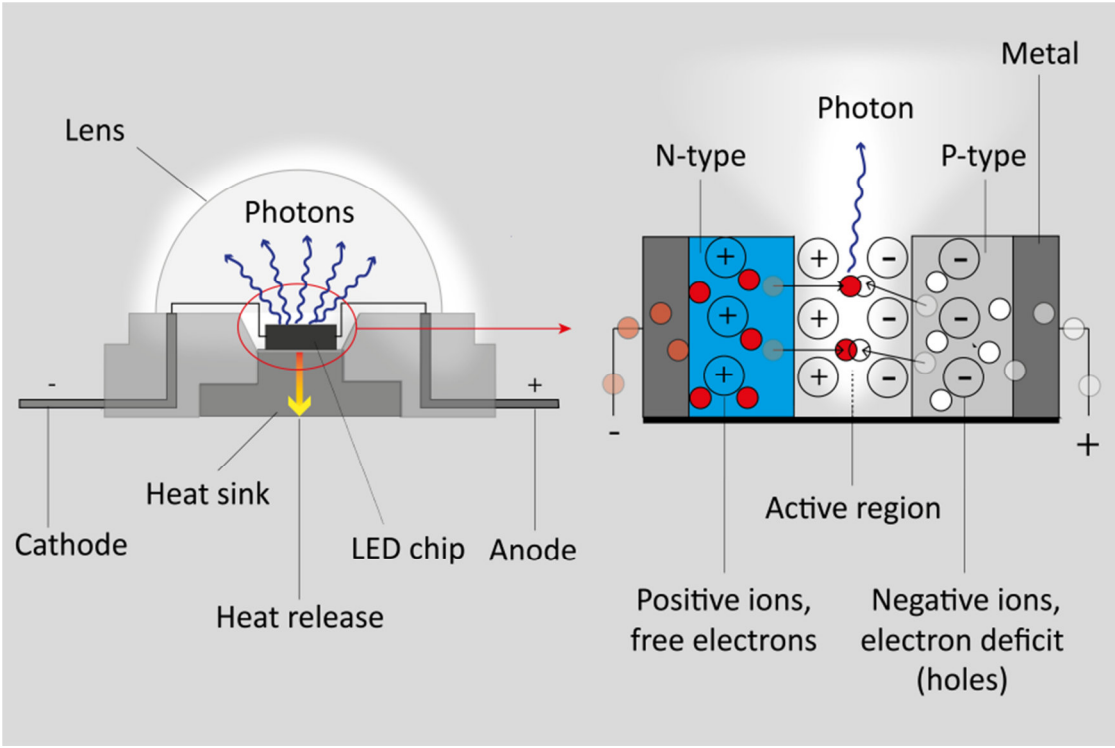

Figure 1.2-1 Simplified diagram of how low-power (homostructured) LEDs work. To increase efficiency, however, most (high power) LED chips are built up in heterostructures, having a more complex internal structure with more than one semiconductor material, which can also include multiple quantum wells (see also refs. [27-30]).

A blue-to-green (365-550 nm) InGaN (Indium Gallium Nitride) semiconductor has a wider energy gap than an orange-to-red (560-650 nm) emitting AlGaInP (Aluminium Gallium Indium Phosphorus) diode or a red-to-infrared (630-940 nm) GaAlAs (Gallium Aluminium Arsenide) chip (Fig 1.2-2). Thus, recombination of electrons from one semiconductor material to another controls the wavelengths and thus the colour and energy of emitted light. Lastly, white LEDs can be obtained by combining different LED chips in colour-mixed LEDs (cm-LEDs) or by coating single blue chips with a photon-converting layer in phosphor-converted LEDs (pc-LEDs) [13]. Cm-LEDs are rendered tri- or tetrachromatic to specific colour temperatures mostly by mixing blue (440-460 nm), green (520-540 nm), red (610-620 nm) and amber (580-595 nm) emitting diodes [13]. For further information about the theoretical background and employment of these technologies see refs. [27-30].

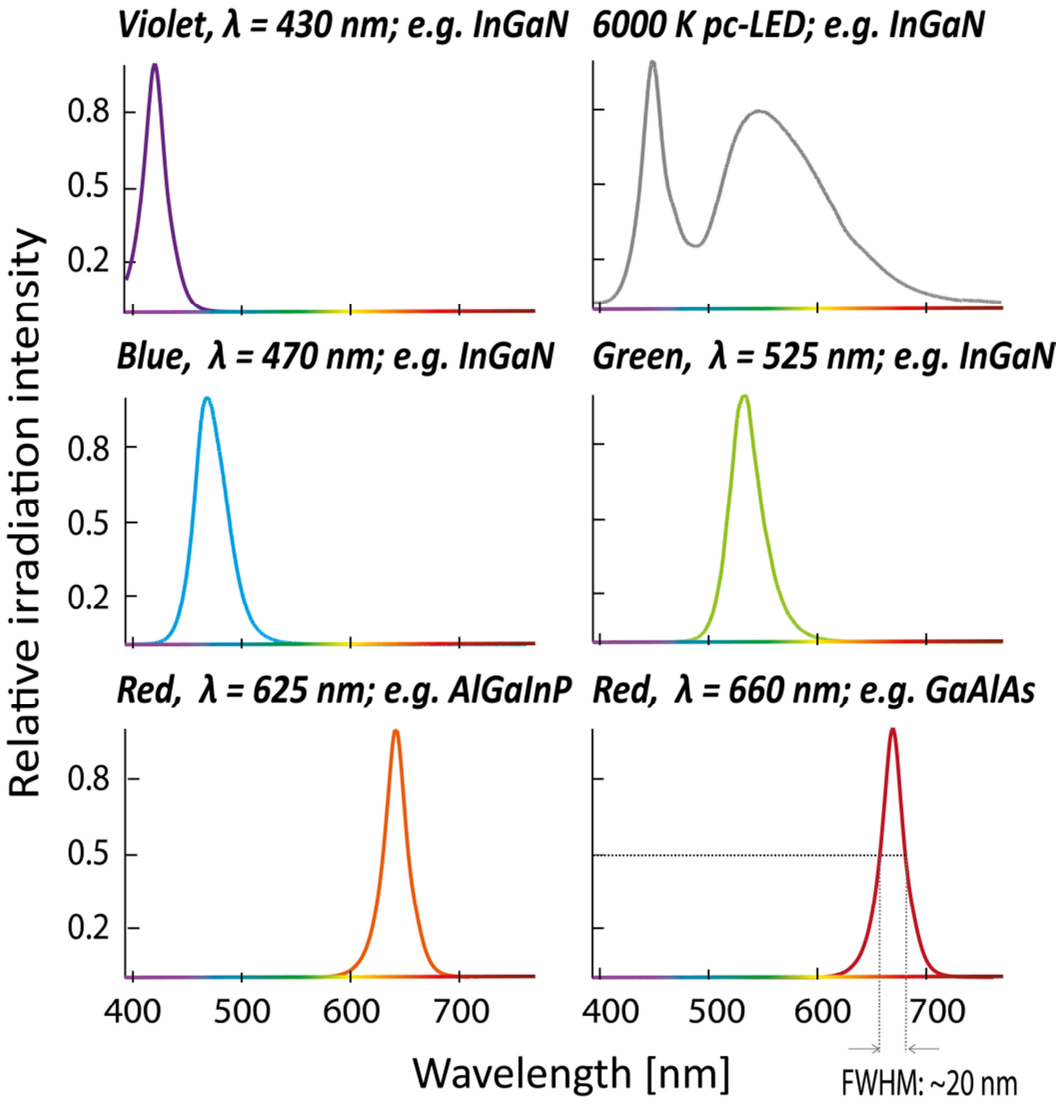

Figure 1.2-2 Emission spectra of different LEDs. The full-width-at-half-maximal (FWHM) corresponds to the difference of two wavelength values (usually ~20 nm) at which the LED attains 50% of its maximal intensity.

1.2.2 FLs

Concerning FLs, electrodes located at each side of a gas filled glass tube are heated up to allow electrons to be emitted into the space in front of the electrodes (thermionic emission) ([31]; Fig. 1.2-3). An electric field is thereby built up, accelerating the electrons until their energy is high enough to excite gaseous mercury atoms, distributed in the space between both electrodes, from the ground stage to a higher energetic level. An excited mercury atom falls back to its ground stage and releases the energy difference by emitting a photon with an energy of ~5.5 eV (E_λ = 8.83×10^{-19} J). This high energetic ultraviolet photon can then be absorbed by the phosphor coating on the inner face of the tube and be transformed into less energetic, visible and photosynthetic active light (λ_e = 380-750 nm or rather E_λ = 1.7-3.2 eV). The energy difference (40-70 %) is dissipated as heat, limiting drastically the efficiency of a FL [31].

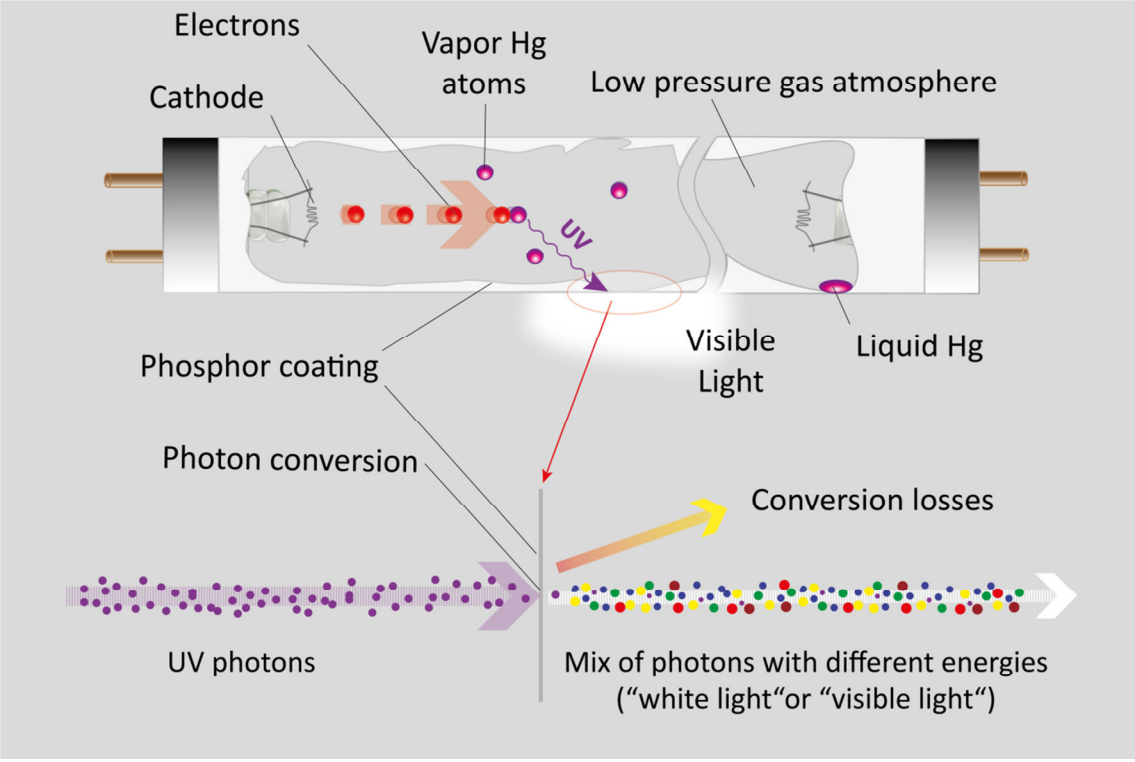

Figure 1.2-3 Simplified diagram of how fluorescent lamps (FLs) work.

Emission spectra of different types of FL including grow-light, warm white, and cold daylight, are depicted in Fig 1.2-4. Grow-light FLs spectra have high levels of red light (630-680 nm), which matches the chlorophyll *a* and *b* absorption peaks within the red spectral range. Therefore, this type of FLs can be used for growing photosynthetic organisms, although they are more expensive and less energetically efficient than FLs having their major emissions at shorter wavelengths (e.g. cool daylight FLs) [20]. Warm white FLs spectra may not be suitable to grow algae in an energy efficient manner, as a significant proportion of their emission peaks lie outside the major photosynthetic ranges (420-450 and 630-690 nm).

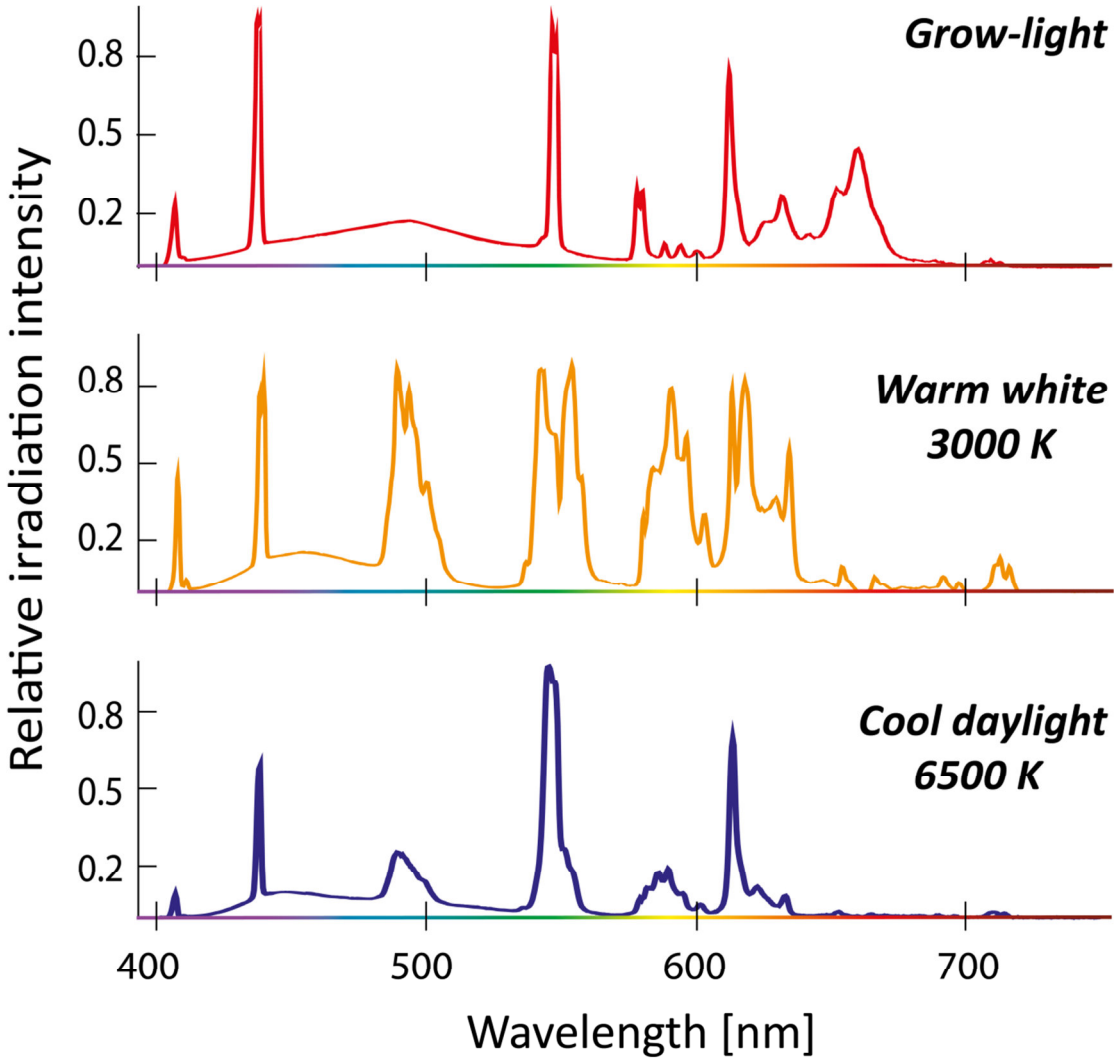

Figure 1.2-4 Emission spectra of different types of FLs, including grow-light, warm white, and cold daylight.

1.3 Economics and efficiency

As light quality influences growth and the biochemistry of microalgae, artificial lighting can be used to manipulate the final biomass to specific uses, particularly those for high-end markets. In order to design an artificial lighting system for microalgae, electric and photosynthetic efficiency of FLs and LEDs must be considered. Upon conversion of electric current to light in LEDs and FLs (see section 1.2) energy losses occur due to thermal dissipation, inward light reflection and reabsorption, among other factors. The reduction of these inefficiencies has resulted in higher power conversion efficiencies (PCE; ratio between electric input and optical output energy: $W_{output(optical)}/ W_{input}$) for LEDs (up to 50%) [13], as compared to gas discharge lighting technologies such as FLs (~30%) (Table 1.3-1) [28, 31].

Table 1.3-1 Comparison between LEDs and fluorescent lamps (FLs) largely based on data from US-DOE [13] and Kane *et al.* [31].

	LEDs		**Fluorescent lamps**	
	LED type	**Value**	**FL type**	**Value**
PCE (%)[a]	Blue (InGaN) Red (AlGaInP) Green (InGaN) Amber (AlGaInP) Cool white pc-LEDs	~50 ~40 ~17[b] ~8[b] ~30	Cool white T8	<30
Lifetime (h)[c]	Standard LEDs	~25,000-50,000; up to 100,000 (at T ≤ 70°C)	Standard FLs Long lifetime FLs	~12,000-20,000 ~50,000
Emission range(nm)	Single colour LEDs White LEDs (pc-LEDs)	FWHM: ~20 400-700	Coloured and white FLs	400-700
Cost of single illuminant (€/W_{input})[d]	SMD 5050 LED strips (60LEDs/m)	≥0.5-1.6[e]	FL T8 lamps (58 W)	~0.1-0.3[f]

Table 1.3-1 (continued).

Cost of Complete Systems (€/W_{input})[c]	High Power LED module	~4-6[g]	FL T8 lamps (58 W)	~0.7-2[h]
Pros	Quick response (ns scale), allowing the flashing of LEDs at high frequencies; Tailored light design easy applicable.		Well established in microalgal production.	
Cons	When heated up, efficiency and lifetime decreases drastically: AlGaInP-chips are more sensitive than InGaN to temperature. Cooling of LEDs is recommended if a high PPFD is achieved using high power LEDs or a high stock density; Limited market for single colour LED lamps in photosynthetic efficient wavelengths (i.e. 430 nm and 660 nm).		FLs containing mercury, as being highly detrimental to the environment and difficult to recycle; Electrodes can burn out, causing complete failure of the lamp.	

a. Power conversion efficiency **(**PCE) only reveals the efficiency of an illuminant; thus, the overall system efficiency (OSE) should also be considered, as it takes into account electrical drivers, reflectors, or rather every obstacle and electrical resistance between the input power source and the irradiated object (i.e. a photobioreactor) [32]. FLs can have a much lower OSE than LEDs, considering that they release photons in all directions and reflectors are needed, absorbing optical energy, when light is required in only one direction. LEDs have already reflectors incorporated, where losses have already been considered in the PCE.
b. To increase the efficiency and thermal stability of LEDs, some LED manufactures are producing more efficient InGaN chips with a phosphor cover, converting the emitted blue photons into light within the green and amber wavelength ranges (i.e. Luxeon® Rebel Phosphor-Converted (PC) Amber LED; http://philipslumileds.com) [33, 34].
c. LED lifetimes may exceed the lifetimes of power converter. Many power converters have a lifetime of 30.000-50.0000 h (source: Osram constant current LED power supplies, http://osram.com).
d. Light sources are typically compared using Kilolumen (a measure of light intensity perceived by the human eye). Hence, as this comparison is unsuitable for photosynthetic purposes, the prices are given taking into account the input wattage of an illuminant. Suppliers are only examples; other suppliers might offer cheaper and more sustainable products.
e. e.g. http://okledlights.com; http://rs-online.com.
f. It depends on the supplier; http://rs-online.com.
g. e.g. Philips (GreenPower LED, e.g. ref. DR/B 120).

Presently, among white LEDs, cool white phosphor converted-LEDs (pc-LEDs) yield the highest PPFD per input wattage (PPFD/W) and can be highly photosynthetic active due to their blue emission peak ($\lambda_e \approx$ 440-460 nm) [30], fitting almost perfectly to the blue absorption spectrum of light harvesting pigments (LHPs) in many plants and algae [2, 24, 35]. Both FLs and pc-LEDs emit light within the range of photosynthetically important long wavelengths ($\lambda_e >$ 650 nm), whereas most colour mixed-LEDs display a sharp decrease of light emission at shorter wavelengths [13]. Furthermore, white pc-LEDs and FLs emit a broad spectrum of light with high photon releases at the blue and green spectral ranges, decreasing at $\lambda_e >$ 650 nm. As pc-LEDs and FLs have similar emission spectra, pc-LEDs might be well suited for replacing FLs within the same colour temperature ranges, without causing significant changes in algal growth rates and biochemical properties. This replacement would thus provide a more competitive energy usage for biomass production [2, 3, 36].

Nevertheless, unlike FLs or pc-LEDs, single-colour LEDs have usually higher PCEs, as they can emit at specific wavelengths without using phosphor layers and thus avoiding losses (> 30%) for converting higher to lower energy photons [13]. However, single colour LEDs emitting within the green-amber light range show often very low PCEs, a problem known as the "green gap" or "green-yellow gap" [34]. In addition, usually more photons are released by LEDs emitting at longer wavelengths (e.g. red), resulting in higher PPFD/W ratios as compared to LEDs emitting at shorter wavelengths (e.g. blue) [3], since blue photons are more energetic than red photons. Specifically, red (λ_e = 660 nm) LEDs can emit the double amount of photons than blue LEDs, whereas green LEDs were found to emit ~3 times less photons than red LEDs [14, 18, 34, 37, 38]. At face value, these results suggest that the 660-nm red LEDs are able to sustain biomass growth with the highest energy efficiency [3]. However, LEDs with $\lambda_e >$ 680 nm also release photons with photosynthetically inefficient wavelengths ($\lambda >$ 695 nm) [39, 40], leading to less photon utilization by the algae and thus less biomass production per input wattage. Nevertheless, caution is needed, as PPFD/W ratios and PCE may vary with the LED manufacturer. Finally, the fast response time of LEDs compared to that of FLs can also be beneficial, as it can be used to grow algae under customised flashing light, increasing biomass production [17, 41, 42] and perhaps allowing algae to exceed the proposed maximal photosynthetic efficiency of 17% [3]. For further information about flashing and controlling LEDs see Schulze *et al.* [1] (Annex 1).

1.4 Effects of light quality on microalgal growth

1.4.1 Pigments and light requirements of microalgae

The amount of photons at blue or red wavelengths that can be captured by a molecule of chlorophyll in algae is dependent on the cellular architecture, pigment composition and chloroplast arrangement. Interestingly, the evolutionary history of microalgae as purported by Keeling [43] seems to account for the preference of microalgae for growing under either blue ($\lambda \approx$ 420-470 nm) or red ($\lambda \approx$ 660 nm) light (Table 1.4-1). This preference correlates well with the evolutionary megagroup of each microalga, which in turn seems to reflect the pigment composition of the light harvesting complexes present in their chloroplasts [44].

Table 1.4-1 Impacts of light quality in microalgal growth parameters and preferred growth wavelengths (λmax) of several algae classified according to Keeling [43] and percentage of diminished biomass production under alternative wavelengths (λmin).

Microalga	λ_{max} (nm)	λ_{min} (nm)	% less at λ_{min}	Outcome	Refs.
Cyanobacteria					
Synechocystis sp. PCC 6803	612 620 660	535 470	n.i.	LEDs peaking at 612, 620 and 660 nm showed better growth than green (535 nm) and blue (470 nm) LEDs.	[45]
Arthrospira platensis	[620-645]	[460-475]	75	*Arthrospira platensis* (syn. *Spirulina platensis*) grown under red light showed higher growth rates.	[46]
Arthrospira platensis	630	470	80	Red LED light was considered to be the most effective light source for photoautotrophic cultivation compared to blue, green, yellow and white LEDs. Red LEDs gave rise to the highest growth rates and biomass production at light intensities of 300-3000 μmol m^{-2} s^{-1} as compared to blue LEDs. Green LEDs also promote higher biomass production than blue LEDs.	[47]
Chlorophytes					
Acutodesmus obliquus CNW-N	660 470	s	-	*Acutodesmus obliquus* (syn. *Scenedesmus obliquus*) showed always lower biomass production under blue (470 nm) LEDs as compared to red, green and white (daylight) LEDs. Furthermore, *A. obliquus* FSP-3 grown under FLs showed higher biomass production than under white (daylight) LEDs.	[48]
Acutodesmus obliquus FSP-3	660 470	s	-		
*Botryococcus braun*ii Bot-144	660	470[a]	21	Carbon fixation was highest under blue light. Red LED more effective regarding the supplied optical energy. Shapes of aggregates changed between blue and red LEDs.	[8]
Chlorella kasseri	660	470	18	Red LEDs produced highest number of cells with highest weight, blue LEDs led to increased cell size.	[19]

Table 1.4-1 (Continued).

Microalga	λ_{max} (nm)	λ_{min} (nm)	% less at λ_{min}	Outcome	Refs.
Chlorella sp.	660	460	7	White LED light resulted in slightly more biomass than blue or red LED light alone. Mixed LED light (red : blue; 1:9, 3:7, 5:5, 7:3, 9:1) showed always higher biomass production than white, red or blue light alone, whereas a ratio of 5:5 showed highest, 32% more, biomass production than red light alone.	[18]
Chlorella pyrenoidosa	660	n.i.	-	No need for additional blue light. Photosynthesis only slightly affected by flashing LEDs (5 ns on-cycle, 45 ns off-cycle).	[42]
Chlorella sp.	660	460	37	Red LEDs are the most effective in nutrient removal from agriculture digestates and growth as compared to white, yellow (590 nm) and blue LEDs, in decreasing order.	[14]
Chlorella sp.	[650-680]	[440-470]	21	Mixotrophic culture of *Chlorella* sp. and *Saccharomyces cerevisiae*; Biomass productivity was highest under red followed by blue and green LEDs.	[49]
Chlorella sp. FC-21	660	450	27	Red light was found to be the most suitable light source (2.5 times higher specific growth rate than FL). Mixed LEDs of red and blue (3:1) or additional white LED (1:1:1) did not increase the growth rate (no CO_2 supplementation).	[50]
Chlorella vulgaris	n.i.	n.i.	-	Blue LEDs (420-450 nm) showed higher biomass production than FLs.	[51]
Chlorella vulgaris	660	450	39	Similar biomass production under red, white and yellow (590 nm) LEDs as well as blue and purple (410 nm). Green light showed lowest biomass production (65% less than the red LEDs).	[37]
Chlorella vulgaris	625 660	470	56	Red light is most efficient for nutrient removal. Blue light resulted in a 56% decrease of the growth rate and final biomass production.	[18, 52]

Table 1.4-1 (Continued).

Microalga	λ_{max} (nm)	λ_{min} (nm)	% less at λ_{min}	Outcome	Refs.
Chlorella vulgaris	430	625	70	LEDs peaking at 625 nm were not suitable to grow *C. vulgaris.* Mixing blue and red LEDs increased biomass production but was still 17% less than sole blue LED lights.	[53]
Dunaliella salina	660	n.i.	-	25% blue photons with 75% red photons resulted in higher growth rate than only red light.	[16]
Haematococcus pluvialis	470 421	625	3 15	LEDs with emission peaks at 380, 421, 470 and 625 nm had higher volumetric productivity than FLs. Blue light induced cell growth arrest.	[54]
Haematococcus pluvialis	470	625[a]	45	Blue LEDs, compared to red, green and white, increases cell size and growth kinetics. Blue light caused suppression of cell growth. White light was less efficient than blue light.	[55]
Scenedesmus sp.	670 450	s	-	White light irradiated algae had a 45% higher production rate than those under single blue or red LEDs. When red light was mixed with blue light (almost regardless to the mixing ratios), production rates were 50 % higher than only under white light.	[56]
Mychonastes homosphaera	660	n.i.	-	*Mychonastes homosphaera* (syn. *Chlorella minutissima*) produced 8% less biomass under red and white LEDs compared to FLs.	[36]
Tetraselmis suecica F&M-M33	624	470	50	Biomass productivity was equal between cool white LEDs and red LEDs as well as between green and blue LEDs, respectively. Approximately 75% more cells were observed when grown under red light compared to those under white, blue and green LEDs. Furthermore, cells under red light were more motile and smaller.	[57]

Table 1.4-1 (Continued).

Microalga	λ_{max} (nm)	λ_{min} (nm)	% less at λ_{min}	Outcome	Refs.
SAR: Stramenopiles					
Nannochloropsis oceanica CY2	475 630	s	-	*N. oceanica* CY2 showed similar biomass production under blue, red, yellow (~590 nm) and white LEDs thus was slightly higher under FLs.	[58]
Nannochloropsis sp.	470	680	26	Cells exposed to green LEDs (550 nm) showed higher growth rates than those under red LED light.	[15]
Phaeodactylum tricornutum	blue, ?	red, ?	22	Blue LED light results in NPQ and has higher photoprotective potential. Evidence found that diatoms need blue light to acclimatize to high light intensities.	[59]
Skeletonema costatum	456	656[a]	9	With increasing spectrum absorption coefficient[b] among different LED light sources, growth rate increased and saturation of light quantity decreased. Cell numbers between green and red LED light were similar.	[60]
Achnanthes sp.	450	650[a]	44	Blue LED light was more efficient in terms of net photosynthesis rates than FLs, yellow and red LEDs in all diatoms, especially for *Nitzschia* sp. *Nitzschia* sp. showed removal of dissolved inorganic nitrogen, and phosphorus, acid volatile sulphide from growth medium in decreasing order as follows: blue LEDs > FLs > red LEDs > yellow LEDs. Blue light yielded highest chlorophyll content in *Nitzschia* sp.	[61]
Amphora sp.	450	650[a]	35		
Navicula sp.	450	650[a]	33		
Nitzschia sp.	450	650[a]	47		
SAR: Alveolata					
Alexandrium tamarense	450	650[a]	39	Cells showed highest growth rate under blue LED light, followed by FL, red- and yellow LED light in decreasing order.	[61]

Table 1.4-1 (Continued).

Microalga	λ_{max} (nm)	λ_{min} (nm)	% less at λ_{min}	Outcome	Refs.
Hacrobia: Haptophytes					
Isochrysis galbana	460	660	80	Blue light (470 nm) was considered to be more economical than FLs. A mix of red and blue LEDs gave same optical density than fluorescent or sole blue light.	[26]
Isochrysis galbana	red, ?	blue, ?	32	Flashed blue light provided highest biomass production compared to continuous FL as well as flashed red or white LEDs. Cell weight was not affected by light quality	[62]
Isochrysis sp.	n.i.	n.i.	-	Broad band blue light source obtained higher photosynthesis rate than white light. Cell concentration was similar between both light sources.	[63]

Abbreviations: **a**: growth rates; **b:** Spectrum absorption coefficient reveals the quantum efficiency of photosynthetic effective photons absorbed by microalgae. It also reflects the efficiency of a light source to promote growth of microalgae; **FAME:** fatty acid methyl esters; **FLs:** fluorescent lamps; **n.i.:** not investigated **s:** similar biomass production; **SAR:** Stramenopiles-Alveolata-Rhizaria megagroup.

As discussed by Keeling [43], a primary endosymbiotic event between a eukaryote and a chlorophyll *b*-containing ancestor of cyanobacteria gave rise directly or indirectly to most photoautotrophic eukaryotes (Fig.1.4-1). Cyanobacteria, especially those lacking chlorophyll *b*, use chlorophyll *a* ($\lambda_a \approx$ 430 and 680 nm) as well as accessory phycobiliproteins such as phycoerythrin ($\lambda_a \approx$ 550 nm) and phycocyanin ($\lambda_a \approx$ 620 nm) as LHP [64], making them capable of utilizing mostly red and yellow light and, to a significantly lesser extent, blue light [45-47]. The first endosymbiotic event with the ancestor of cyanobacteria as the endosymbiont led to the appearance of chlorophytes (green algae) and rhodophytes (red algae) [65].

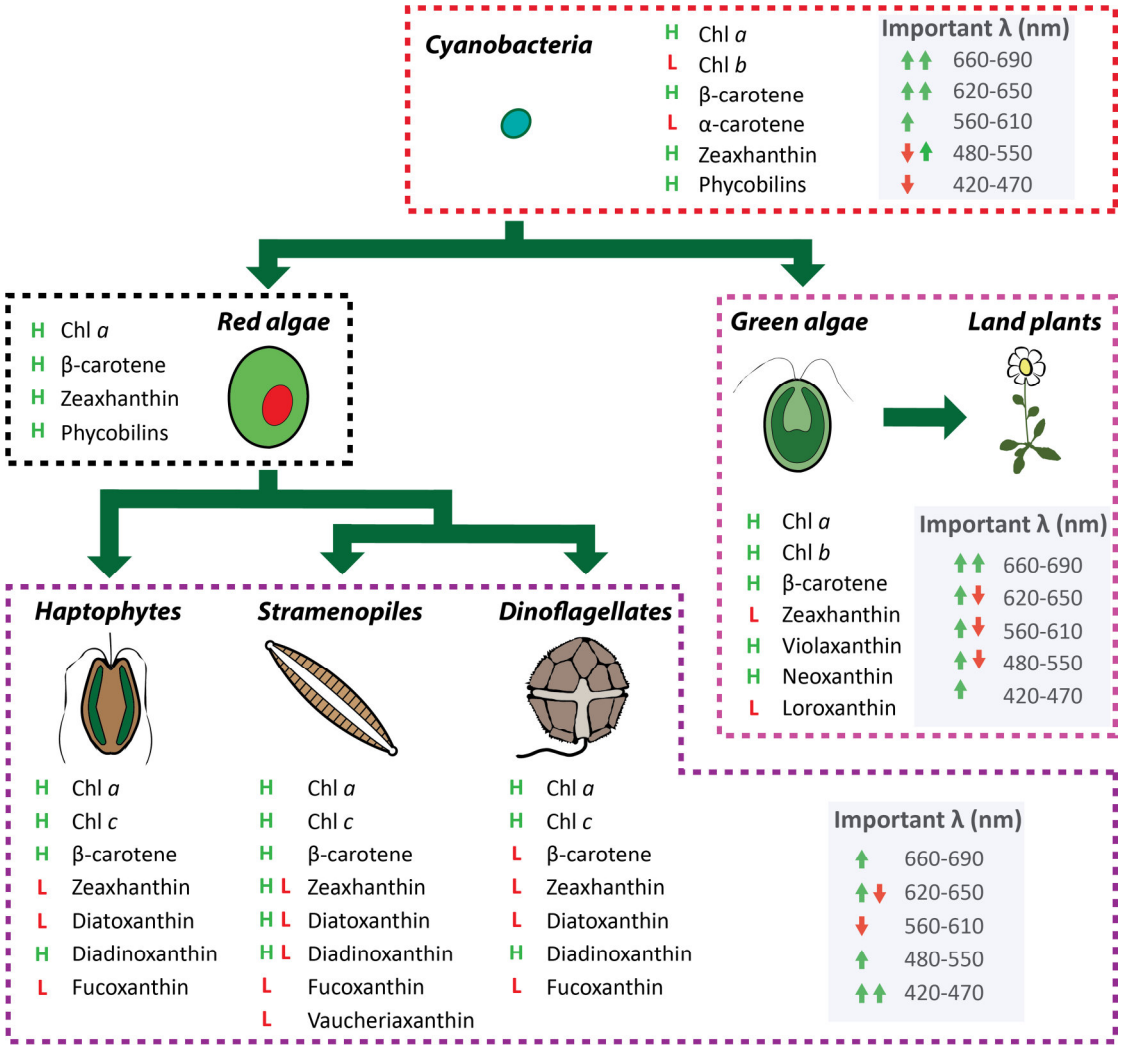

Figure 1.4-1 Approximate light requirements of microalgae based on results from Table 1.4-1, main pigments, and the evolutionary relationships among major microalgal megagroups. Pigment distribution was obtained from Takaichi [44] and evolutionary history is in accordance with Keeling [43]. Arrows denote the relative importance of different wavelengths: two upward green arrows, very important; one upward green arrow, important; one upward green arrow and one downward red arrow, important / accessory; one downward red arrow, accessory. Abbreviations: Chl: Chlorophyll, H: high pigment content, L: low pigment content, H L: variation between high and low pigment contents among species.

Red light is crucial for the growth of chlorophytes (and land plants) [44]. However, these organisms are able to utilize blue light more efficiently than cyanobacteria, probably due to the loss of chlorophyll *b* by many cyanobacterial species [65] and due to a higher diversity of carotenoids in photosynthetic eukaryotes (Fig. 1.4-1). As a trade-off, chlorophytes lack the ability of utilizing yellow and green light extensively as they lost phycobilins during evolution [64]. Therefore, for chlorophyll *a*-containing microalgae, "major" wavelengths are within the 420-470 nm and/or 660-680 nm ranges and "accessory" wavelengths are located below, between or above the aforementioned ranges.

Secondary endosymbiotic events involving heterotrophic eukaryotes and green algae gave rise to mixotrophic euglenids and chlorarachniophytes with a pigment composition and most probably light requirements similar to those of the ancestors of their plastids. Conversely, microalgae such as rhodophytes and glaucophytes are probably more adapted to shorter wavelengths (blue, green, yellow) than chlorophytes as they retained phycobilins during evolution [43].

Cryptomonads and haptophytes (e.g. *Isochrysis*), belonging to the Hacrobia megagroup, and the heterokontophytes (e.g. diatoms) and dinoflagellates, belonging to the SAR (Stramenopiles-Alveolata-Rhizaria) megagroup, are assumed to have evolved from secondary endosymbiosis of a heterotrophic eukaryote engulfing a rhodophyte, whereupon most species lost phycobilins, developing instead a higher diversity of carotenoids, and acquiring chlorophyll *c*, a type of chlorophyll known to absorb strongly in the blue light range [66]. As a result, Hacrobia and SAR algae are usually better equipped for using bluish light compared to cyanobacteria or chlorophytes (see Table 1.4-1). Serial and tertiary endosymbiosis resulted in other eukaryotic photo-heterotrophs (mostly dinoflagellates) with preferred wavelengths probably similar to those of the ancestors of their endosymbionts, although only few studies on the light requirements of these microalgae have been found.

Therefore, shared evolutionary history of microalgae as suggested by Keeling´s [43] tree of endosymbiotic events may provide information about the light requirements of algae within groups as depicted in Fig.1.4-1.

1.5 Effects of light quality on microalgal traits

Red to far-red light ($\lambda_e \approx$ 630-750 nm) is known to cause high growth rates and smaller cells [19, 46, 49, 67-69] by accelerating the cell cycle in many microalgae of diverse evolutionary lines. However, far-red light can suppress volumetric biomass production when supplemented to a broadband light source [69], as it regulates light harvesting mechanisms in microalgae [68].

Red to far-red light can be detected by photoreceptors such as phytochromes in land plants and charophytes as well as multiple light sensing photoreceptors in cyanobacteria [70, 71]. In free-swimming chlorophytes, no obvious genes encoding phytochromes have been found. Instead, an "animal-like" cryptochrome seems to be the long sought-after red receptor in chlorophytes, which is unable to detect far-red [72]. This multitude of red/far-red photoreceptors in different evolutionary lines strongly indicates that caution must be used when extrapolating how the red/far-red light range is detected and how it regulates growth. Clearly, further research is needed in order to understand how different photosynthetic organisms detect and respond to this range of the electromagnetic spectrum.

Concerning shorter wavelengths, blue light influences gene expression as well as several metabolic pathways in algae and plants via photoreceptors such as cryptochromes, phototropins, aureochromes and neochromes [71, 73]. Blue light is, for example, responsible for endogenous breakdown of carbohydrate reserves [74], which may explain why the haptophyte *Isochrysis* sp. T-ISO exposed to blue light and grown in a chemostat displayed lower carbohydrate content than under other wavelengths [63]. However, the opposite or no significant effect has been found in green algae grown in batch [8, 57].

Blue light, most probably via photoreceptors such as phototropins, seems to induce pigment accumulation in several species (Table 1.5-1) [16, 54, 72, 75]. Moreover, as the energy of blue photons is higher than that required for photosynthesis [20], blue light might result in non-photosynthetic quenching (NPQ), generating reactive oxygen species (ROS) [16]. Therefore, to protect the photosynthetic apparatus against ROS, algae as well as plants accumulate photoprotective pigments (e.g. xanthophylls) [12, 16, 24, 76, 77].

Table 1.5-1 Light quality effects on microalgal biochemical composition at specific wavelengths (λmax).

Light	λ_{max} (nm)	Alga	Effects	Refs.
Blue	[440-470]	*Chlorella sp.*	Higher lipid content in biomass when compared to red (650-680 nm) LED.	[49]
	500	*Chlorella sp.*	Blue light induces slightly higher lipid production compared to red light.	[75]
	470	*Dunaliella salina*	β-carotene and lutein accumulation was observed when blue light was supplemented to red (660 nm).	[16]
	470	*Haematococcus pluvialis*	Accumulation of red pigments.	[55]
	[380-470]	*Haematococcus pluvialis*	Astaxanthin accumulation.	[54]
	n.a.	*Isochrysis sp.* (T-iso)	Blue light causes higher protein content accompanied by low carbohydrate and chlorophyll content per cell compared to a white FLs.	[63]
	n.a.	*Isochrysis galbana*	Higher DHA and phospholipids content in fatty acids than red LEDs under intermitted light (*f* = 10Khz)	[62]
	475	*Nannochloropsis oceanica* CY2f	Blue and red (~630 nm) LEDs showed highest EPA content in biomass compared to FLs as well as white and yellow LED.	[58]
	470	*Nannochloropsis sp.*	Highest palmitoleic acid (C16:1) thus lowest eicosapentaenoic acid (EPA) content in FAME compared to red, green and white LEDs under phototrophic condition. Total FAME per dry weight was highest under blue, green and white light, lowest under red when grown mixotrophically. Similar FAME contents under phototrophic condition.	[15]
	450	*Nitzschia sp.*	Blue light yielded highest chlorophyll content compared to red (650 nm) and yellow (590 nm) LEDs.	[61]
	n.a.	*Phaeodactylum tricornutum*	Lager pool of xanthophyll cycle pigments and higher chlorophyll *a* content compared to red and white LED light (low light conditions).	[59]
	[460-475]	*Spirulina platensis*	Lowest chlorophyll and phycocyanin content in biomass compared to yellow, green, red and white LEDs.	[46]

Table 1.5-1 (Continued).

Light	λ_{max} (nm)	Alga	Effects	Refs.
	470	*Tetraselmis suecica* F&M-M33	Blue light induces higher chlorophyll accumulation compared to cool white and red, green and blue LEDs. Higher carbohydrate content of cells grown under blue LEDs compared to red LED.	[57]
Green	n.a.	*Chlorella vulgaris*	Green light induces higher chlorophyll accumulation compared to blue, yellow, orange and red broad band light spectra.	[78]
	550	*Nannochloropsis sp.*	Higher arachidonic acid (AA) content under phototrophic conditions compared to FL as well as blue, red, white LEDs.	[15]
Red	660	*Botryococcus braunii* Bot-144	Evidences for higher carotenoid/chlorophyll ratio compared to blue and green LEDs.	[8]
	660	*Chlorella minutissima*	Increased C18:2 and decreased C18:3 in FAME. No fatty acid changes between FLs and white LED. Total FAME unaffected among all light sources.	[36]
	660	*Chlorella sp.*	Highest biogas production compared to yellow, blue and white LED.	[14]
	680	*Nannochloropsis sp.*	Higher oleic acid (C18:1) contents in FAME compared to blue, green and white LEDs under phototrophic conditions.	[15]
	n.a.	*Tetraselmis suecica* F&M-M33	EPA content increased under red light compared to blue, green and white LED.	[57]
Far-red	n.a.	*Dunaliella bardawil*	Supplemented far-red light to FLs induced high carotenoid accumulation.	[69]

FAME: fatty acid methyl esters; **FLs:** fluorescent lamps; **N.A.:** Spectrum not available or broadband spectrum.

1.6 Using LEDs for microalgal production

1.6.1 Estimation of preferred wavelengths

To maximize the photosynthetic efficiency, all photons released from a source of light should be captured by the photosynthetic apparatus of microalgae. A strategy to achieve a high level of light utilization is the complete spectral matching of a light source with the photosynthetic active spectrum (PAS). However, this strategy can only be an approximation, as the measurement of the PAS of microalgae is still a difficult endeavour [79]. The determination of a general PAS for single taxonomical groups or rather megagroups, as done for green algae [80], may help estimate the light quality required for a species belonging to specific taxon. Absorption spectra of intact cells, however, are easier to be determined and may give a rough idea of the light quality needed for optimal growth. When the wavelengths of peaks from absorption spectra [81, 82] and the preferred wavelengths for growth (λ_{max}, λ_{min}; Table 1.4-1) of algae within a given megagroup are compared, a relatively good spectral match is apparent. However, the wavelength of the peak with the highest absorption seldom matches the preferred wavelength for optimal growth (either $\lambda_{max} \approx$ 420-470 nm or $\lambda_{max} \approx$ 660-670 nm) of cyanobacteria and green algae. These species usually show better growth and biomass production under LEDs 660 (λ_e = 600nm; Table 1.4-1), whereas the maximal absorption is usually measured in the blue range of the electromagnetic spectrum [81, 82]. This may be explained by the fact that absorption spectra of cells include the contribution of all cellular components able to absorb or scatter light, which may not necessarily contribute to the light harvesting processes needed for photosynthesis, masking thereby the true light requirements for growing a specific microalga.

1.6.2 Tailored light sources

A tailored LED-based light source for high volumetric production, at the present state of the art, may include pc-LEDs as a good starting point, covering with their broadband phosphor emission ($\lambda_e \approx$ 560 nm; Fig. 1.2-2) the green, yellow and amber (500-610 nm) wavelength ranges. Violet-blue (preferably $\lambda_e \approx$ 420-450 nm) and red ($\lambda_e \approx$ 660-670 nm) wavelengths can then be further adjusted to the species selected for cultivation. However, white pc-LEDs, especially those with cooler colour temperatures, also emit photons with $\lambda_{e\_blue} \approx$ 440-460 nm (Fig. 1.2-2), increasing the levels of available blue light. Moreover, as discussed before, the taxonomy of the selected microalga may be used to predict the most

important LEDs for growth (Fig. 1.4-1; Table 1.4-1) and/or production of specific biomolecules (Table 1.5-1). Concerning red-to-blue ratios, land plants have shown optimal biomass production when red LED light was supplemented with 10-30% blue light [83]. This suggests that similar red and blue ratios may also be suitable for green algae, as their plastids are closely related to those of terrestrial plants in terms of structure, metabolism and biochemical composition. Indeed, this assumption seems to be correct, as mixing of red with blue photons in this proportion has often been reported to increase biomass production compared to red light alone [16, 38, 48, 84]. Regarding other taxa such as cyanobacteria and SAR microalgae, higher blue light content may be needed. Nonetheless, a relative dearth of studies on red-to-blue ratios for these species allows no final conclusion.

The success of increasing biomass productivity via tailored supplemental artificial light depends on the remaining environmental parameters for photosynthesis such as PPFD, light path length, CO_2 concentration, pH, macro- and micronutrient availability, temperature, among other factors [4, 68]. For example, nitrogen starvation can cause chromatic adaptation of cyanobacteria and red algae, resulting in degradation of phycobilisomes (i.e. phycobilin-containing light harvesting complexes), leading to diminished green light absorption [68]. Furthermore, the light path length of the bioreactor can influence the choice of wavelengths coming from a light source. An increased amount of green-amber wavelengths might be beneficial for green and SAR algae grown in photobioreactors (PBR) with a long light path and/or highly density cultures as photons are less absorbed, allowing them to travel deeper into the culture. In turn, the same light quality might be unsuitable for algae growing in thin layer PBR with shorter light path lengths and/or low density cultures. Lastly, Miao *et al.* [60] concluded that the light saturation point for *Skeletonema costatum* exposed to a suitable light source is lower than an unsuitable source of light. If this result is confirmed in other species, it could allow the growth of microalgae at lower PPFD, decreasing energy consumption, when tailored light sources are selected for specific microalgal strains, growth phases and/or PBR.

1.7 Justification of the dissertation

Although studies about the cultivation of microalgae under different light qualities supplied by LEDs have increased in number over the last 2-3 years, there are still important gaps in the knowledge of how microalgae respond to light. For example, published data on the combined use of LEDs for microalgae grown under optimized multichromatic light in order to increase photosynthetic efficiency have not been found. Furthermore, amongst the

few studies investigating the effects of light quality on biochemical components (e.g. total lipids, fatty acids, proteins and/or carbohydrates) in microalgae, only partial reports focusing on more than one or two specific biochemicals have been published. Therefore, no general metabolic response patterns can be ascertained. Lastly, no studies were found linking growth and biochemical parameters to morphologic and physiological changes in algae growing under light at specific wavelengths. Unfortunately, a significant number of studies working with monochromatic LEDs used for phototrophic growth have not measured light intensity and light properties with appropriate sensors. This has often led to misleading results and inadequate experimental design, hindering the establishment of an accurate body of knowledge of the general response of algae to light quality. Specifically, the effects of light quality on the growth, biochemical and morphologic properties of *Nannochloropsis oculata* and *Tetraselmis chuii* have not been studied satisfactorily. Both species have different promising key applications, such as the production of biofuels, nutra- and/or pharmaceuticals due to their high contents of unsaturated fatty acids and triacylglycerols [85], whereas the flagellated green microalga *T. chuii* is a useful species for aquaculture due to its high EPA and DHA contents and high motility [86]. Interestingly, the aforementioned microalgae belong to different evolutionary pathways. *N. oculata* is classified as a Stramenopiles microalga, belonging to the unranked Stramenopiles-Alveolata-Rhizaria (SAR) megagroup. Conversely, *T. chuii* is a Chlorophyta microalga belonging to the unranked Archaeplastida megagroup [43]. As these species belong to different evolutionary lines, it is likely that they respond to light quality in different ways, especially in terms of the preferred growth wavelengths within the blue and red regions of the electromagnetic spectrum [1] as well as within the range of the so called “accessory” wavelengths. However, possible similarities in the response of each microalga to light quality cannot be excluded at this stage.

1.8 Objectives

In order to fill in the gaps found in the current state of the art, the main objective of this study is to explore the application of different (blue, red, white) LED light sources to the cultivation of microalgae. Hence, a specific objective of the present dissertation is to investigate the effect of light quality on the growth rate, biochemical composition, morphology and physiology of two microalgal species with distinct evolutionary histories, namely *N. oculata* and *T. chuii*. With this purpose in mind, the present study investigates and

discusses how combinations of different artificial light sources impinge on the growth of microalgae as well as what is the role of “preferred wavelengths” [1] of particular taxonomical groups in determining the response of microalgae to light quality. These results are compared to microalgae grown under light of FLs developed for photosynthetic growth, as these FLs are currently the most productive growth light sources for microalgal production in terms of biomass/PPFD production. Hence, the obtained know-how may result in the establishment of cost-cutting measures as well as in a more efficient production of high value products from microalgae as compared to production systems using alternative light sources, such as FL.

2 Material and methods

2.1 Microalgae

Two marine microalgae, *N. oculata* (Stramenopiles) and *T. chuii* (Chlorophyta), were provided by the CCMar, University of Algarve, Faro, Portugal and by the Universidad de Cádiz, Spain, respectively. Microalgal cultivation was performed in the Departamento de Tecnologías del Medio Ambiente, Universidad de Cádiz in Spain.

2.2 Growth conditions

Each treatment was carried out in three 1-L borosilicate glass flasks filled up with 700 mL of algal culture. The growth medium consisted of 0.1 µm filtered seawater from the Atlantic shoreline of Cádiz, Spain (salinity 38), enriched with modified F/2 medium, whose composition was 4.39 mg L^{-1} EDTA, 3.15 mg L^{-1} $FeCl_3$, 100 mg L^{-1} $NaNO_3$, 5 mg L^{-1} NaH_2PO_4 and micronutrients: 0.098 mg L^{-1} $CuSO_4$, 0.105 mg L^{-1} $ZnCl_2$, 0.10 mg L^{-1} $CoCl_2$, 1.8 mg L^{-1} $MnCl_2$ and 0.63 mg L^{-1} Na_2MoO_4. The temperature for the culturing chamber was 22± 2 °C. Each culture with a volume of 700 mL was aerated by 0.2-µm-filtered air enriched with 5% CO_2 at a flow rate of 0.5 L min^{-1}.

2.3 Light treatment

Algae were exposed to single purple (LED 405), blue (LED 465), pure-red (LED 630), deep red (LED 660) as well as cool- and warm white pc-LEDs (CW LED, WW LED; Fig. 2.3-1A and B, respectively). Furthermore, each alga was exposed to dichromatic light with a high (HRLB) or low (HBLR) red-to-blue ratios (Fig. 2.3-1C) as well as a multichromatic emission spectrum adapted to the absorption spectrum of the algae, mixing low (HBmix) or high (HRmix) red-to-blue ratios with "accessory" [1] wavelengths (Fig. 2.3-1D). These treatments were divided into three experiments for each alga. In Experiment 1, the effects of light emitted by LED 405, LED 465, LED 630, LED 660, CW LED and WW LED on microalgal growth and biochemical components were investigated. In Experiments 2 and 3, the effects of HRLB and HBmix as well as HBLR and HRmix on microalgal growth were investigated, respectively. Reference cultures for each experiment and inocula were grown under FL used for phototrophic growth (Sylvania Gro-Lux) (Fig. 2.3-1B).

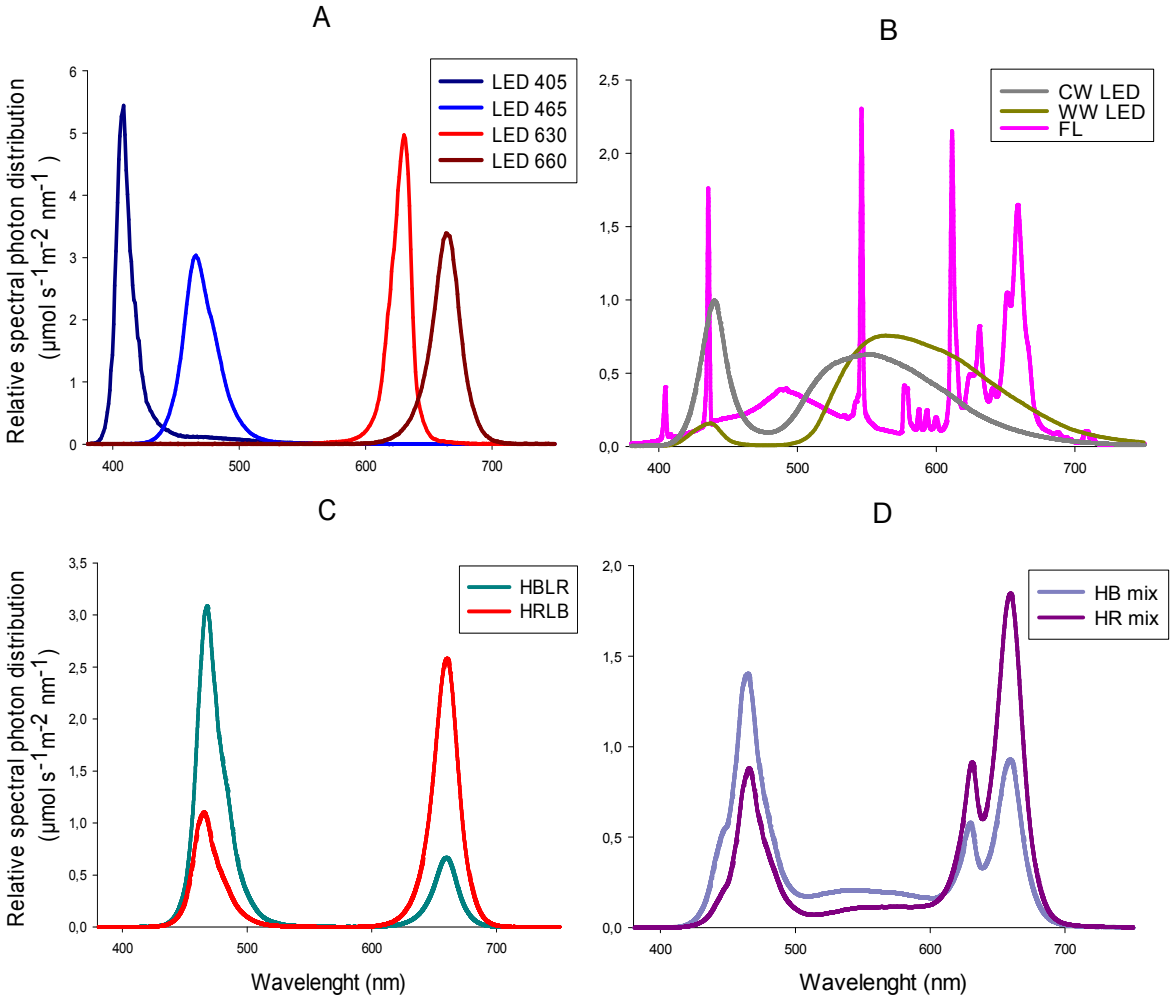

Figure 2.3-1 Photon distribution between 380 and 750 nm of the light sources under study. (A) single colour LEDs, peaking at λ_e = 405 nm (LED 405), 465 nm (LED 465), 630 nm (LED 630) and 660 nm (LED 660); (B) Mixed spectra light sources: Cool (CW LED) and warm (WW LED) white LED as well as a FL for plant growth (Sylvania Gro-Lux), (C) two-colour mix adapted spectra with high blue and low red (HBLR) and high red with low blue (HRLB) light emission; and (D) multi-colour mix spectra with high (HBmix) and low (HRmix) blue light content.

The relative spectral photon distribution of single light sources (Fig.2.3-1) was measured via Ocean optics 4000+. To quantify the spectrum, the PPFD of ~100 µmol $s^{-1}m^{-2}$ was determined via Apogee MQ 100 quantum sensor. The spectral response of the used quantum sensor (Apogee MQ 100) was corrected by applying factors calculated by the relative spectral light distribution of the light sources and the response spectrum of the quantum sensor according to [21]. As the error for quantum sensors is usually higher at near monochromatic light sources than compared to broad band light sources [22], the obtained correction values for the single colour LEDs were further tested and validated by measuring the optical energy (Optical power meter, Thor Labs Inc.) at the peak wavelengths of the LEDs followed by the conversion of optic energy into PPFD. For further details see Annex 3.

All cultures were subjected to a 24-h photoperiod using the light source under study. The PPFD of ~100 µmol $s^{-1}m^{-2}$ at the surface of the reactor was adjusted by changing the distance

between bioreactor and LEDs. The used LEDs (LED strip SMD 5050) were glued on a closure head of a cable channel mounted on a wooden board. This design allows exchanging or removing the closure head and the LED arrays to adjust the emission spectra for the second and third experiments (Fig. 2.3-2).

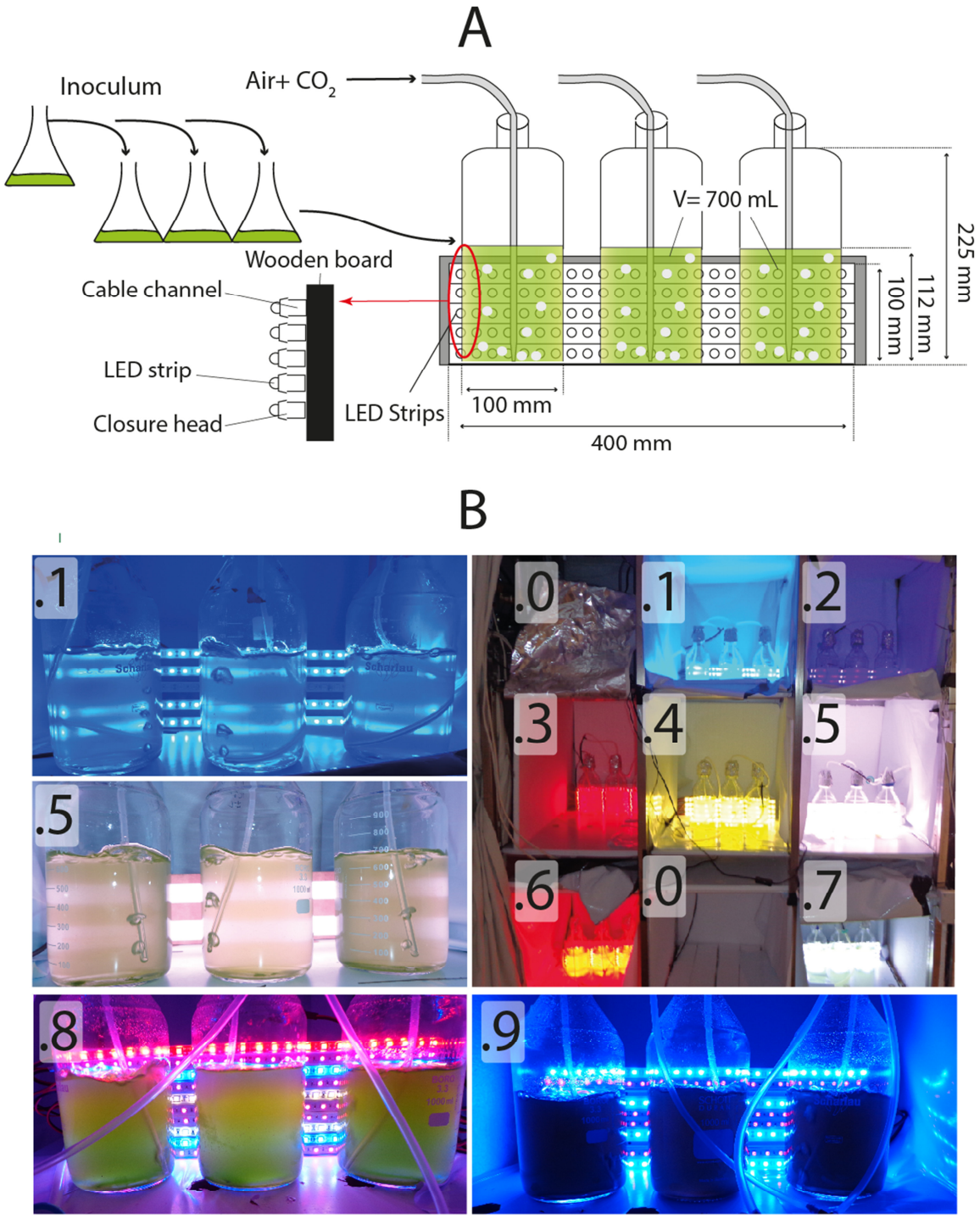

Figure 2.3-2 Design of the experiments. (A) represents a draft of the experimental setup for all experiments. (B) shows representative photographs of *T. chuii* under different light conditions, in which B.1 shows algae grown under LED 465, B.2 LED 405, B.3 LED 660, B.4 WW LED, B.5 FL, B.6 LED 630, B.7 CW LED, B.8 HRmix and B.9 HBLR. Initial operating volume (V) was always 700 mL. Chambers indicated as B.0 were used as reserves and for controlling CO_2 and airflow.

2.4 Sampling

In all experiments, samples for daily multiple cell counts via a Neubauer cell count chamber were taken (two per flask, six per treatment per day). In addition, daily samples for pH measurement, dissolved nutrient analyses as well as optical density (OD) determination of each treatment and flask were taken. OD was measured at 680 nm. Ash free dry weight (AFDW) determinations were performed at critical time points during cultivation time (see results). Two cultures of algae were harvested from each treatment at late exponential phase. However, only biomass from the first experiment was analysed for its biochemical contents in terms of protein, carbohydrates, total lipids and fatty acids as well as elemental composition in terms of nitrogen, hydrogen and carbon (LECO CHNS-932, Leco Corporation). Furthermore, morphologic traits of cells grown during the first experiment were investigated upon harvesting. The remaining flask was maintained and monitored by daily cell counts (n = 6) and OD measurements (n = 3) until cell concentration was stagnating (stationary phase). At the end of the first experiment the absorption spectra of the single cultures was determined.

2.5 Analytical methods

N. oculata and *T. chuii* were centrifuged at 3,000×*g* for 10 and 5 min, respectively. Pellets for elementary analysis, protein, total lipid and fatty acids analyses were freeze dried and stored at room temperature for further analysis. Furthermore, remaining moisture and ash content in the dry biomass was determined. Therefore ~10 mg of biomass was filled in a ceramic crucible and dried at 105°C for 24 h to obtain the dry weight (DW). Weight difference between initial biomass and DW represented the moisture content in the samples. Subsequently the DW was burned at 560 °C for 8 h and ash was weighed. The AFDW of the samples was calculated by subtracting the moisture weight and the ash weight (AW) from the initial biomass weight.

2.5.1 Proteins

Protein determination was carried out according to Lowry *et al.* [87] and modified according to Pomory [88]. A sample of 5-10 mg (DW) was suspended in 10 mL 1 M NaOH, vortexed and boiled at 100 ºC for 20 minutes in a heat bath. Upon centrifugation at 18,000×*g*, the supernatant containing the protein extract was transferred into a clean tube. An additional volume of 5 mL of 1 M NaOH was added to the pellet, vortexed and boiled again for 20

minutes in the heat bath. Subsequently the supernatant was added to the previous one. An aliquot of 0.5 mL of the extract was taken and mixed with 5 mL of a solution containing 0.5 g $CuSO_4 \bullet 5H_2O$ dissolved in 100 mL 1% sodium citrate ($C_6H_7NaO_7$), mixed in a proportion of 1:50 with 2% sodium carbonate (Na_2CO_3), vortexed and left for 10 minutes at 25 °C. In the following step 0.5 mL Folin-Ciocalteu's reagent ($C_{10}H_5NaO_5S$, mixed 1:1 with distilled water) was added and left for 120 minutes at 25 °C. The OD was measured spectrophotometrically at a wavelength of 750 nm (Genesys 10uv). Standard curve was done with different concentrations of bovine serum albumin (BSA) standard solution (0.5 mg mL^{-1}). The standard was done by dissolving 50 mg of albumin in 100 mL NaOH (1 M) and boiling for 20 min in a heat bath. Thereafter the standard solutions underwent the same procedure as the extracts. The standard curve used is given in Annex 4.

2.5.2 Total lipids

Total lipids were determined according to Bligh and Dyer [89]. A sample of 2-40 mg of freeze dried algal was transferred to test tubes and aliquots of 0.8 mL distilled water were added to soften the samples. Upon a 20-minute incubation period at room temperature, 2 mL of methanol and 1 mL of chloroform were added and algal cells were disrupted by a disperser (IKA Ultra-Turrax) in an ice bath for 60 s. Thereafter 1 mL of chloroform was added and homogenised for 30 s, followed by the addition of 1 mL of distilled water and homogenisation for another 30 s. Phase separation was performed by centrifuging at 3500×*g* for 8 minutes. Subsequently 1 mL of the bottom phase (extract), containing the chloroform and the lipids, was transferred into a new, pre-weighed tube. The extract was evaporated at 60 °C for at least 24 h followed by 3-h cooling-down step in a desiccator at room temperature. Finally lipids were determined gravimetrically.

2.5.3 Fatty acids

Fatty acids were determined as follows: approximately 30-40 mg of freeze dried algae were transferred into derivatisation vessels, 1.5 mL of a methanol/acetyl chloride (20:1) mix was added and homogenised with an IKA Ultra-Turrax disperser by means of two intervals of 60 and 30 s, respectively. Subsequently 1 mL *n*-hexane was added and vessels were incubated at 90°C in a water bath for 70 minutes. Samples were cooled down and 1 mL of distilled water as well as 4 mL of hexane were added and vortexed for 1 minute in order to transfer the fatty acid methyl esters from the polar (methanol/water) to the non-polar (*n*-hexane) phases. Phase separation was achieved by centrifugation at 2000×*g* for 5 minutes. The upper phase

(extract) was transferred to a glass tube and algal suspensions were washed twice with 4 mL hexane. Extracts were washed with sodium sulphate in order to remove moisture, undergoing filtration afterwards. Finally the hexane was evaporated under nitrogen atmosphere at 55°C and the remaining extract containing the fatty acid methyl esters (FAME) was transferred to a GC-flask for gas chromatography-mass spectrometry analysis at a later stage.

2.5.4 Biomass

Aliquots of algae were filtered by a previously heated (560°C), washed (ammonium bicarbonate) and weighed glass fibre filter (0.7 μm, Whatman filter). Subsequently the filter was washed twice with 20 mL of 0.5 M isotonic ammonium bicarbonate solution [90]. After drying for 24 h at 105°C, dry weight (DW) plus the filter weight was registered. Finally, the filter was incubated at 560°C for 8 h with subsequent ash weight (AW) determination. AFDW was calculated by subtracting AW from DW.

2.5.5 Nutrients

For nutrient analysis, the algae were separated from the medium by filtering (0.7 μm nominal pore glass fibre filter) and the filtrate was stored frozen (-20°C) until analysis. Nutrient determination were spectrophotometrically analysed using a Spectroquant Nova 60 (Merck Chemicals).

Dissolved phosphate-based phosphorous in the medium (RP; mg $P\text{-}PO_4^{3-}$ L^{-1}) was analyzed according to (Standard me American Public Health Association [91], method 4500-P E by using Merck-Chemicals test kit 1.17942.0001. Samples were brought into a sulphuric solution where PO_4^{3-} ions react with molybdate ions, forming molybdophosphoric acid. Then ascorbic acid reduces the molybdophosphoric acid to phosphomolybdenum blue as being determined spectrophotometrically.

Dissolved nitrate based nitrogen in the medium (mg $N\text{-}NO_3^-$ L^{-1}) determination was performed using a Spectroquant test kit (Cod. 1.14773.0001 (Merck; [92]). In this method, NO_3^- ions react with a benzoic acid derivative to form a red nitro compound that is determined spectrophotometrically in the presence of concentrated sulphuric acid (Spectroquant Nova 60, Merck Chemicals).

Dissolved ammonium based nitrogen in the medium (mg $N\text{-}NH_4^+$ L^{-1}) was analyzed according to American Public Health Association (1999), method 4500-NH3 D by using Merck-Chemicals test kit 1.14752.0001. For this analysis the pH of the sample was raised to form $N\text{-}NH_4^+$ into ammonia based nitrogen ($N\text{-}NH_3$). The $N\text{-}NH_3$ reacts with a chlorinating

agent to form monochloramine. Monochloramine forms then with thymol a blue indophenol derivate whose concentration can be determined spectrophotometrically.

2.5.6 Morphological traits

Cell cultures from the first experiment (single light treatments) were diluted to a cell concentration of ~1000 cells mL^{-1} and stored in seawater containing diluted formaldehyde (1% v/v). Sedimentation chambers with a volume of ~3 mL were filled with the cell suspension and cell length was determined by an inverse microscope connected to NIS-Element software version 4.1 (Nikon Cop.).

Additionally, cell surface area of each treatment was analysed from photos taken during length measurements (n = 20) via ImageJ software version 1.48 (Research Service Branch, NIH, Bethesda, MD). In order to quantify lengths and areas of algae, pictures of a calibration master plate containing a 1 mm long bar, subdivided in 10 µm steps (Graticules Ltd.) were taken to calibrate the software for each lens. Software calibration was implemented by setting the pixels in photographs from algae in relation to amount of pixels representing a known distance obtained by the master plate under different magnifications.

Additionally, according to Pereira *et al.* [93], a more detailed analysis of the cell cycle and lipid distribution within cells was acquired in a Zeiss AXIOMAGER Z2 microscope, connected with a coollSNApHQ2 camera and AxioVision software version 4.8 (Carl Zeiss MicroImaging GmbH, Göttingen, Germany) using a 100 × objective lens. Lipids were visualized using BODIPY (4,4-difluoro-1,3,5,7-tetramethyl-4-bora-3a,4adiaza-*s*-indacene) according to Cooper *et al.* [94]. Therefore a first stock solution of BODIPY (5 mM) in DMSO was prepared. This first stock solution was diluted 1:50 with distilled water, obtaining a second stock solution with a final concentration of 100 µM and 2% DMSO. Finally, the preserved algae in formaldehyde (see above) were diluted 1:10 with the second stock solution resulting in a final concentration of 0.2 % DMSO and 10 µM BODIPY in the algal suspension. Obtained images of fluorescence and algae were combined and further improved with ImageJ software version 1.48 (Research Service Branch, NIH, Bethesda, MD).

2.5.7 Absorption spectra

Qualitative absorption spectra were determined by the on-filter absorption method according to Mueller and Fargion [95], using glass fibre filters (Millipore 1502500; pore size = 1 µm). Briefly, cultures were filtered and the filters holding the wet algae were transferred to a microscope slide containing a drop of filtered seawater (pore size: 1 µm) in order to avoid

the formation of air bubbles between the microscope slide and the filter. The microscope slide with the fixed filter was carefully placed into a spectrophotometer (Jenway 7315) and the absorption was measured using 1-nm steps from 380 to 750 nm. As blank, the absorption spectrum of a filter containing only filtered seawater was used. To observe variations in absorption spectra due to changing biomass concentrations on the filter, spectra of different filtered volumes from FL treated cultures were determined. Since the baseline noise of the blank filter without algae was higher than OD = 0.005 [95] (see Annex 5), absorption spectra were corrected by subtracting the noise from the OD (λ) as proposed elsewhere [95]. Obtained spectra were normalized at 750 nm. Effects of filter scattering were compensated by light-path amplification according to Cleveland and Weidemann [96] (eq. 2):

$$OD_{corrected}(\lambda) = 0.378\ OD_{observed}\ (\lambda) + 0.523\ OD_{observed}\ (\lambda)^2 \quad (2)$$

Finally, to compare absorption spectra between species as well as light treatments, the measured absorption between 380 and 750 nm was integrated in 1-nm steps and the obtained area was normalized to 100.

2.6 Data treatment

2.6.1 Growth model

To model microalgal growth kinetics, experimental data based on cell counts and AFDW determination were adjusted to the Verhulst logistic kinetic model [97], which describes microbial growth as sinusoidal pattern (eq. 3) as a mathematical derivation of the time.

$$\frac{dx(t)}{dt} = \mu_{AFDW,cell}\ x(t)\left(1 - \frac{x(t)}{x_m}\right) \quad (3)$$

where $\mu_{AFDW,\ cell}$ represents the maximal growth rate of AFDW and cell count based data, *x(t)* the concentration of either AFDW or cell numbers at a certain time point *t* and x_m the maximal concentration in the medium of AFDW or cells. Integration of eq. 3 leads to eq. (4 in which the maximal specific growth rate (μ), initial concentration (x_0) and x_m were estimated by fitting *x*(*t*) data to the corresponding kinetic models, minimizing the sum of squared residuals via iteration using the Microsoft Excel Solver tool [98]. This tool employs a non-linear programming algorithm called GRG2, an implementation of the generalized reduced gradient

algorithm [99]. The fitting parameters used were: Precision[4] 1 × 10^{-5} Tolerance[5] = 5; Convergence[6] = 1 × 10^{-4}.

$$x(t) = \frac{x_0 \times x_m \times e^{\mu_{AFDW,cell} * t}}{x_m - x_0 + x_0 \times e^{\mu_{AFDW,cell} * t}} \quad (4)$$

where $x(t)$, x_0, x_m, and $\mu_{AFDW,cell}$ correspond to the concentration of either AFDW or cell numbers at a certain time point t, initial concentration, the maximal concentration in the medium of AFDW or cells and growth rate expressed as AFDW or cells, respectively.

The estimated minimal and maximal cell concentration (x_m and x_0) from equation 4 was then used to determine the productivity (P; mg AFDW or cell L^{-1} d^{-1}) according to eq. (5 [98]:

$$P_{batch,AFDW,cell} = \frac{0.9 \times x_m - 1.1 \times x_0}{t_{(0.9\,x_m)} - t_{(1.1\,x_0)}} \quad (5)$$

Equation 5 minimizes effects of varying lag and stationary phases on the production rate of algae by considering only the time, space and concentration differences at which the lag and exponential phases ended—i.e. the time points when biomass or cell concentration increased by 10% from the initial values, $t_{(1.1\,x_0)}$ and the time point when 90% of maximal concentration was reached, $t_{(0.9\,x_m)}$, respectively. For further details regarding the growth model see Ruiz *et al.* [98].

In order to apply the data from AFDW and cell count determination to the model, for each time point the obtained data were sorted according to size. Data modelling was carried out with data of the lower, middle and the higher limit of each time point and treatment (three modelling steps per treatment). Sample size for *N. oculata* and *T. chuii* and each modelling

[4] Precision is an optional variable in Solver, which can vary between zero and one. It specifies the precision with which constraints must be satisfied. The relationship between the cell reference and the constraint value cannot be violated by more than the value set. The smaller the precision value is, the higher the precision.

[5] The tolerance can be set by decimal number between zero and 100, specifying the Integer Optimality percentage tolerance. It specifies that Solver can stop if it has found a feasible integer solution whose objective is within this percentage of the best known boundary of the objective of the true integer optimal solution. A larger percentage tolerance would tend to speed up the solution process.

[6] The convergence represents an optional variable in Solver. It is a number between zero and one specifying the convergence tolerance. In the GRG2 method used by Solver, a relative change in the target cell value lower than this tolerance leads to an interruption after five iterations.

step corresponded to 18 and 16 cell count determinations as well as 9 and 8 AFDW determinations, respectively. Total sample size was derived from 54 and 48 cell count determinations and 27 and 24 AFDW determinations per treatment for *N. oculata* and *T. chuii*, respectively. Obtained growth parameters were treated according to section 2.6.4.
In order to draw conclusions about the application of given light qualities in continuously cultures, AFDW-based growth rate and maximal production data were applied to a further model proposed by Ruiz et al [100].

$$P_{cont,AFDW} = x_{AFDW}\ (\theta^{-1} - \frac{1}{\mu_{AFDW}} * \theta^{-2}) \quad (6)$$

where $P_{cont,AFDW}$ represents the production rate expressed as AFDW in a continuously culture, x_{AFDW} the maximal AFDW concentration under batch conditions and θ correspond to the hydraulic retention time (HRT).

Since the production rate in a continuously culture is maximal if the HRT equals 2 μ^{-1} [100], HRT in eq. 6 can be substituted, resulting in eq. 7:

$$P_{cont,AFDW} = \frac{x_{AFDW} * \mu_{AFDW}}{4} \quad (7)$$

2.6.2 Nitrogen consumption

Based on the assumption that nutrient consumption and microbial growth (microalgae) occur in an autocatalytic behaviour, Ruiz *et al.* [98] developed a function for the nutrient concentration in the medium dependent on time (S(t)) (eq. 8):

$$S(t) = \frac{\left(\frac{X_0}{Y_0} + S_0\right)(S_0 - S_{na}) - S_{na}(S_0 - \left(\frac{X_0}{Y_0} + S_0\right))e^{\mu_n t}}{(S_0 - S_{na}) - (S_0 - \left(\frac{X_0}{Y_0} + S_0\right))e^{\mu_n t}} \quad (8)$$

Parameter S(t) and (X_0) are the experimental data from the dissolved nitrogen concentration at a certain time point *t* and initial biomass concentration obtained by eq. (4, respectively. The nitrogen content of the biomass used for inoculation Y_0 (mg N mg DW^{-1}), initial dissolved nitrogen concentration S_0 (mg N-NO_3^- L^{-1}), dissolved nitrogen concentration unassimilated in form of NO_3^- S_{na} (mg N-NO_3^- L^{-1}) and nitrogen based maximal specific growth rate of the microalgae μ_n (d^{-1}) were solved iteratively. In order to maintain reliable

results restrictions were applied whereas the S_{na} value should be greater or equal to 0 and Y_0 between 0.01 to 0.1 mg N·mg DW^{-1} [101].

2.6.3 Approximate photosynthetic efficiency

The approximate photosynthetic efficiency until t = 120 h and t = 96 h for *N. oculata* and *T. chuii* was determined according to Pilon *et al.* [24] by using for all treatments the same volume (V = 0.7 L) and area (A = 157 cm^2), regardless of the reduction of volume and area due to sampling during the experiment. The energy applied to the PBR by light was calculated according to eq. 9 and 10. First, the higher energy value (HHV; KJ g^{-1}) was calculated by applying data from the element analysis to eq. 9 [102]:

$$HHV = -3.393 + 0.507[\%C] - 0.341[\%H] + 0.067[\%N] \quad (9)$$

where %C, %H and %N represent the percentage of carbon, hydrogen and nitrogen in DW, respectively.

The output energy (E_{out}; KJ) was calculated as follows:

$$E_{out} = HHV * DW(t_{harvest}) * V \quad (10)$$

where $DW(t_{harvest})$ is the dry weight at the time of biomass harvesting and V the reactor volume (0.7 L). By introducing the Avogadro's number (N_A = 6.02 × 10^{23} mol^{-1}) to eq. 1 the energy (KJ) of 1 mole of photons ($E_{1mol\ photons}$) that is released by the light sources within the photosynthetically active range (400-700 nm) was calculated (eq. 11):

$$E_{1mol\ photons} = \int_{\lambda=400}^{\lambda=700} \frac{h * c * N_A}{\lambda} \quad (11)$$

where h represents the Max Planck constant (6.626 x 10^{-34}J s^{-1}), *c* the speed of light (299,792,458 m s^{-1}) and λ = wavelength of light (m).

The optical energy in KJ applied to the algae (E_{in}) for each light condition (PPFD: 100 µmol s^{-1} m^{-2}; reactor surface area 157 cm^2) was calculated according to equation 12:

$$E_{in} = \frac{E_{1mol\ photons} * 100\ \mu mol\ photons * t_{harverst} * 0{,}0157\ m^2}{10^6 * s * m^2} \quad (12)$$

Finally, the energy usage or rather photosynthetic efficiency (Φ) in % was calculated as follows:

$$\Phi = 100 * \frac{E_{out}}{E_{in}} \quad (13)$$

where the output energy (E_{out}) and input energy (E_{out}) was calculated according to eq. 10 and 12, respectively.

CO_2 fixation F_{CO_2} was calculated based on the carbon content in biomass (%C), the produced DW at time point of harvest as well as the stoichiometric relation between C and CO_2 (44/12) [14]:

$$F_{CO_2} = \frac{DW(t_{harvest}) * \%C * 44g\ CO_2}{12g\ C} \quad (14)$$

2.6.4 Statistical analysis

Data analyses were done with Excel and GraphPad Prism 5 programmes. The data were evaluated by one-way ANOVA with Tukey's multiple comparison tests. Linea relationships were tested via two-tailored Perlson´s test. Qualitative data for the determination of fatty acid profile determination were normalized using arcsine transformation before carrying out statistical data analysis. Significant level for all tests was $p < 0.05$.

3 Results

3.1 Growth parameters and modelling

The following section presents the growth parameters $P_{AFDW\&cell}$, $\mu_{AFDW\&cell}$ and $X_{AFDW\&cell}$ of all experiments carried out in this study. The applied growth model had the purpose of normalizing the calculation of the growth parameters without being influenced by the duration of lag phases or initiation of stationary phases. The estimated parameters are thus a function of all data applied to the model of algal growth used in this study. To obtain triplicates of growth parameters for statistical analysis, for each time point, the data were sorted by size and applied three times in sequence to the model, each time with the lowest, medium and highest values (three data modelling). More specifically, for each day, only two cell count determinations and one biomass estimate were applied to the model, maintaining always $R^2 \geq 0.91$. Representative cell growth curves and the three modelling steps are depicted in Fig. 3.1-1. The obtained cell growth parameters obtained by modelling are given in Tables A.6-1 and A.6-2 in Annex 6 for *N. oculata* and *T. chuii*, respectively. Original growth curves expressed as AFDW and cell counts are provided in Fig. A.7-6 in Annex 7.

In all experiments, *N. oculata* and *T. chuii* showed, during the first 24 h, a very short lag phase, followed by an exponential phase ending at time point t = 120 h and t = 96 h, respectively. At this time point, two out of three flasks were harvested for (biochemical) analysis. When cell concentration plateaued, indicating the beginning of stationary phase, the experiment ended and the remaining cultures were analysed for the time points t = 196 h and t = 168 h for *N. oculata* and *T. chuii*, respectively.

AFDW was measured at t = 0 and at time points shown by arrows in Fig. 3.1-1. For *N. oculata* and *T. chuii* the AW content was 5.59±2.69 and 4.98±1.75% of DW, respectively. AFDW was used mainly to monitor growth, since sample volume was limited. Sampling on the harvesting day was carried out in order to calculate photosynthetic efficiency and CO_2 capture. Upon plotting AFDW against the OD of the same time points (n = 64 and n = 52 for *N. oculata* and *T. chuii*, respectively), a linear correlation between the two values was found (Fig.3.1-2). Because the Pearson's correlation was always $r \geq 0.97$ ($p < 0.01$) and the data included values of different experiments, time points and light treatments, this correlation was considered to be universally valid for each alga. However, as the number of AFDW

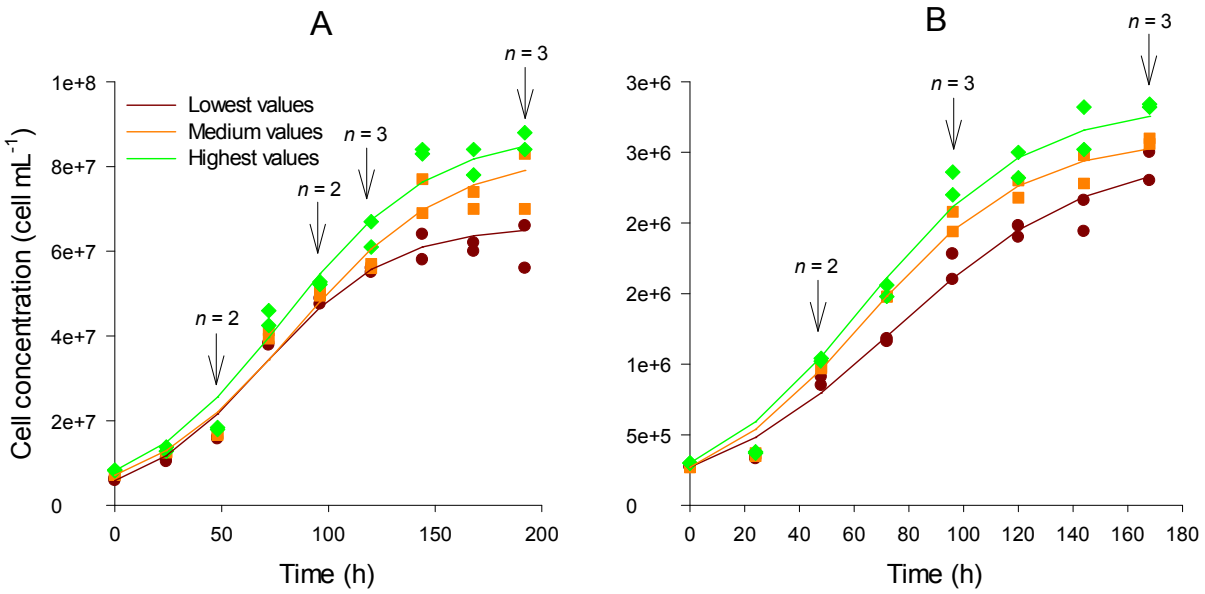

Figure 3.1-1 Verhulst model (eq. 4) applied to growth curves for *N. oculata* (A) and *T. chuii* (B) under FL treatment. Replicates of cell counts (n = 6) were sorted by size in three pairs and model (solid lines) was applied to the lowest (circles), medium (squares) and highest pairs (diamonds). Averaged results from the data modelling are given in Tables A.6-1 and A.6-2. Arrows indicate time points and number (n) of AFDW determinations.

determinations per treatment were low (n = 13 and n = 12 for *N. oculata* and *T. chuii*, respectively), the OD was used to predict the AFDW data being applied to the growth model (see Tables A.6-1 and A.6-2) on a daily basis according to eq. 15 and 16 obtained by the regression line in Fig. 3.1-2A and B.

$$AFDW_{N.oculata} = (0.3498 \pm 0.0099)\, OD + (0.0377 \pm 0.0111) \quad (15)$$

$$AFDW_{T.chuii} = (0.8999 \pm 0.0317)\, OD - (0.0382 \pm 0.0201) \quad (16)$$

There was also a correlation between cell concentration and OD (n = 117 and n = 104 for *N. oculata* and *T. chuii*, respectively). However, in this case, cell counts rather than OD values were used for modelling, as sufficient determinations were performed for the three modelling steps and the residual plot showed a remarkable increase of variance with OD for *T. chuii* (data not shown).

To test data replicability across Experiments 1, 2 and 3 (see 2.3 for details), growth parameters of cultures under light treatments used as reference (FL(1), FL(2) and FL(3), respectively) were compared and were found to be statistically different. In

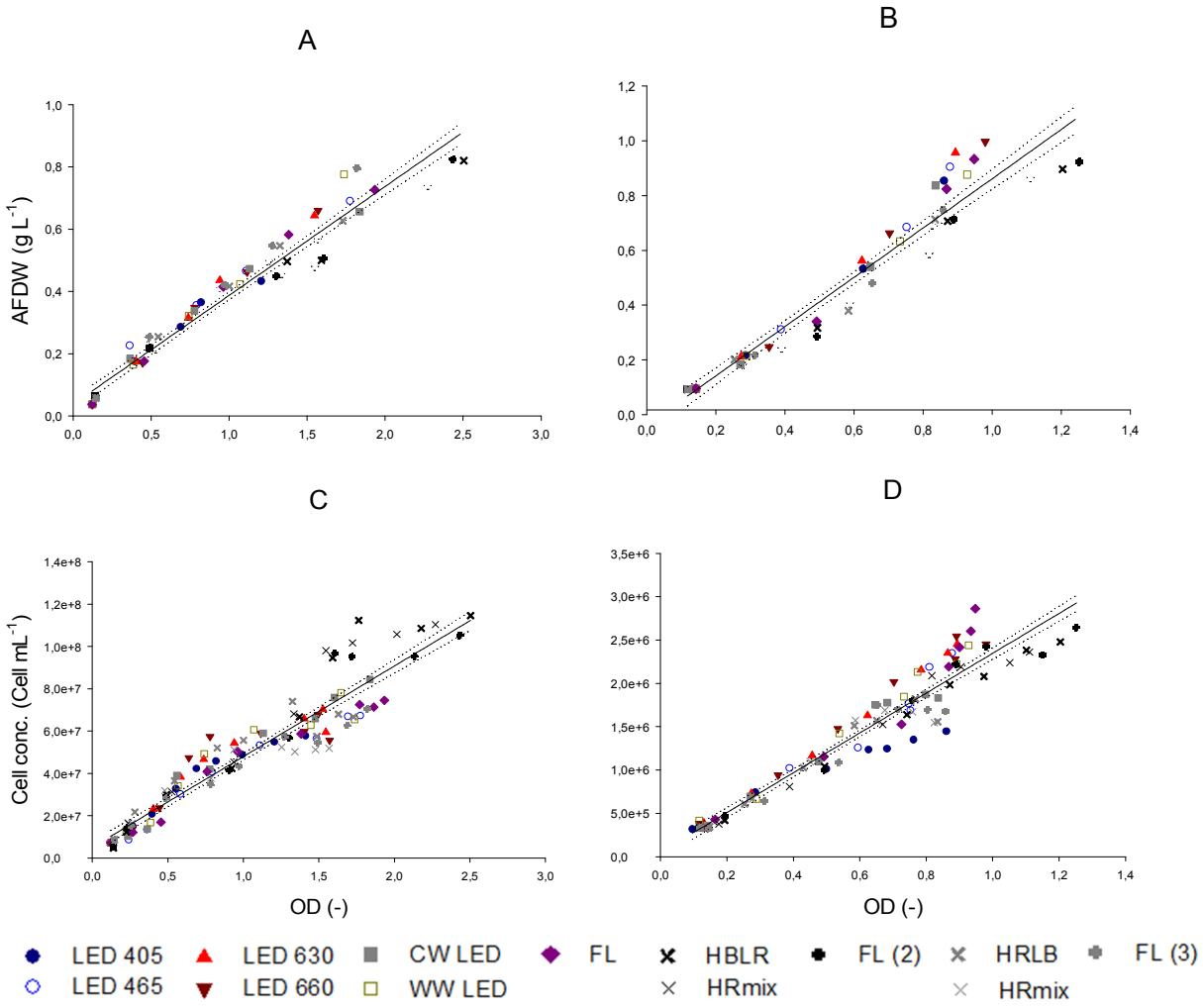

Figure 3.1-2 Linear relationship between OD and AFDW (top) and OD and cell concentration (bottom) for *N. oculata* (A and C) and *T. chuii* (B and D). Equation for the correlation between OD and AFDW with confidence 95% band (dotted line) was for *N. oculata* and *T. chuii* AFDW = (0.3498±0.0099) OD + (0.0377±0.0111) (R^2 = 0.95 and r = 0.98) and AFDW = (0.8999±0.0317) OD - (0.0382±0.0201) (R^2 = 0.9414 and r = 0.97), respectively. Equation of the correlation between OD and cell counts was for *N. oculata* and *T. chuii* Cell conc.= (4.281 ± 0.136) × 10^6 OD + (5.124 ± 1.581) × 10^6 (R^2 = 0.90 r = 0.95) and Cell conc. = (2.299±0.062) × 10^6 OD + (3379±50397) (R^2 = 0.93 and r = 0.97).

Experiment 3, FL-treated cells (FL(3)) showed the highest productivity and maximal biomass (AFDW) and cell concentration compared to the cells under the same light treatment in Experiments 1 and 2 (Tables A.6-1 and A.6-2). These differences could have been induced by dissimilar inoculum strengths, CO_2 flow rates or other factors. However, these differences seemed to have been negligible among treatments within the same experiment. Hence, in order to compare light treatments between experiments and treatments, a normalization of the quantitative data from Tables A.6-1 and A.6-2 was done by setting all results and parameters as relative values to the ones obtained with the FL treatments. The relative growth data derived from AFDW- and cell count-based data modelling are given in Fig. 3.1-3 and 3.1-4, respectively.

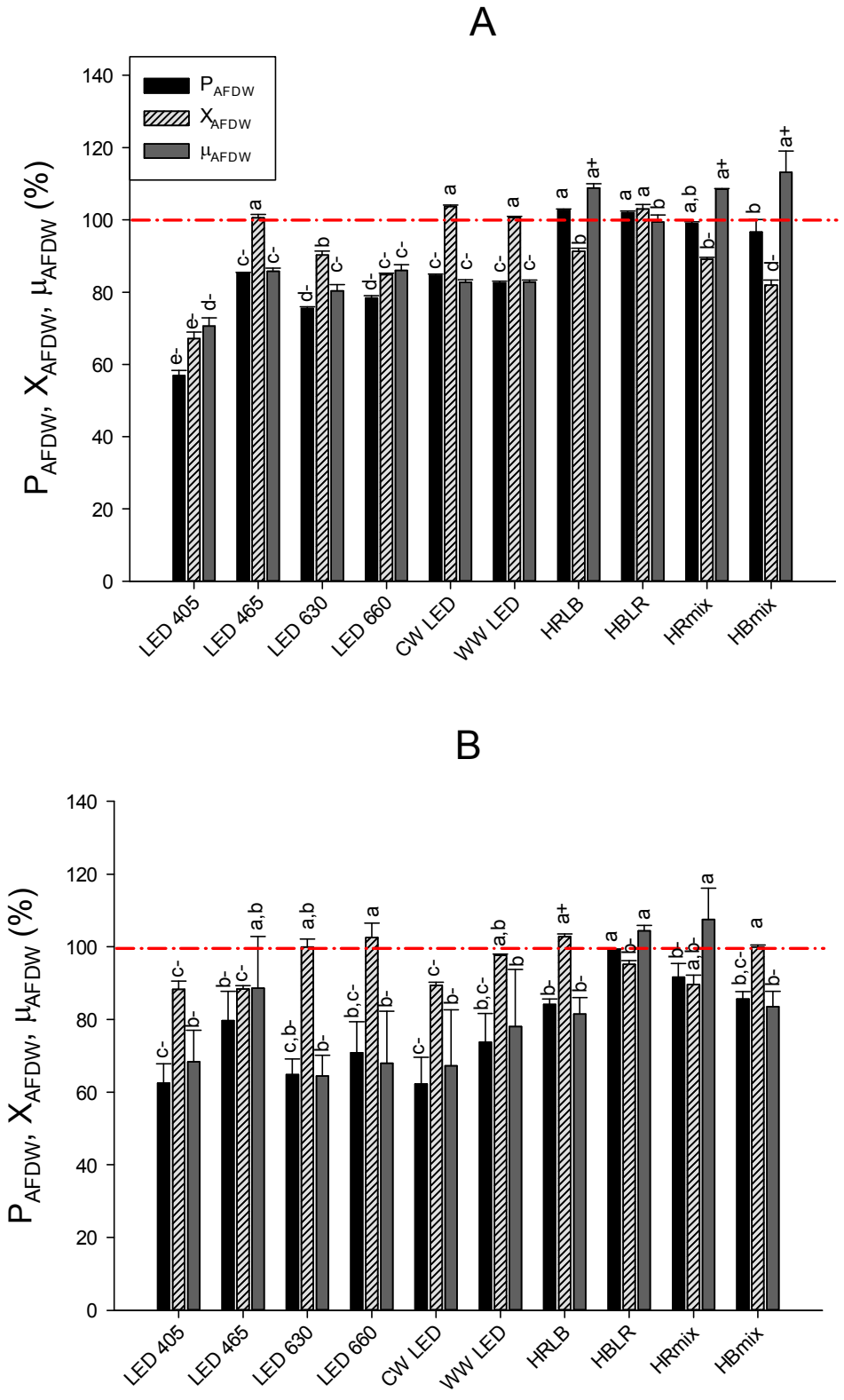

Figure 3.1-3 Normalized AFDW-based growth parameters: productivity (P_{AFDW}), maximal concentration (X_{AFDW}) and growth rate (μ_{AFDW}) for *N. oculata* (A) and *T. chuii* (B). Reference data (red dashed line) was obtained with cells growing under FL. Statistical differences ($p < 0.05$) within AFDW productivity (black bar, left), maximal AFDW concentration (light grey bar, middle) and AFDW-based growth rate (dark grey bar, right) among light treatments are indicated by different letters. Statistically higher or lower values as compared to those of the reference (FL) cultures are given as + and - signed letters, respectively. Unsigned letters indicate no statistical differences were found between cells under a given light treatment and under FL (see also Table A.6-1 in Annex 6).

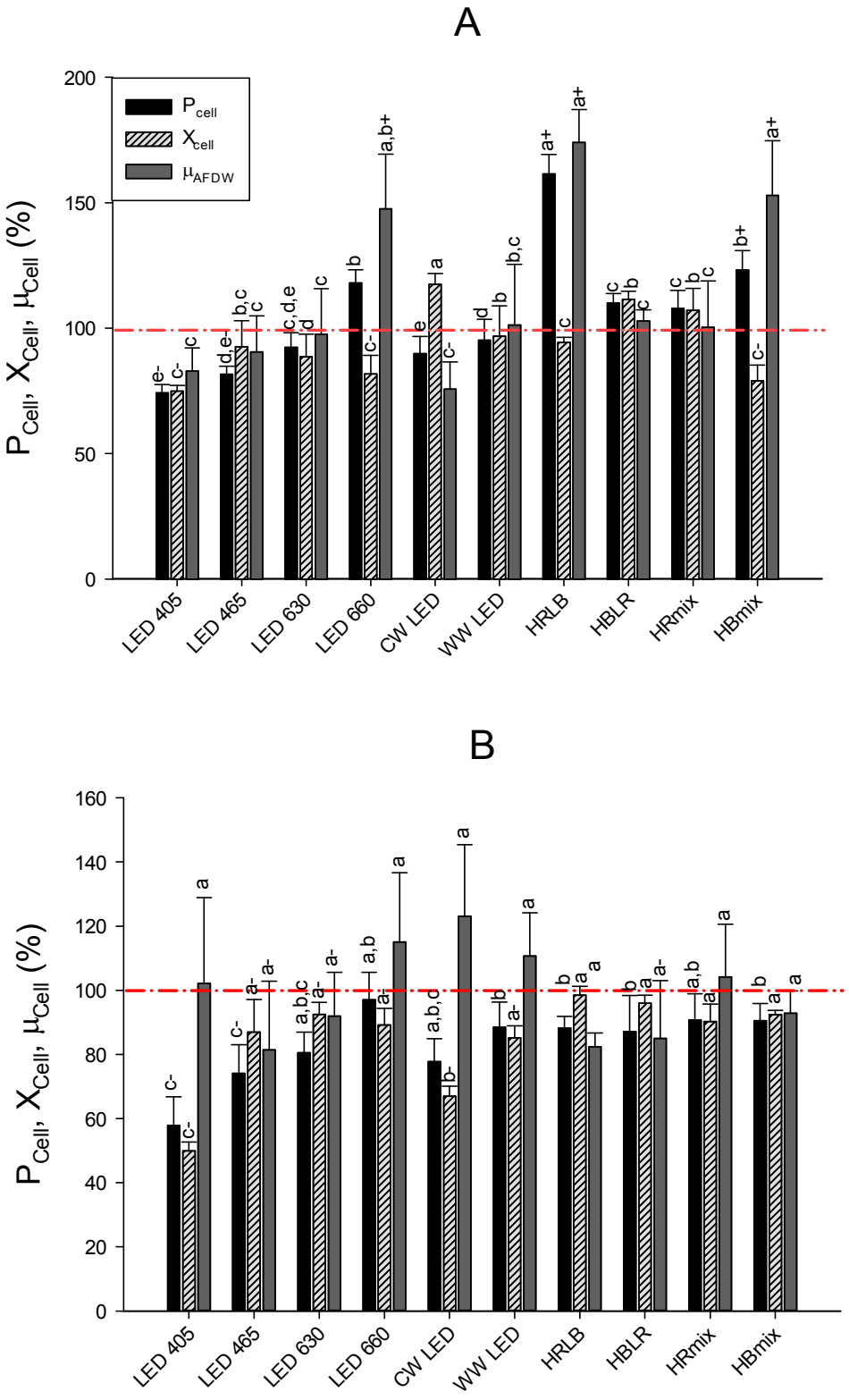

Figure 3.1-4 Normalized cell count-based growth parameters with data: productivity (P_{AFDW}), maximal concentration (X_{AFDW}) and growth rate (μ_{AFDW}) for *N. oculata* (A) and *T. chuii* (B). The reference data (red dashed line) was obtained with cells growing under FL. Statistical differences ($p < 0.05$) within cell productivity (black bar, left), maximal cell concentration (light grey bar, middle) and cell count-based growth rate (dark grey bar, right) among treatments are indicated by different letters. Statistically higher or lower values as compared to those of the reference (FL) cultures are given as + and - signed letters, respectively. Unsigned letters indicate no statistical differences were found between cells under a given light treatment and under FL (See also and A.6-2 in Annex 6).

When data are normalized one can observe that specifically designed lamps for photosynthesis used as reference (FL) and diverse LED light combinations, such as HBLR, HRLB, HBmix and HRmix, provide higher biomass growth parameters (P_{AFDW}, μ_{AFDW} and X_{AFDW}) for *N. oculata* and *T. chuii* as compared to non-optimal lamps such as CW LED or WW LED (Fig. 3.1-3). A high spectral matching of emission and absorption spectra (e.g., HRmix and HBmix) increased the biomass growth rate (μ_{AFDW}) of *N. oculata* compared to other treatments. Nevertheless, the final volumetric biomass concentration of algal cultures under the latter tailored light mixes decreased as compared to FL, HBLR and HRLB treatments. All AFDW-based growth parameters were similar between CW LED and WW LED treatments for *N. oculata* and *T. chuii* cultures (Fig. 3.1-3, Table A.6-1).

For both algae, cell count-based growth parameters (P_{cell}, μ_{cell} and X_{cell}; Fig. 3.1-4) tended always to be higher under light sources with high red content (e.g. LED 630, WW LED, FL, HRLB and HRmix treatments) and under those having considerable amounts of photons with a wavelength of 660 nm (HBLR or HBmix). More specifically, for *N. oculata*, highest cell productivity was obtained under the latter light sources (e.g. LED 660, FL, HRLB, HBLR, HRmix, HBmix), whereas *T. chuii* only showed significantly higher cell-based productivities under LED 660 and FL treatments (Table A.6-2 in Annex 6 and Fig. 3.1-4). *N. oculata* showed the highest cell-based growth rates under light sources with a high deep-red content (LED 660, HRLB) and under the tailored HBmix treatment (Fig. 3.1-4).

In general, AFDW productivity was lower in *N. oculata*, ranging between 60-122 mg L^{-1} d^{-1} (LED 405 in Exp. 1 and HBLR in Exp. 3, respectively) as compared to *T. chuii*, which varied between 136-220 mg L^{-1} d^{-1} (LED 405 and FL(1) in Exp. 1; see Table A.6-1, Annex 6). Growth rates of *N. oculata* (0.42-0.59 d^{-1}) were also lower compared to those of *T. chuii* (0.75-1.34 d^{-1}). Volumetric cell productivities were 0.99-1.98 × 10^7 and 3.08-5.47 × 10^5 cell L^{-1} d^{-1} for *N. oculata* and *T. chuii* cultures, respectively (Table A.6-2, Annex 6). The cell growth rate varied between 0.62-1.22 d^{-1} for both algae and the maximal cell concentration reached 5.57-11.84 × 10^7 and 1.44-2.88 × 10^6 cells L^{-1} for *N. oculata* and *T. chuii*, respectively. The observed differences in terms of cell count-based growth parameters between the two species are most probably due to the smaller cell size of *N. oculata* (see section 3.2).

AFDW productivity in a continuously operated culture was estimated using the maximal growth rate and maximal concentration obtained under batch conditions (Annex 8). Similarly to batch conditions, FL led always to one of the highest productivities among all treatments

and experiments. However, it is worth to mention that significantly higher biomass productivity under LED 465 light was obtained as compared to cultures under LED 630 and LED 660. For further information please refer to Annex 8.

3.2 Cell morphology and cell cycle

Among all cultures no contaminations were found. Both algae showed different morphologic changes among light treatments. The length of 200 algae per treatment was estimated according to Fig. 3.2-1. Since *T. chuii* cells were preserved for two weeks in formaldehyde and cell size changes could have occurred [103], an additional experiment was carried out for measuring the length of cells (n = 200) from the same culture before and after preservation. Comparing both types of samples, no statistical differences ($p > 0.05$) were found between average cell lengths before and after preservation: 12.17±1.77 and 12.33±1.19 µm, respectively.

The results of length and surface determinations as well as weights of *N. oculata* and *T. chuii* cells exposed to the different light treatments in the first experiment are given in Table 3.2-1. Further representative pictures of distinct cultures are pointed out in Fig. 3.2-2.

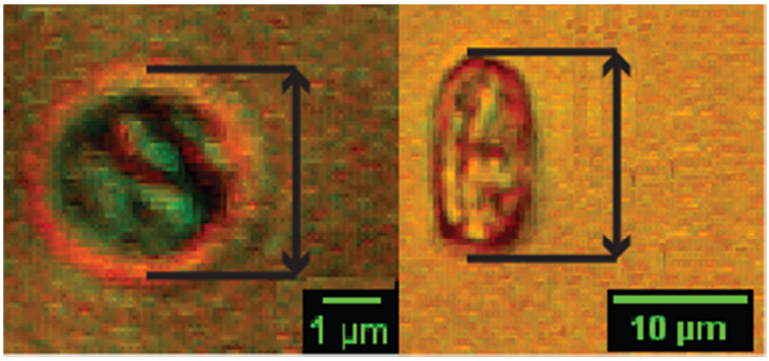

Figure 3.2-1 Illustration of cell length measurements. Left: *N. oculata*, right: *T. chuii*.

Table 3.2-1 Morphological cell parameter among all treatments from the first experiment. Different letters indicate statistical differences among treatments within each parameter.

N. oculata	**LED 405**	**LED 465**	**LED 630**	**LED 660**	**CW LED**	**WW LED**	**FL**
Cell surface area (μm^2)	7.52 ± 3.09 c	8.46 ± 3.27 b,c	8.06 ± 3.07 b,c	9.01 ± 3.51 b	9.12 ± 3.53 b	9.25 ± 3.43 b	10.50 ± 3.91 a
Cell weight (pg $cell^{-1}$)	6.13 ± 0.15 c	8.37 ± 0.29 a	6.54 ± 0.29 b,c	5.31 ± 0.12 d	7.56 ± 0.49 a,b	6.97 ± 0.52 b	8.00 ± 0,22 a,b
Cell length (µm)	3.18 ± 0.38 d	3.48 ± 0.44 c	3.36 ± 0.47 d	3.46 ± 0.44 b	3.64 ± 0.40 b	3.50 ± 0.37 b	3.91 ± 0.41 a
T. chuii							
Cell surface area (μm^2)	79.66 ± 3.84 b	70.73 ± 6f.02 c	76.24 ± 5.07 b	67.35 ± 4.58 c,d	66.94 ± 3.25 c,d	65.58 ± 5.17 d	102.57 ± 4,24 a
Cell weight (pg $cell^{-1}$)	444.1 ± 25.8 a	439.5 ± 6.4 a	328.7 ± 12.6 b	298.8 ± 29.1 b	326.7 ± 19.5 b	340.9 ± 25.0 b	409.4 ± 28,1 a
Cell length (µm)	12.04 ± 1.04 b	12.56 ± 1.01 a	12.49 ± 1.20 a	12.69 ± 1.25 a	11.36 ± 1.03 c	12.39 ± 1.12 a	12.60 ± 1,15 a

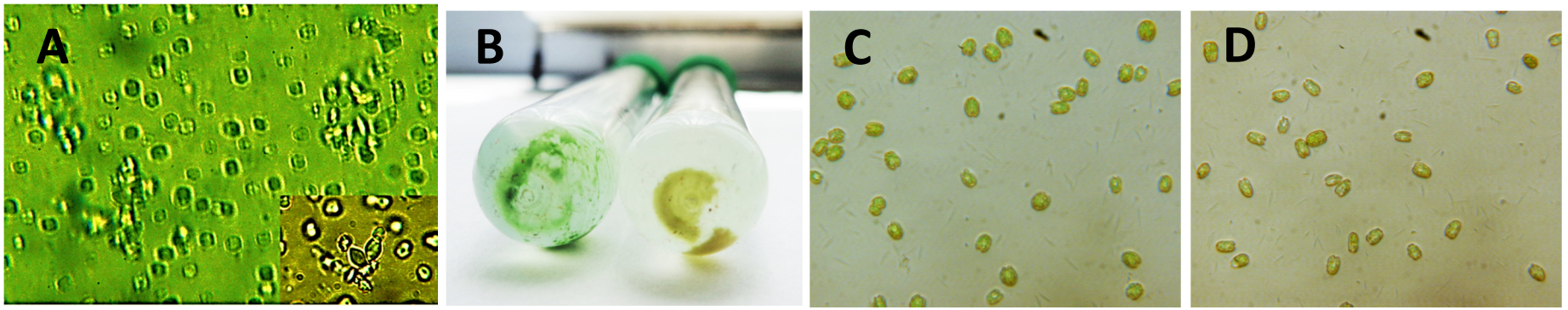

Figure 3.2-2 (A) *N. oculata* culture exposed to LED 660 treatment at t = 196 h. Inset image at the bottom right shows a more detailed cell aggregate. Cell walls of *N. oculata* can be observed within aggregates. (B) Colour difference between *N. oculata* cultures exposed to LED 405 (greenish colour; left test tube) and FL (yellowish colour; right test tube). (C) *T. chuii* cells under LED 405 assume often a coccoid shape, whereas cells exposed to LED 660 are usually more rod-like or cordiform (D).

The cell surface area among *N. oculata* treatments was highest under FL (32.34±5.46 μm^2) and up to 30% smaller at LED 405-treated algae. Cell weights were highest under FL and LED 465 and in average ~25 % smaller under LED 405 and LED 660 treatments. Cell length was again highest under FL treatment and lowest under LED 405 and LED 660 treatments. Cell length correlated significantly ($r = 0.95$, $p < 0.05$) with P_{AFDW} although the number of tested samples ($n = 7$) and R^2 (0.90) was low. Final visual observations at $t = 192$ h revealed that *N. oculata* cultures exposed to LED 630 and LED 660 developed many whitish aggregates containing cell wall debris and apparently intact cells (Fig. 3.2-2A). Cultures under LED 405 showed fewer aggregates compared to all other treatments. Furthermore, *N. oculata* cultures exposed to FL showed a fast colour shift from green to yellow, while LED 465-, LED 630-, LED 660-, CW LED- and WW LED-treated cultures showed the same shift but at a slower pace (see Annex 9, Fig. A.9-8). Cultures exposed to LED 405 remained green during the whole cultivation period (Fig. 3.2-2B).

T. chuii cells exposed to FL showed also the largest cell surface area (102.57±4.24 μm^2), followed by LED 405-, LED 630- and LED 465-treated algae. Cells exposed to LED 405 and LED 465 as well as FL were heaviest as compared to those under LED 630, LED 660, CW LED and WW LED treatments.

The longest cells were found under LED 465, LED 630, LED 660, WW LED, FL and shortest cells under LED 405 and CW LED. Thus, measurements of cellular length could not clearly distinguish cultures with larger or smaller cells among treatments, since the shape of cells changed significantly, while cell lengths changed only slightly (≤ 10%).

LED 405-, LED 465 and FL-treated *T. chuii* cultures were dominated by cells with a coccoid, compact shape with low motility and often with no flagella (Fig. 3.2-2C). On the other hand, cultures exposed to LED 630 and LED 660 (Fig. 3.2-2D) contained a larger amount of long, flagellated cells with high motility (Fig. 3.2-2D). *T. chuii* cultures illuminated with LED 630 and LED 660 showed the highest motility among all treatments, whereas lowest motility was found in cultures lit with LED 405 and LED 465. *T. chuii* cells exposed to CW LED and WW LED showed no clear trend between high or low motility.

Detailed microscopy observation allowed further distinction of cell shapes among cultures. With the assumption that the cell size of microalgae increases with cell cycle progression, as often reported [67, 104, 105], a cell cycle for *N. oculata* and *T. chuii* is proposed.

The cell cycle of *N. oculata* was reconstructed starting with (1) rod-shaped “daughter” cells, (2) larger rod-to-coccoid-shaped followed by a (3) coccoid-shaped cell and finally an

(4) even larger rod-to-coccoid-shaped “mother” cell. It appeared that the location and the amount of lipids changed with the progression of the cell cycle (Fig. 3.2-3). Notable is also an apparent splitting of the lipid body into two in the last stage (4), indicating an imminent cell division.

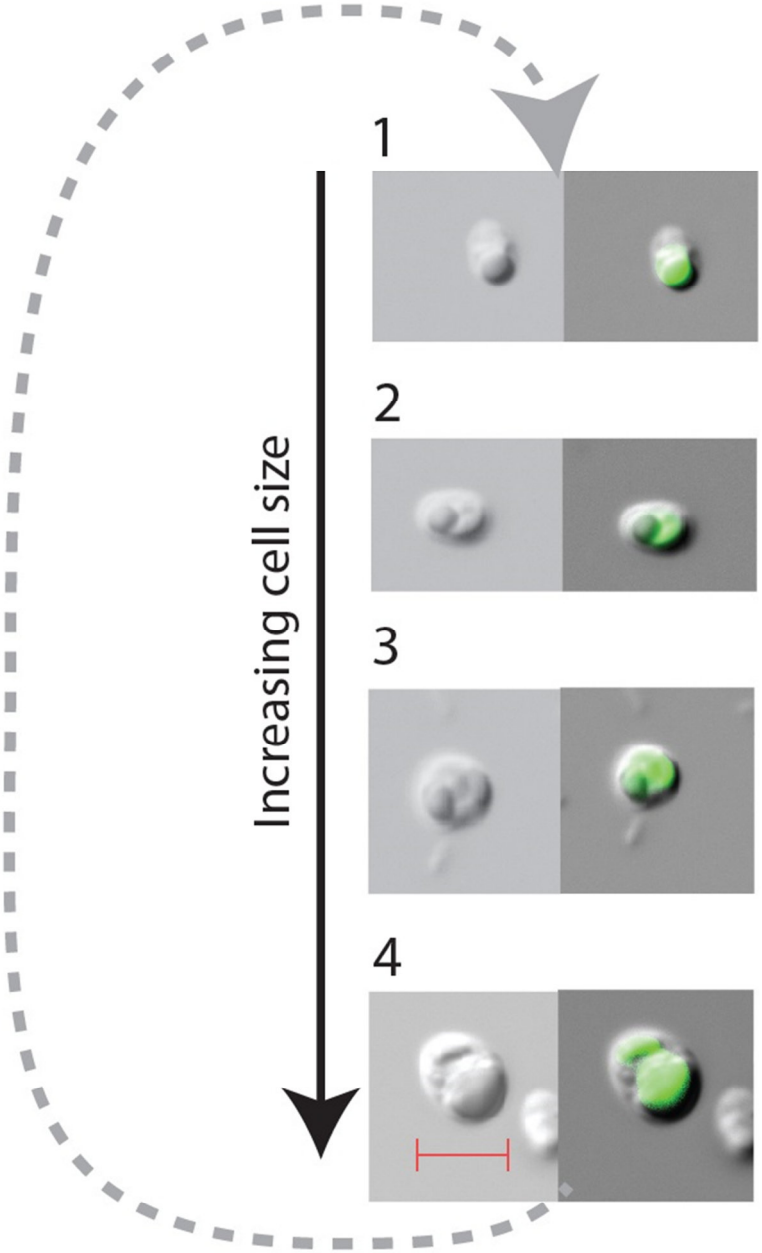

Figure 3.2-3 Proposed cell cycle of *N. oculata*. Cell size increases and lipid bodies accumulate as the cell cycle progresses. It starts with (1) rod-shaped daughter cells, (2) rod-to-coccoid-shaped cells, (3) coccoid-shaped cells and (4) larger rod-to-coccoid-shaped “mother” cells. The photographs on the left were taken by differential interference contrast (DIC), whereas photographs on the right show DIC merged with BODIPY 505/515 fluorescence (green), which indicates lipid distribution. Red bar represents 5 µm and is applicable to all photographs.

In contrast to *N. oculata*, the growth cycle of *Tetraselmis* cells (Fig. 3.2-4) seems to be more complex as cells undergo large morphologic changes during growth. In stage $1_{T.\ chuii}$, elliptical daughter cells were released by the mother cell ($6_{T.\ chuii}$). In stage $2_{T.\ chuii}$, matured cordiform daughter cells are formed followed by a morphologic switch into stage $3_{T.\ chuii}$, corresponding to flagellated cells with high motility and a clearly visible U-shaped chloroplast. Algae in stage $4_{T.\ chuii}$ had larger cells with apparently lower motility. In stage $5_{T.\ chuii}$ cells lose their flagella and cell division is initiated. In the subsequent stage $6_{T.\ chuii}$, cell division occurs and two coccoid daughter cells within the mother cell wall are formed.

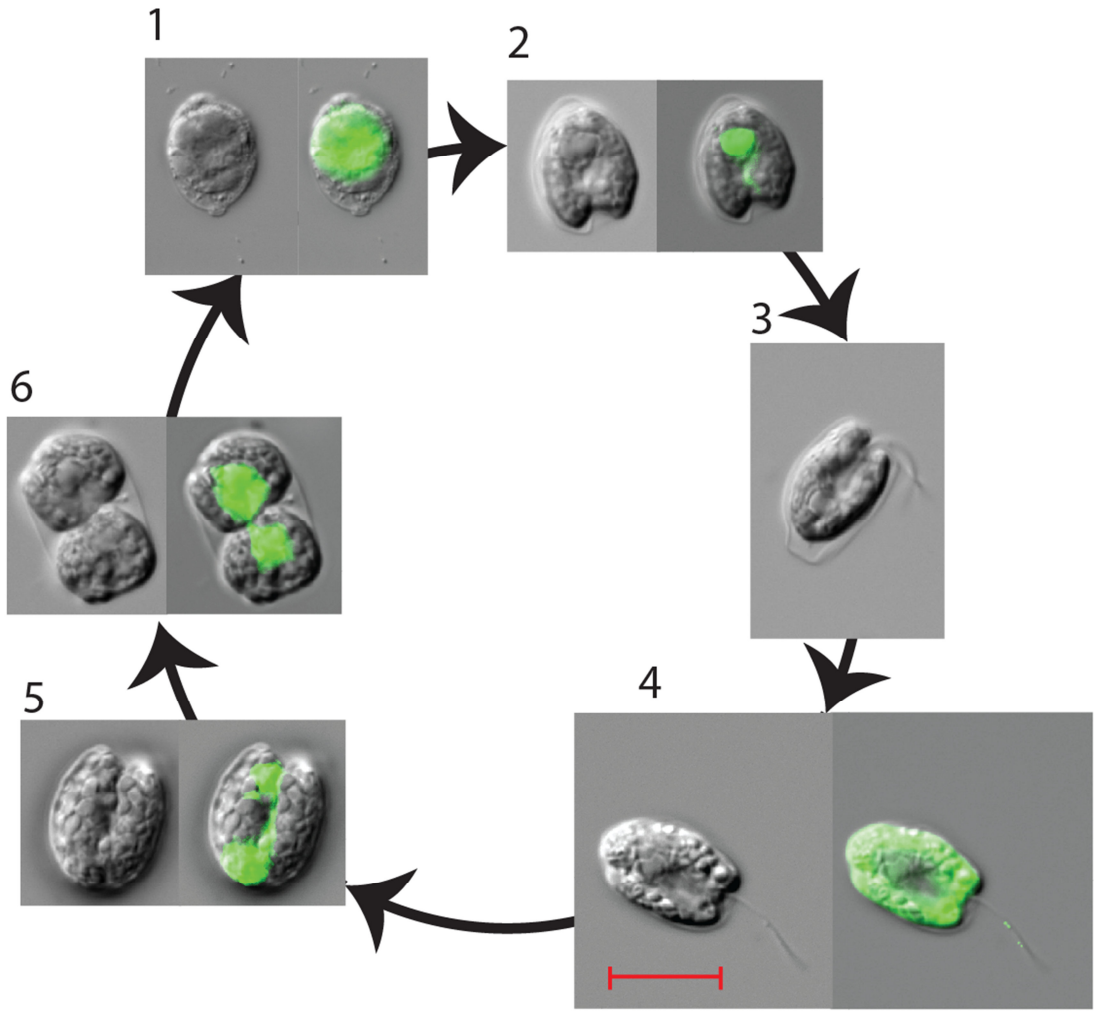

Figure 3.2-4 Proposed cell cycle for *T. chuii,* starting with the release of elliptical daughter cells (1), which transit into matured cordiform cells (2). In stage (3), small flagellated cells appear, increasing in size towards the next stage (4). Thereafter cells lose flagella (5) and cell division is initiated. In the subsequent stage (6), cell division occurs and two coccoid daughter cells within the mother cell wall are formed. The left photographs of cells were taken by differential interference contrast (DIC), whereas photographs on the right hand side show DIC merged with BODIPY 505/515 fluorescence (green), which indicates lipid distribution. A remarkable lipid relocation could be observed starting from stage 1 and 2, during which lipids apparently move to the cytoplasm, co-localizing again with the U-shaped chloroplast by stage 4. In stages 5 and 6 the lipid bodies move back towards the cytoplasm and are equally partitioned between the two daughter cells. Red bar represents 10 µm and is applicable to all photographs.

A remarkable lipid reallocation could be observed in the transition of stage $1_{T.\ chuii}$ to $2_{T.\ chuii}$ during which the lipid bodies seem to be excluded from the developing U-shaped chloroplast. Between stages $2_{T.\ chuii}$ and $4_{T.\ chuii}$ this exclusion process seems to revert, whereas between stage $5_{T.\ chuii}$ and $6_{T.\ chuii}$ the lipid bodies move back towards the cytoplasm before they start dividing into two sets of lipid bodies, one in each daughter cell.

3.3 Absorption spectra

The pigment composition varied between *N. oculata* and *T. chuii,* being mirrored by their absorption spectra (Fig. 3.3-1). Chlorophyll *a,* peaking at 440, 625 and 680 nm [106, 107] could be found in both species. However, *T. chuii* contained chlorophyll *b* peaking at ~650

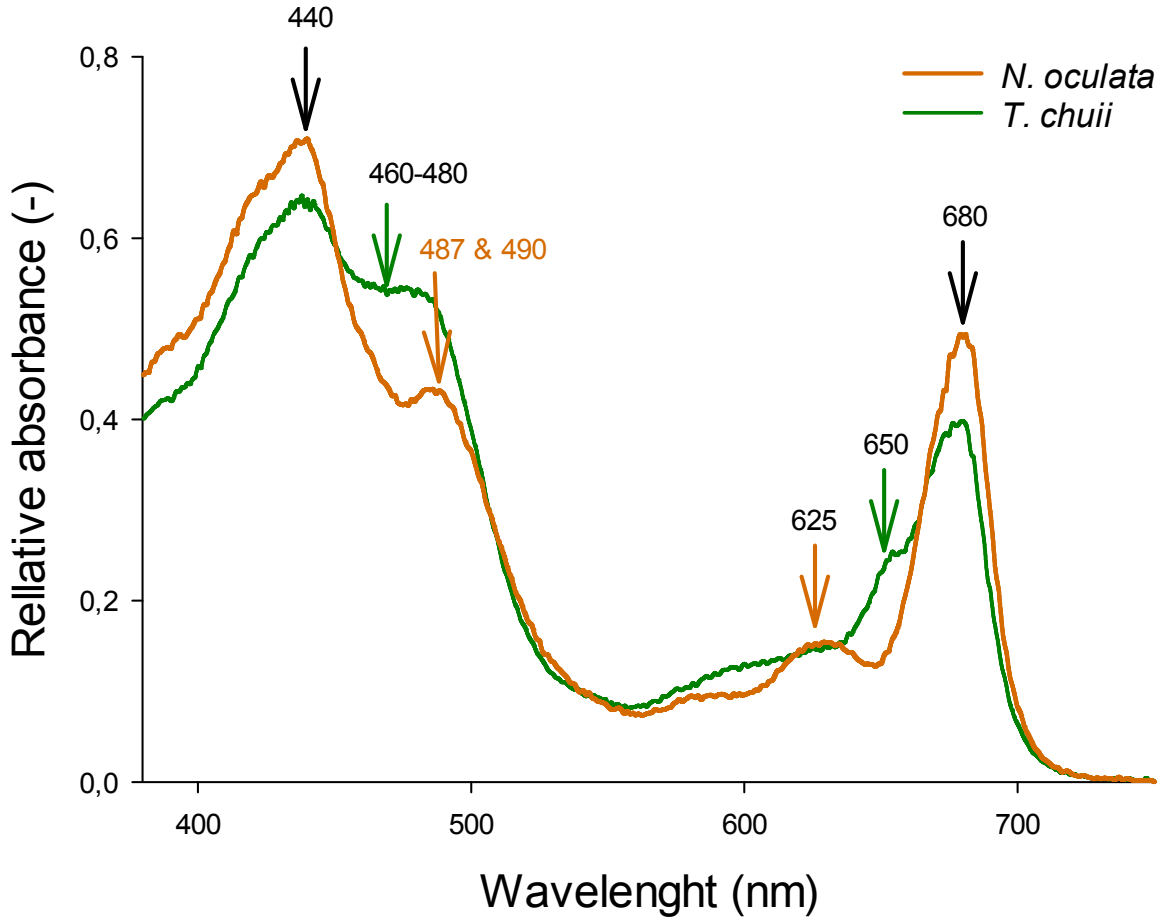

Figure 3.3-1 Comparison of absorption spectra between *N. oculata* and *T. chuii* whole cells. Arrows with wavelengths indicating the peaks of major pigments. Absorption spectra represent the average of five different dilutions measured in duplicates for each alga as given in Annex 5**.**

nm and 460-480 nm and thus, in contrast to *N. oculata*, had a higher absorption within these ranges. The peak of *N. oculata* from 487-490 nm can be related to antheraxanthin and violaxanthin pigments [24, 108]. Regarding distinctiveness of light absorption between both algae, *N. oculata* showed a higher absorption between 380 and 450 nm and 660-700 nm, whereas *T. chuii* absorbed more photons between 450 and 500 nm and 550-660 nm.

Absorption spectra of treatments with monochromatic light varied only slightly. Variation in the blue region was perhaps due to different algal concentrations on the filter and/or due to the filter itself (see Annex 5). Nevertheless, repeated measurements confirmed the observed different absorption spectral profiles of *N. oculata* exposed to LED 405 compared to other treatments (higher between 500-660 nm and lower between 390-490; Fig. 3.3-2A). The absorption spectra of *T. chuii* (Fig. 3.3-2B) did not show high variations among light treatments, probably due to shifts caused by different concentrations of algae on the filter. Nevertheless, CW LED and WW LED lights induced slightly higher absorption between 500-660 nm compared to other treatments. Visual observation confirmed that CW LED- and WW LED-lit cells had a more greenish tint when compared to cells under other light treatments. Interestingly, this chromatic shift appeared to be similar to that of *N. oculata* exposed to LED 405. However, the chromatic shift of *T. chuii* cultures exposed to different light qualities were less pronounced and were thus harder to establish.

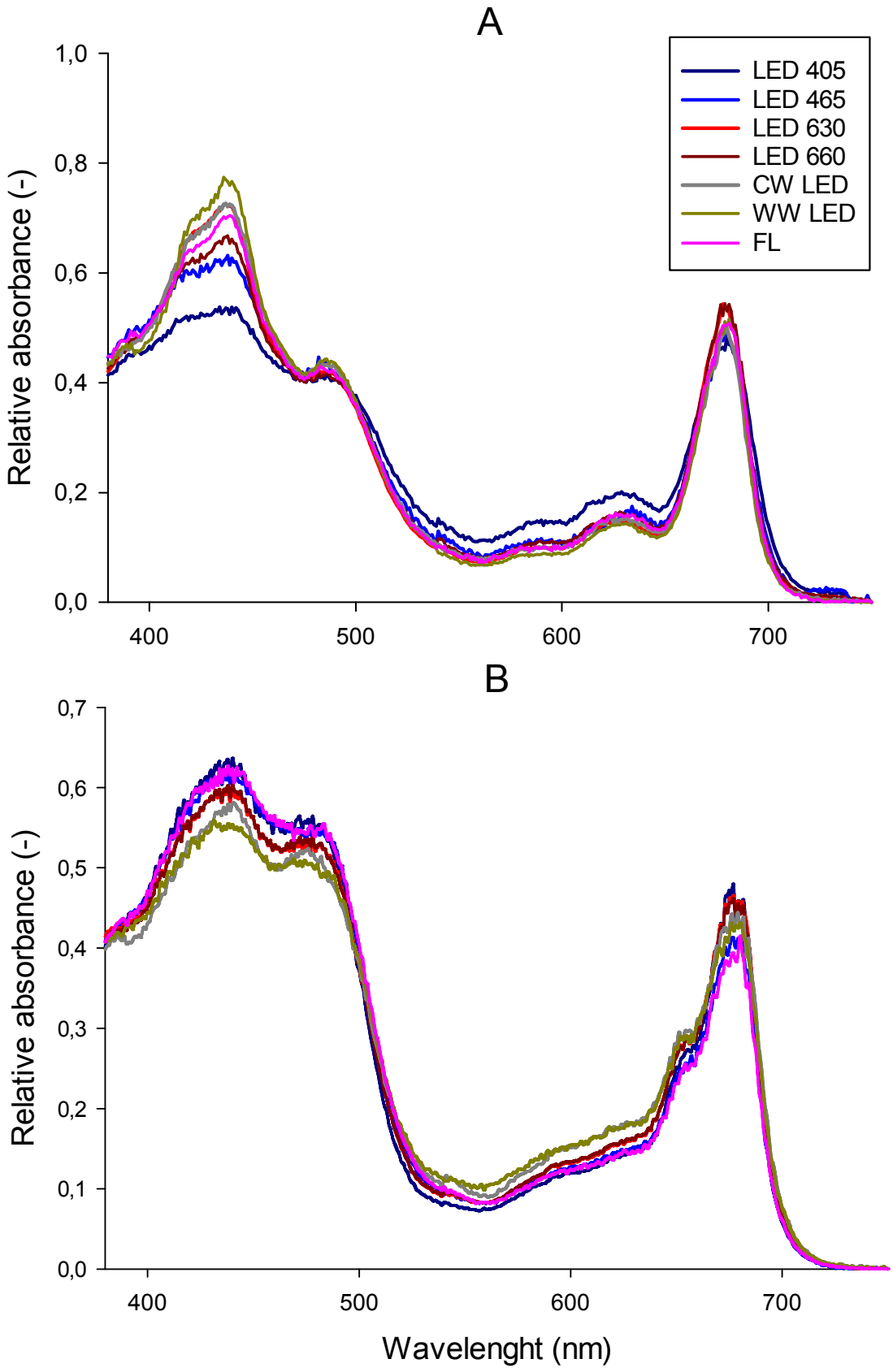

Figure 3.3-2 Absorption spectra of *N. oculata* (A) and *T. chuii* (B) culture at the end of the experiment. Each curve represents the average of two absorption spectra of the same sample.

3.4 Biochemical components

N. oculata cultures exposed to FL light showed highest total lipid content (48.4±0.9 % of AFDW) and lowest in LED 465-treated cultures (36.2±2.0 % of AFDW), although no statistical differences were found between the latter and other cultures under white LED light (CW, WW) and other monochromatic treatments (Fig. 3.4-1A). The highest protein content in *N. oculata* was found in cultures exposed to LED 405 (55.7±4.0 % of AFDW), whereas cells illuminated with FL showed the lowest values (30.6±2.2% of AFDW). Highest carbohydrate contents were found in LED 465-, LED 630- and LED 660-treated cultures (average: 27.2±2.3 % of AFDW, with no statistical differences among each other), and lowest under LED 405 (7.1±4.4 % of AFDW). Considering the aforementioned findings, a trend for a degradation of carbohydrates and an accumulation of proteins became obvious in cells under light sources containing wavelengths below 450 nm (LED 405, CW LED, WW LED and FL), whereas total lipids remained unaffected under these conditions.

T. chuii showed highest total lipid contents in LED 405- and CW LED-treated cultures (average: 23.4±0.6 % of AFDW). Significantly less total lipid content was found in algae grown under LED 465, LED 630, LED 660, WW LED and FL. Highest protein content in biomass was observed in *T. chuii* exposed to LED 405 and CW LED light (38.9±1.6 and 42.0±0.7 % of AFDW, respectively; $p < 0.05$). Remarkable low protein content was found in cultures exposed to LED 465, LED 630, LED 660 and WW LED, with the lowest value corresponding to FL-treated cultures (27.2±1.0% of AFDW). Carbohydrates were lowest under LED 405 and CW LED: 37.3±1.5 and 35.0±0.7 % of AFDW, respectively. Also cultures exposed to WW LED showed a statistically lower carbohydrate content than those exposed to LED 465, LED 630, LED 660 and FL. The highest carbohydrate content was found in FL-lit cultures (55.1±1.1 % of AFDW). In summary, *N. oculata* and *T. chuii* exposed to LED 405 and CW LED showed always lower carbohydrate contents as compared to cells illuminated with LED 465, LED 630 and LED 660.

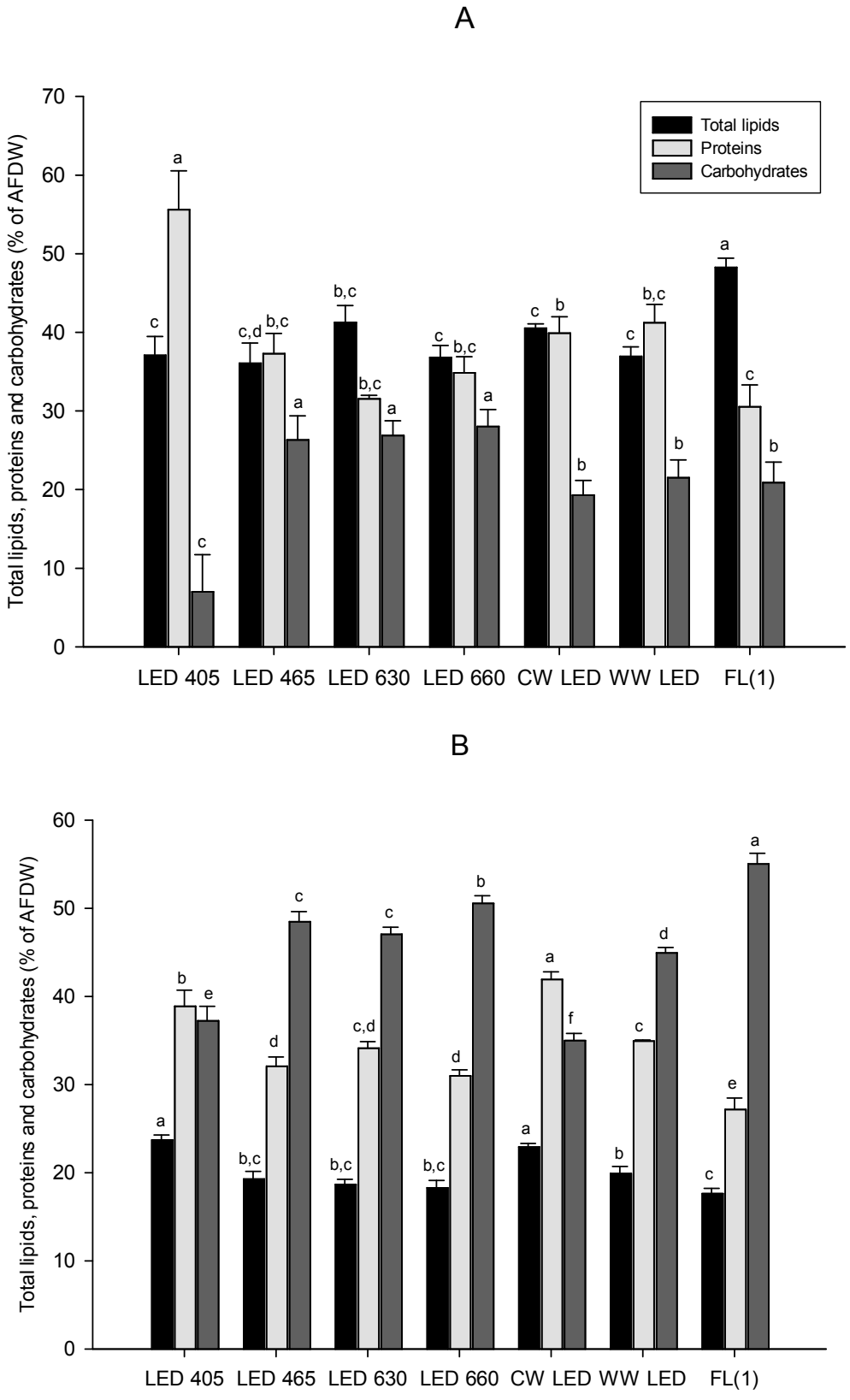

Figure 3.4-1 Biochemical composition in % of AFDW for *N. oculata* (A) and *T. chuii* (B). Statistical differences ($p < 0.05$) within contents of total lipid (black bar), protein (light grey bar) and carbohydrates (dark grey bar) are indicated by different letters.

The intracellular nitrogen content in the algae and the observed protein content in AFDW was used to calculate protein conversion factors for each treatment (Table 3.4-1). The carbon:nitrogen (C:N) ratios per treatment and per algal strain is shown in Table 3.4-1, as can be used to draw conclusions about the nitrogen distribution in the algae.

N. oculata showed the highest nitrogen-protein (N-prot) factor when exposed to LED 405, followed by CW LED and WW LED, whereas lowest factors were found under FL treatment. An inverse pattern could be observed in C:N ratios, being lowest in LED 405-treated cultures followed by those lit with CW LED and WW LED and highest when exposed to FL. LED 630 and LED 660 led also to relatively low N-prot factors and high C:N ratios. Similarly to LED 630 and 660, LED 465 contributed to a low N-prot factor. In contrast, the latter cells displayed C:N ratios similar to those under CW LED and WW LED.

The pattern mentioned above is reflected by a linear relationship between N-prot factor and C:N ratio in *N. oculata*, showing a R^2 among all treatments of 0.86 (r = 0.93; n = 7). If data from the LED 465 treatment is excluded, then an even better correlation (R^2 = 0.94, r = 0.97; n = 6) is found.

T. chuii showed highest N-prot factors in LED 405, 465, CW LED and WW LED treatments and lowest when exposed to LED 630, LED 660 and FL. C:N ratios were lowest under LED 405 and CW LED, LED 630 and highest under FL. Contrary to *N. oculata*, *T. chuii* showed no specific trend between N-prot factors and C:N ratios among treatments, and consequently no linear regression was found (R^2 = 0.15; r = 0.39; n = 7).

Table 3.4-1 Nitrogen-protein (N-prot) factors and carbon:nitrogen (C:N) ratios among different algae and treatments. Statistical differences are given with different letters in the same column.

Treatment	N-prot factors		C:N ratios	
	N. oculata	*T. chuii*	*N. oculata*	*T. chuii*
LED 405	7.94 ± 0.56 a	7.81 ± 0.36 a	5.79 ± 0.10 c	8.30 ± 0.12 c
LED 465	6.00 ± 0.32 b,c	7.63 ± 0.22 a	6.89 ± 0.03 b	9.90 ± 0.27 b
LED 630	5.76 ± 0.09 c,d	7.36 ± 0.13 b	7.87 ± 0.17 a	8.80 ± 0.25 c,d
LED 660	6.14 ± 0.29 b,c	7.19 ± 0.17 b	7.53 ± 0.13 a	9.89 ± 0.26 b
CW LED	6.52 ± 0.27 b	7.71 ± 0.14 a	6.81 ± 0.18 b	7.72 ± 0.10 c,d
WW LED	6.53 ± 0.29 b	7.94 ± 0.03 a	6.68 ± 0.10 b	9.36 ± 0.12 b,c
LED FL	5.48 ± 0.41 d	7.47 ± 0.29 b	7.91 ± 0.09 a	11.29 ± 0.03 a

Taken together, these results suggest that LED light sources with considerable blue content (LED 405, 465, CW LED, WW) tend to promote high N-prot factors in contrast to light sources with high red content (LED 630, LED 660, FL). Interestingly, this trend is apparent in both algae, despite their distinct evolutionary paths.

3.4.1 Fatty acids

The fatty acid profiles of *N. oculata* and *T.* chuii showed significant differences depending upon the light treatment (Tables 3.4-2 and 3.4-3). However, the saturated fatty acid (SFA) showing the highest levels in *N. oculata* and *T. chuii* under all light regimes were palmitic acid (C16:0; ~31-49 % of total fatty acids [TFA]) and, to a lesser extent, myristic acid (C14:0; ~0-9%). The most abundant monounsaturated fatty acid (MUFA) in *N. oculata* was palmitoleic acid (C16:1), ranging between 26 and 34 % of TFA. Conversely, low contents of oleic acid (C18:1) were observed in this alga. Oleic acid was, however, the most abundant MUFA (~12-20 % of TFA) in *T. chuii*, followed by gadoleic (C20:1) and palmitoleic acids. In *N. oculata,* major *n*-6 fatty acids were AA (C20:4), and in *T. chuii*, linoleic acid (LA; C18:2), ranging between 3 to 7 % and 4 to 15 % of TFA, respectively. In *N. oculata*, a major *n*-3 fatty acid was EPA (C20:5) with levels between 8-14 % of TFA. In *T. chuii*, the major *n*-3 fatty acid was α-linolenic acid (ALA; C18:3; ~22-30% of TFA) and only relatively low contents of EPA were observed (3-7% of TFA).

In *N. oculata*, the highest content of SFA was found under CW LED and WW LED treatments, whereas LED 405-treated cells showed the lowest levels ($p < 0.05$). Myristic acid was found to be highest in cultures under LED 405, LED 465 and FL. Exposure to LED 405 induced the highest contents of MUFA and PUFA. Moreover, EPA, being the only detected *n*-3 fatty acid in *N. oculata*, was found to be highest in cells under LED 405, resulting in a low *n*-6 to *n*-3 ($\sum n$-6/$\sum n$-3) ratio (0.54±0.12). *N. oculata* exposed to red LED light treatments showed the highest $\sum n$-6/$\sum n$-3 ratio. Worth to mention is also the low MUFA content in the CW LED and WW LED treatments.

Table 3.4-2 Fatty acid profile of *N. oculata* exposed to different light qualities. Values are given as percentage of total FAME (n = 3). Different letters within each fatty acid indicates statistical differences.

Fatty acid %	LED 405	LED 465	LED 630	LED 665	CW LED	WW LED	FL
C14:0	9.07 ± 0.38 a	9.23 ± 0.44 a	5.38 ± 0.73 c	6.42 ± 0.55 b,c	7.09 ± 0.35 b	5.15 ± 0.26 c	9.44 ± 1.47 a
C16:0	33.82 ± 0.23 c	41.86 ± 0.31 c	38.92 ± 0.01 b,c	41.19 ± 2.75 a,b,c	45.60 ± 1.37 a,b	48.56 ± 4.99 a,b	38.65 ± 3.24 c
C18:0	0.38 ± 0.05 b	0.62 ± 0.12 a,b	0.90 ± 0.29 a	0.81 ± 0.02 a,b	0.55 ± 0.09 a,b	0.65 ± 0.12 a,b	0.79 ± 0.06 a,b
C16:1	33.82 ± 0.36 a	33.54 ± 1.03 a	33.99 ± 0.43 a	30.49 ± 1.15 a,b	28.63 ± 0.71 b	26.06 ± 2.88 b	28.56 ± 0.33 b
C18:1	1.90 ± 0.11 b	1.90 ± 0.05 b	3.12 ± 0.23 a	3.93 ± 0.48 a	2.07 ± 0.31 b	1.94 ± 0.21 b	4.18 ± 0.38 a
C18:2 (*n*-6)	0.72 ± 0.01 a,b	0.38 ± 0.32 b	1.49 ± 0.61 a,b	1.80 ± 0.26 a	0.86 ± 0.25 a,b	0.89 ± 0.08 a,b	1.46 ± 0.44 a,b
C20:4 (*n*-6)	6.60 ± 0.81 a	3.34 ± 0.32 c	6.42 ± 0.36 a	6.19 ± 0.23 a	4.58 ± 0.44 b,c	6.04 ± 0.82 a	6.27 ± 0.10 a
C20:5 (*n*-3)	13.59 ± 1.43 a	9.10 ± 0.31 b,c	7.82 ± 0.31 b,c	7.74 ± 0.37 c	9.51 ± 0.58 b,c	8.64 ± 0.98 b,c	10.73 ± 1.20 b
∑ SFA	43.26 ± 0.56 c	51.71 ± 0.25 a,b	45.19 ± 1.00 b,c	48.42 ± 2.23 a,b,c	53.25 ± 0.97 a	54.35 ± 4.84 a	48.88 ± 1.72 a,b,c
∑ MUFA	35.72 ± 0.24 a	35.45 ± 0.98 a,b	37.11 ± 0.66 a	34.41 ± 1.64 a,b	30.69 ± 0.53 b,c	28.00 ± 3.09 c	32.74 ± 0.71 a,b,c
∑ PUFA	20.91 ± 0.61 a,b	12.82 ± 0.95 c	15.74 ± 1.29 b,c	15.73 ± 0.87 b,c	14.96 ± 1.22 b,c	15.57 ± 1.88 b,c	18.46 ± 1.74 b
∑ *n*-3	13.59 ± 1.43 a	9.10 ± 0.31 b,c	7.82 ± 0.31 b,c	7.74 ± 0.37 c	9.51 ± 0.58 b,c	8.64 ± 0.98 b,c	10.73 ± 1.20 b
∑*n*-6	7.32 ± 0.82 a,b	3.72 ± 0.64 c	7.91 ± 0.98 a	7.99 ± 0.49 a,b	5.45 ± 0.68 a,b,c	6.93 ± 0.90 a,b	7.73 ± 0.54 a,b
∑*n*-6/∑*n*-3	0.54 ± 0.12 b	0.41 ± 0.06 c	1.01 ± 0.08 a	1.03 ± 0.01 a	0.57 ± 0.05 b,c	0.80 ± 0.01 a,b	0.72 ± 0.03 b
PUFA/SFA	0.48 ± 0.02 a	0.25 ± 0.02 b	0.35 ± 0.04 b	0.33 ± 0.03 b	0.28 ± 0.03 b	0.29 ± 0.06 b	0.38 ± 0.05 a,b

Table 3.4-3 Fatty acid profile of *T. chuii* exposed to different light qualities. Values are given as percentage of total FAME (n = 3). Different letters within each fatty acid indicates statistical differences.

Fatty acid %	LED 405	LED 465	LED 630	LED 660	CW LED	WW LED	FL
C14:0	0,84 ± 0,24 a	0,63 ± 0,03 a	0,57 ± 0,02 a	0,60 ± 0,01 a,b	0,76 ± 0,31 a	0,69 ± 0,20 a	0,91 ± 0,06 a
C16:0	36,54 ± 1,13 a	33,22 ± 0,83 b,c	33,39 ± 0,11 b,c	34,04 ± 0,41 b,c	31,85 ± 0,58 c	34,54 ± 1,08 a,b	36,48 ± 0,93 a
C18:0	0,29 ± 0,08 a,b	0,35 ± 0,04 a,b	0,38 ± 0,04 a,b	0,42 ± 0,02 a	0,35 ± 0,03 a,b	0,37 ± 0,09 a	0,23 ± 0,01 b
C16:1	2,31 ± 0,25 a,b,c	5,05 ± 0,18 a,b	1,83 ± 0,26 c	2,62 ± 0,15 a,b,c	2,37 ± 0,40 a,b,c	3,18 ± 0,40 a,b,c	5,12 ± 0,96 a,b
C18:1	15,05 ± 0,36 b	20,01 ± 0,28 a	13,24 ± 0,31 c	15,77 ± 0,20 b	12,49 ± 0,62 c	16,03 ± 0,71 b	19,78 ± 0,32 a
C20:1	2,68 ± 0,35 b,c	5,10 ± 0,36 a	4,45 ± 0,27 a	3,40 ± 0,38 b	2,57 ± 0,30 c	2,57 ± 0,09 c	2,71 ± 0,22 c
C18:2 (n-6)	14,16 ± 1,23 a	6,81 ± 0,42 b	13,69 ± 0,34 a	14,91 ± 0,21 a	15,71 ± 0,68 a	7,59 ± 0,55 b	4,42 ± 0,11 c
C18:3 (n-3)	24,56 ± 1,62 b,c	22,06 ± 0,54 c	26,35 ± 1,55 a,b	22,08 ± 0,59 c	27,82 ± 1,75 a,b	30,08 ± 1,19 a	25,91 ± 0,79 b
C20:5 (n-3)	3,45 ± 0,46 d	6,55 ± 0,60 a	5,84 ± 0,44 a,b,c	5,93 ± 0,14 a,b	5,93 ± 0,72 a,b	4,76 ± 0,48 b,c	4,36 ± 0,23 c,d
∑ SFA	37,67 ± 1,12 a	34,20 ± 0,81 c	34,34 ± 0,06 c	35,05 ± 0,44 b,c	32,96 ± 0,86 c	35,61 ± 1,20 b	37,62 ± 0,98 a,b
∑ MUFA	20,05 ± 0,43 c	30,16 ± 0,77 a	19,52 ± 0,84 c,d	21,79 ± 0,31 c,d	17,42 ± 1,15 d	21,77 ± 1,16 c	27,60 ± 0,65 b
∑ PUFA	42,16 ± 1,17 c	35,42 ± 1,39 d	45,88 ± 0,77 b	42,92 ± 0,36 b,c	49,46 ± 1,07 a	42,43 ± 0,31 c	34,69 ± 1,07 d
∑ n-3	28,01 ± 1,19 c	28,61 ± 1,04 b,c	32,19 ± 1,11 a	28,01 ± 0,51 c	33,75 ± 1,65 a	34,84 ± 0,72 a	30,27 ± 0,96 b
∑n-6	14,16 ± 1,23 a	6,81 ± 0,42 b	13,69 ± 0,34 a	14,91 ± 0,21 a	15,71 ± 0,68 a	7,59 ± 0,55 b	4,42 ± 0,11 c
∑n-6/∑n-3	0,51 ± 0,06 a,b	0,24 ± 0,01 c	0,43 ± 0,03 b	0,53 ± 0,02 a	0,47 ± 0,04 b	0,22 ± 0,02 d,c	0,15 ± 0,00 d
PUFA/SFA	1,12 ± 0,06 b	1,04 ± 0,06 c	1,34 ± 0,02 a,b	1,22 ± 0,02 b	1,50 ± 0,06 a	1,19 ± 0,04 b	0,92 ± 0,05 c

T. chuii showed highest content of SFA under LED 405 and FL treatments ($p < 0.05$; average: 37.65±0.81 % of TFA) and significantly less under CW LED (32.96±0.86 % of TFA). Moreover, similarly to those under LED 465, FL-treated *T. chuii* cultures showed also elevated content of MUFA (27.6±0.65 and 30.16±0.77 % of TFA, respectively). CW LED-treated cultures displayed both the lowest MUFA and the highest PUFA contents (49.46±1.07 % of TFA), whereas the lowest PUFA levels were obtained for cells under LED 465 and FL (average: 35.06±1.18 of TFA). In *T. chuii*, ALA was the only *n*-3 PUFA observed. The highest levels were found in cells under CW LED and WW LED (average: 28.95±1.83 % of TFA) and lowest under LED 465 and LED 660 (22.07±0.51% of TFA). The ratio of $\sum n$-6/$\sum n$-3 was highest in LED 660- and lowest under FL-treated *T. chuii* cultures (0.94±0.04 and 0.34±0.01% of TFA, respectively; $p < 0.05$). CW LED-lit cultures yielded the highest PUFA/SFA ratio (1.5±0.06), whereas cells under FL and LED 465 showed the lowest ratio (0.92±0.05 and 1.04±0.06, respectively).

3.5 Nutrients and growth parameters

Daily observations of pH did not reveal significant differences between treatments, but rather among experiments. In Experiment 1, all treatments showed an average pH of 7.68±0.34 and 7.68±0.22, in Exp. 2, 7.35±0.07 and 7.04±0.41, and Exp. 3 7.31±0.22 and 7.02±0.22, for *N. oculata* and *T. chuii*, respectively. These pH differences might be due to slight differences in CO_2 flow rates among experiments.

N. oculata showed an overall lower nutrient utilization compared to *T. chuii*, resulting in uneven dissolved N-NO_3^- concentrations in the media among the treatments at time point of harvest, depending on the light sources under study (Table 3.5-1). Monitored nutrient concentration in the medium (n = 1 per day, n = 7 in total) revealed a high nutrient consumption by *N. oculata* exposed to LED 465 and LED 405 treatment and a low consumption under LED 630 and LED 660. Nevertheless, measurements had only a monitoring purpose and no statistical treatment could be done due to the small sample size (n = 1 per day). *T. chuii* also obtained highest nutrient consumption under LED 465 and lowest under LED 630. The nutrient concentration at day of harvest was for *N. oculata* highest under LED 405, followed by LED 630 and 660 and was lowest under WW LED, FL and LED 465 treatment. The nitrogen content in all *T. chuii* cultures was ≤ 0.1 mg N-NO_3^- L^{-1} after t = 72h. Concentrations of N-NH_4^+ were always below 0.07 mg L^{-1}, representing less than 1% of the total nitrogen in the system, which would otherwise result in insignificant concentrations of nitrite (NO_2^-; see discussion, chapter 4.6).

The $P\text{-}PO_4^{3-}$ consumption of *N. oculata* was highest under LED 405, whereas cultures lit by LED 465, LED 630, LED 660, CW LED, WW LED and FL showed similar results. Among all *T. chuii* cultures, the $P\text{-}PO_4^{3-}$ content in the medium was always below detection limit, indicating a complete utilization by the algae during experimental setup time ($t \approx 1.5$-2 h). Measurements of medium without algae showed a concentration of 1.21 mg $P\text{-}PO_4^{3-}$ L^{-1}. Therefore the concentration at the time point of inoculation was around ~1 mg $P\text{-}PO_4^{3-}$ L^{-1}.

Table 3.5-1 Nitrate-based nitrogen (R_N; mg $N\text{-}NO_3^-$; $n = 1$) and phosphate-based phosphorous (R_P ; mg $P\text{-}PO_4^{3-}$; $n = 4$) consumption of *N. oculata* and nitrogen consumption of *T. chuii* during the experimental run. Nitrogen content in the medium at the harvesting time point is given as S(t).

	N. oculata			***T. chuii***	
Treatment	**R_N [mg $N\text{-}NO_3^-$ L^{-1} d^{-1}]**	**R_P [mg $P\text{-}PO_4^{3-}$ L^{-1} d^{-1}]**	**S (t = 120) [mg $N\text{-}NO_3^-$ L^{-1}]**	**R_N [mg $N\text{-}NO_3^-$ L^{-1} d^{-1}]**	**S (t = 96) [mg $N\text{-}NO_3^-$ L^{-1}]**
LED 405	1.77	0.71	3.13 ± 0.13 a	2.35	≤ 0.1 ± 0 a
LED 465	1.56	0.39	0.30 ± 0.20 d	2.61	≤ 0.1 ± 0 a
LED 630	0.99	0.45	2.93 ± 0.25 a	1.81	≤ 0.1 ± 0 a
LED 660	1.19	0.45	1.75 ± 0.05 b	2.09	≤ 0.1 ± 0 a
CW LED	1.51	0.37	0.88 ± 0.38 c	1.95	≤ 0.1 ± 0 a
WW LED	1.52	0.41	0.18 ± 0.04 d	2.15	≤ 0.1 ± 0 a
FL(1)	1.51	0.43	0.28 ± 0.04 d	2.30	≤ 0.1 ± 0 a

3.6 Efficiency of light sources used

The used LED light sources were obtained from different suppliers with somewhat low PCEs (measured via power-meter; see Annex 3), being the result of poor electrical design and manufacture. Accordingly, otherwise as discussed before, the OSE of the LED modules could not been taken into account as results for the PE would have been dependent more upon the chosen LED manufacture than the properties of the LEDs. Therefore, only energy efficiencies obtained by biomass energy (E_{out}) to optical energy (E_{in}) ratios led to comparable results among the light sources. To give an overview about the used light sources, approximate relative efficiency data for PPFD/W and PCE/m^2 are provided together with further information in Annex 3, Fig. A.3-3. The daily optical energy (E_{in}) supplied to the PBR is pointed out in Table 3.6-1.

In the first experiment, PE in *N. oculata* cultures was highest in LED 660- and FL-treated cultures (4.6±0.3 and 4.2±0.2 %, respectively; Fig. 3.6-1A). Lowest efficiency was found when *N. oculata* was treated with LED 405 (1.9±0.1 %). Interestingly, *N. oculata* cultures showed consistently similar trends in terms of photosynthetically efficiency as *T. chuii*, in which highest energy efficiencies were found under LED 660 and FL (6.13±0.48% and 6.1±0.03%, respectively) and lowest under LED 405 (2.94±0.32 %).

N. oculata and *T. chuii* showed highest CO_2 fixation until day of harvest when grown under FL light (188.0±11.3 and 311.0±23.7 mg CO_2 L^{-1} d^{-1}) and lowest under LED 405 (108.2±6.4 and 201.1±22.8 mg CO_2 L^{-1} d^{-1}; Fig. 3.6-1B).

Table 3.6-1 Optical energy supplied to photobioreactors in Experiment 1.

Treatment	LED 405	LED 465	LED 630	LED 660	CW LED	WW LED	FL
Optical energy (KJ d^{-1})	39.1	34.5	25.9	24.6	30.5	27.8	28.9

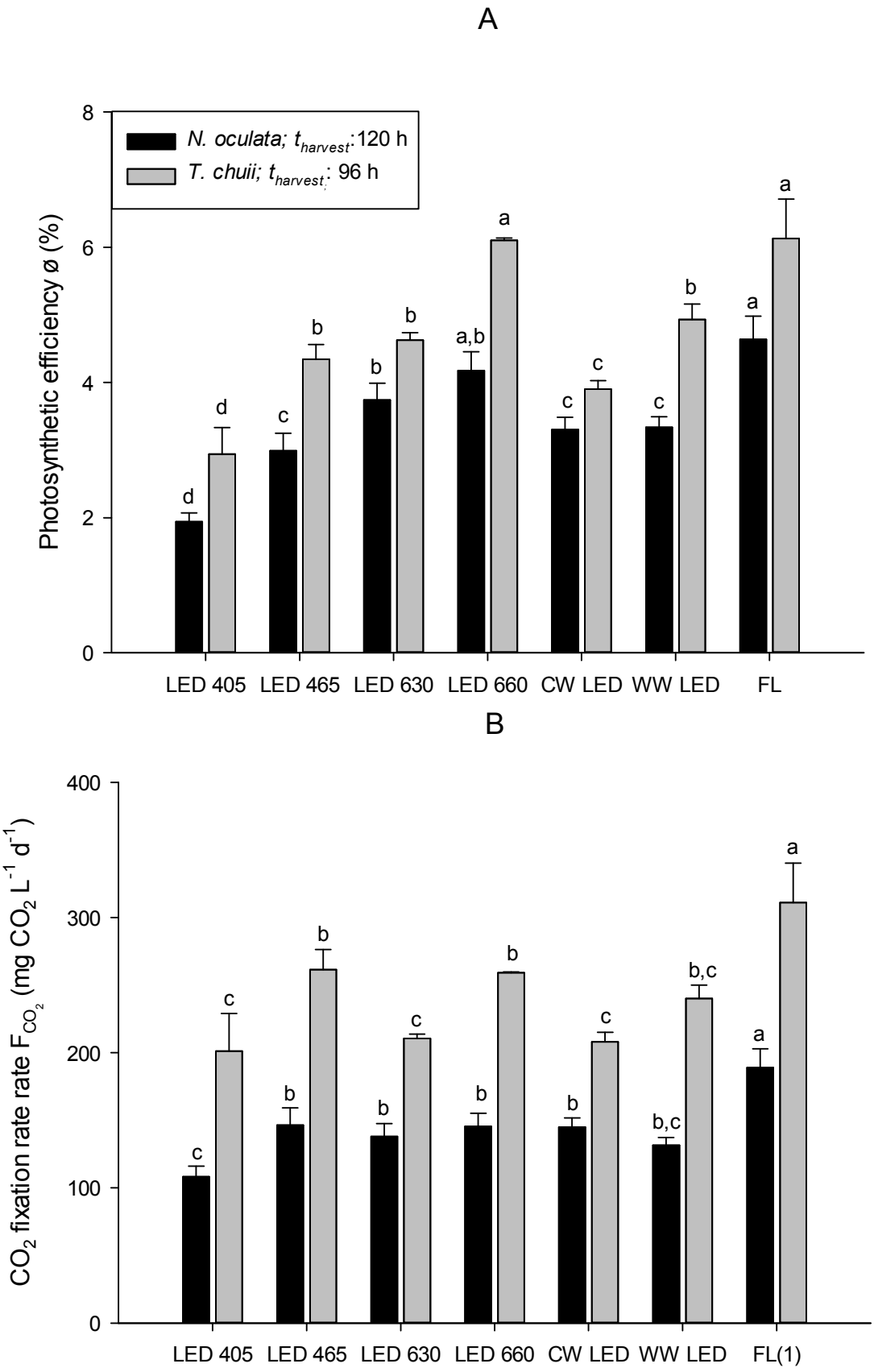

Figure 3.6-1 Photosynthetic efficiency *ø* (PE) and CO_2 fixation rate F_{CO2} until day of harvest of *N. oculata* (black bar) and *T. chuii* (grey bar) exposed to different light qualities. Statistical differences among treatments are indicated by different letters for each alga.

4 Discussion

Light quality was found to affect growth, morphologic changes, total biomass and biochemical composition of *N. oculata* and *T. chuii*. Adjustments of different LEDs to fulfil microalgal light quality requirements was shown to sustain higher biomass production than FLs specifically designed for photosynthetic growth. However, the way how algae respond biochemically and morphologically to light quality might be affected by photon wavelength, which impacts on nutrient utilization and cell growth. How these and other factors may relate to each other is discussed in the following sections.

4.1 Algal growth parameters

In the first experiment, *N. oculata* and *T. chuii* showed similar biomass productivities when they were illuminated with LED 465 and LED 660. Interestingly, a similar trend has been reported for *Nannochloropsis oceanica* [58], while Abiusi *et al.* [57] detected similar productivities for *Tetraselmis suecica* under blue and red LEDs only until the third day of cultivation. In terms of maximal AFDW and cell concentration, *N. oculata* reached a higher $X_{AFDW,cell}$ under LED 465 compared to LED 660, whereas *T. chuii* showed the opposite effect ($X_{AFDW,cell,LED\_660} > X_{AFDW,cell,LED\_465}$). This finding is in agreement with Abiusi *et al.* [57], who reported that red LED-treated *T. suecica* cultures showed a higher X_{AFDW} compared to those under blue light. Nonetheless, their biomass productivity (P_{AFDW}) remained similar under blue and red LED light during the first 72 h of an experiment lasting 14 days. However, after this initial period, red LED-treated cells kept growing, while blue LED-treated algae reached stationary phase at t = 96 h. This resulted in a 50% higher final maximal biomass concentration under red LEDs at t = 336 h. It is likely that algae continue to grow when irradiated by their preferred light quality [1], whereas non-optimal wavelengths can cause growth inhibition when cell or biomass concentrations reach a threshold value (Fig. 4.1-1), as found for different algae [50, 57, 109].

As blue light has been suggested to be a non-optimal wavelength band for green algae as compared to red light [1], similar growth can be observed for cells under this light range until a critical algal concentration is reached. When cell concentration is low and PPFD per cell within a culture is high, NPQ might have only a minor inhibiting effect on algal growth at wavelengths ≥ 450 nm, becoming negligible at late growth stages when biomass concentration is high and PPFD per cell is low [15, 59].

Another factor promoting lower growth rates of *Tetraselmis* under blue light might be nutrient limitation induced by high nutrient uptake rates. Nevertheless, this cannot be the only explanation. Abiusi *et al.* [57] using a fed-batch system to grow *T. suecica*, in order to prevent nutrient limitation from becoming a growth inhibiting factor, reported results similar to those of the present study for *T. chuii*. Hence, a more likely explanation may be linked to growth inhibition caused by low photon penetration into the culture at wavelength bands matching the absorption peaks of whole algal cells rather than those matching only the absorption maxima of light harvesting pigments and/or organic matter dissolved in the medium [110]. Photons emitted by LEDs peaking at ~470 nm cover mainly the carotenoid absorption wavelength band as well as that of chlorophyll *b* (λ_a = 460-480 nm) and, to a lesser extent, of chlorophyll *a* (λ_a = 440 nm) within the blue light range. Chlorophyll *b* is known to absorb strongly in the blue region as compared to the red region [24], which may promote adequate growth of green algae under blue light in batch cultures with low cell concentrations at lag and early exponential phases. However, reduced photon penetration into the culture at later growth phases and higher cell concentrations may lead to growth limitation, as this wavelength band is readily absorbed by cells (Fig. 3.3-1). Therefore LEDs peaking at ~470 nm might be generally well suited for species with a large pool of carotenoids and/or chlorophyll *b* (i.e. SAR and Chlorophyta species).

As chlorophyll *a* peaks were clearly visible in the absorption spectra of whole cells of *N. oculata* (SAR species) and those same peaks were partly obscured in the absorption spectra of *T. chuii* (Chlorophyta), it could be suggested that SAR species may predominantly use chlorophyll *a* as their major light harvesting pigment. In contrast, chlorophytes may rely more heavily on carotenoids and chlorophyll *b* to capture light. These differences would explain why only lower wavelengths (420-450 nm) reveal a distinct preference of a given algal species for either blue or red light. As the absorption peak of chlorophyll *a* lies predominantly within the 420-450 nm range, without having major contributions by accessory pigments (e.g. carotenoids or chlorophyll *b*), LEDs with $\lambda_e \leq 450$ nm would favour the growth of SAR microalgae at expense of any competing chlorophytes.

Low productivities of cultures exposed to LED 405 treatment give this near UV light only an accessory role, probably due to its higher photon energy and consequent induction of growth suppressing NPQ. Nonetheless, it was found that UV-A radiation (320-400 nm) supplemented to other wavelengths in low doses (~4 % of total PPFD) is beneficial for

biomass production of *Nannochloropsis gaditana*, whereas higher supplementation (>10% of total photon flux) may cause photoinhibition [111].

Mixed light sources with photosynthetically suited wavebands and sufficient photon emissions at λ_a = 660 nm were found to be beneficial for microalgal production, compared to only monochromatic light or sources lacking red or blue light (present study; Sánchez-Saavedra and Voltolina [112]). Precise light tailoring (high matching between emission and absorption spectra) may allow algae to absorb photons very efficiently, promoting a high μ_{max}. However, that has the disadvantage of limiting the photon flux towards the centre of the PBR, suppressing growth when cell concentrations increase beyond a threshold value. In turn, this causes lower maximal cell concentrations, as it was found for cells of both species treated with the HRmix in this study.

Conversely, light sources with high red light content (e.g. in HRLB, FL, LED 660) promote higher cell count-based growth (P_{cell}, μ_{cell} and X_{cell}), most probably because red light induces an acceleration of the cell cycle, being accompanied by decreased cell size and weight as found in the present study and elsewhere [19, 46, 49, 67-69]. This effect may also need to be considered for harvesting procedures, as smaller cells might be more difficult to flocculate or centrifuge than larger cells, increasing production costs and decreasing the overall energy efficiency of the process.

4.1.1 Complexity of light measurements

Light quantity strongly influences the maximal biomass concentrations that algal cultures can reach. Therefore, appropriate light quantity measurements are absolutely essential for a meaningful comparison of different studies and require the utmost attention when comparing light qualities used for growing algae. As described above and observed in the present study (see Annex, Fig. A.7-6), algae showed similar growth patterns under all light qualities until a certain time point. Once this point is reached only algae irradiated by their preferred light quality [1] continued to grow. Similar patterns have been described by other authors using an appropriated device for measuring light quantity [50, 57, 109]. Unfortunately, other authors [14, 15, 25] who found clear preferences for a specific light quality for a given alga at early exponential growth phase often used inappropriate devices to measure light intensity (Fig. 4.1-1).

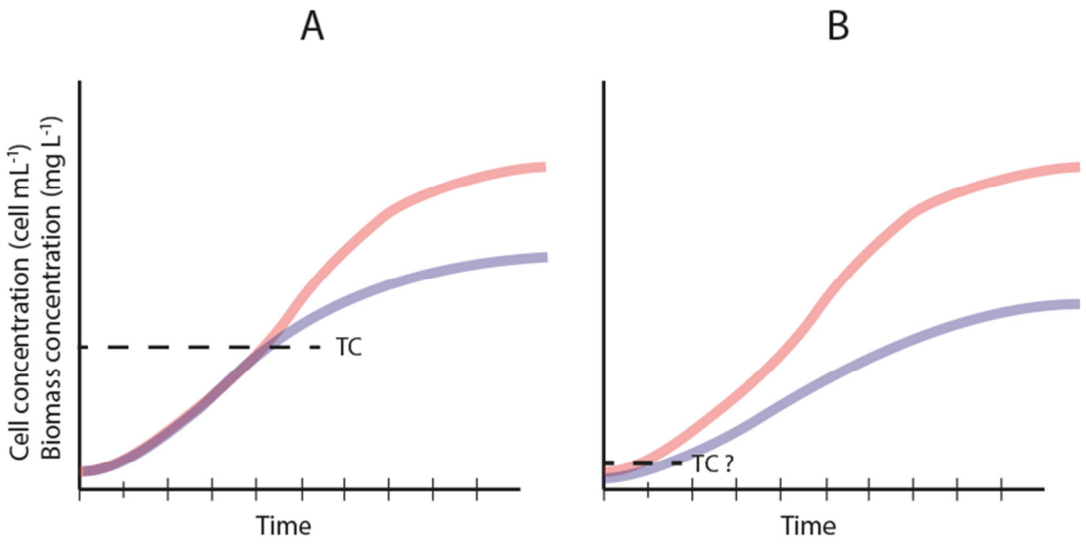

Figure 4.1-1 Simplified growth patterns between light qualities observed by authors using (A) adequate [50, 57, 109] and (B) inadequate [14, 15, 25] devices to measure light intensity. TC indicates the threshold concentration above which algae continue to grow under light with an optimal wavelength range (red) as compared to cells under non-optimal light quality (blue). These differences usually lead to a well-defined TC (A), whereas faulty light intensity measurements often result in an undefined TC (B).

Apparently, the growth patterns observed seem more to be an effect of light intensity rather than light quality [60]. For example, Das *et al.* [15] used luminance (lm m^{-2}; lux) measurements to estimate light intensity. In this case, the effective PPFD (in µmol m^{-2} s^{-1}) of the used red LED (λ_a = 680 nm) might be sevenfold higher than that of blue LED at the same luminous flux (for further details see Annex 2) and thus the PPFD was maybe too high to provide normal growth for *Nannochloropsis* sp. In contrast, Chen *et al.* [58], who measured PPFD via pyranometer, an apparatus considered to be more reliable than only quantum sensors [24], showed similar results for *N. oceanica* and those obtained for *N. oculata* in the present study. Another example of misinterpretation due to faulty measurement of light intensities is the study of Teo *et al.* [25], who found blue light to be the preferred light for growing *Tetraselmis* sp., in contrast with the present work and the Abiusi *et al.* [57] study. Once again, the former authors used a quantum sensor (Light Scout Dual solar quantum light meter), reporting a remarkable low response to blue light compared to red light, which led to exposure to higher PPFD for algae treated with blue LEDs. Thus, the purported enhanced gene transcription and enzyme activities being responsible for higher growth in *Tetraselmis* sp. under blue LEDs cannot be validated by the present study and that of Abiusi *et al.* [57]. Teo *et al.* [25] further mentioned that red light induced cell damage, which would explain the lower growth of *Tetraselmis* sp. under red LED light reported by these authors. However, the

opposite was found by the present study and Abiusi *et al.* [57], as *T. chuii* cells showed higher motility under red light than those exposed to blue light.

Optical density measurements at 680 nm were found to be a fast, reliable method to determine biomass concentration in *N. oculata* and *T. chuii* cultures exposed to different light qualities. Moreover, optical density measurements at 680 nm was also found to be suitable to estimate cell concentration of these cultures. Concerns about different cell sizes affecting significantly the determination of biomass concentration or cell concentration [1] could not be confirmed for *N. oculata* and *T. chuii*.

4.2 Cell morphology, cell cycle and culture maturity

Algae undergo different morphologic changes during their cell and life cycles, being likely affected by light quality and nutrient availability. However, a connection between light quality, absorption spectra, nutrient consumption, cell size, and predominant growth stage-dependent cell morphology within a microalgal culture (defined as "culture maturity" in this work) can be concluded for both species.

For example, ageing *N. oculata* cultures can become pale yellow-brown, which is usually an indication of cyst formation [113]. The colour change is apparently related to an increasing ratio of yellowish carotenoids (canthaxanthin, astaxanthin, vaucheriaxanthin, antheraxanthin, zeaxanthin and violaxanthin) to greenish chlorophyll (car:chl ratio) [106, 114-116]. Progression through the growth cycle and induction of specific car:chl ratios were found to be dependent not only on nutrient depletion from the medium, but also on light quality and quantity [106, 117, 118]. In turn, nutrient uptake by algae is known to be cell-size dependent, for small cells with low volume:surface ratios usually show higher consumption rates than larger cells with high volume:surface ratios [119]. Naturally, algae tend to form small cells in nutrient-rich environments and larger cells in nutrient-depleted growth media as described for *Nannochloropsis* sp. [113, 119]. However, nutrient availability in the medium depends on uptake rates, being probably more affected by wavelength of incident light than cell size. Nevertheless, cell size fluctuations may indicate changes in growth stage-dependent cell morphology for some species (including *N. oculata*) as ageing cultures tend to be dominated by larger cells, while a larger proportion of smaller cells in such cultures may indicate growth limitation/arrest [67, 104, 105]. Interestingly, as LED 405-treated *N. oculata* cells in the present study displayed a greenish appearance and a low amount of cell aggregation, one can conclude that no cysts developed. Such a result might signal that these cells underwent some growth limitation or even growth arrest. This suggestion seems to be supported by the high

nitrogen content remaining in the medium ($S_{t=120h}$ = 3.13 mg N-NO_3^- L^{-1}). The aforementioned (partial) growth arrest might be a consequence of light limitation, as small "particles" (e.g. *N. oculata* cells) are known to absorb shorter wavelengths than larger bodies [110]. Therefore, photons relevant for photosynthesis might have already been absorbed by cells at the periphery of the PBR, thus becoming unavailable for a large proportion of the culture, which is unable to capture enough light to grow efficiently. In contrast, *T. chuii* cells have larger cells, which absorb these wavelengths less efficiently, thus allowing photons to penetrate deeper into the culture and promote long-lasting high nutrient consumption (see chapter 4.6).

The high motility of *T. chuii* cells exposed to LED 630 and LED 660 indicates that the culture was dominated by "swarmer" cells (stage $3_{T.\ chuii}$) as observed for *T. suecica* under red LED light treatment [57]. In LED 465-, CW LED-, WW LED- and FL-treated *T. chuii* cells, stage $4_{T.\ chuii}$ cells were abundant and most probably dominated the culture. However, Abiusi *et al.* [57] observed mostly non-flagellated, encysted (stage $5_{T.\ chuii}$) cells under blue and white light. This discrepancy might be explained by the longer culturing period carried out by these authors compared to that of the present study. The coccoid cells in LED 405- and LED 465-treated cultures might be caused by a significant ratio of cyst cells (stage $5_{T.\ chuii}$) together with some cells still in the motile stage ($4_{T.\ chuii}$).

As with *N. oculata*, one may also assign different predominant cell shapes to *T. chuii* cultures under specific light treatments. However, nutrient consumption rates of *T. chuii* cultures were, in general, significantly higher than those of *N. oculata.* Unfortunately, this difference did not allow to establish a precise correlation between nutrient consumption, cell sizes and shapes, because nutrient levels of *T. chuii* were already under detection limit when cultures were harvested (t = 96 h) and the growth medium was analysed. Nevertheless, in both algae, cultures exposed to LED 630 and LED 660 tended to be dominated by less mature cell stages with smaller cell size and lower cell weight, whereas the opposite was found for cells under LED 465, CW LED, WW LED and FL treatments.

Incidentally, the relationship between nutrient availability and cell size/maturity would also answer the long sought-after question [67] why larger cells are usually found under light sources promoting nutrient assimilation (e.g. blue and white light sources) [19, 57, 67, 104] in comparison with other sources (e.g. red LED light). In other words, average cell size and, in turn, culture maturity are dependent on the ability of a light source to induce nutrient consumption and consequently the duration of exposure to nutrient depletion by microalgae grown in batch (Fig. 4.2-1). Nevertheless, further research is required to confirm the

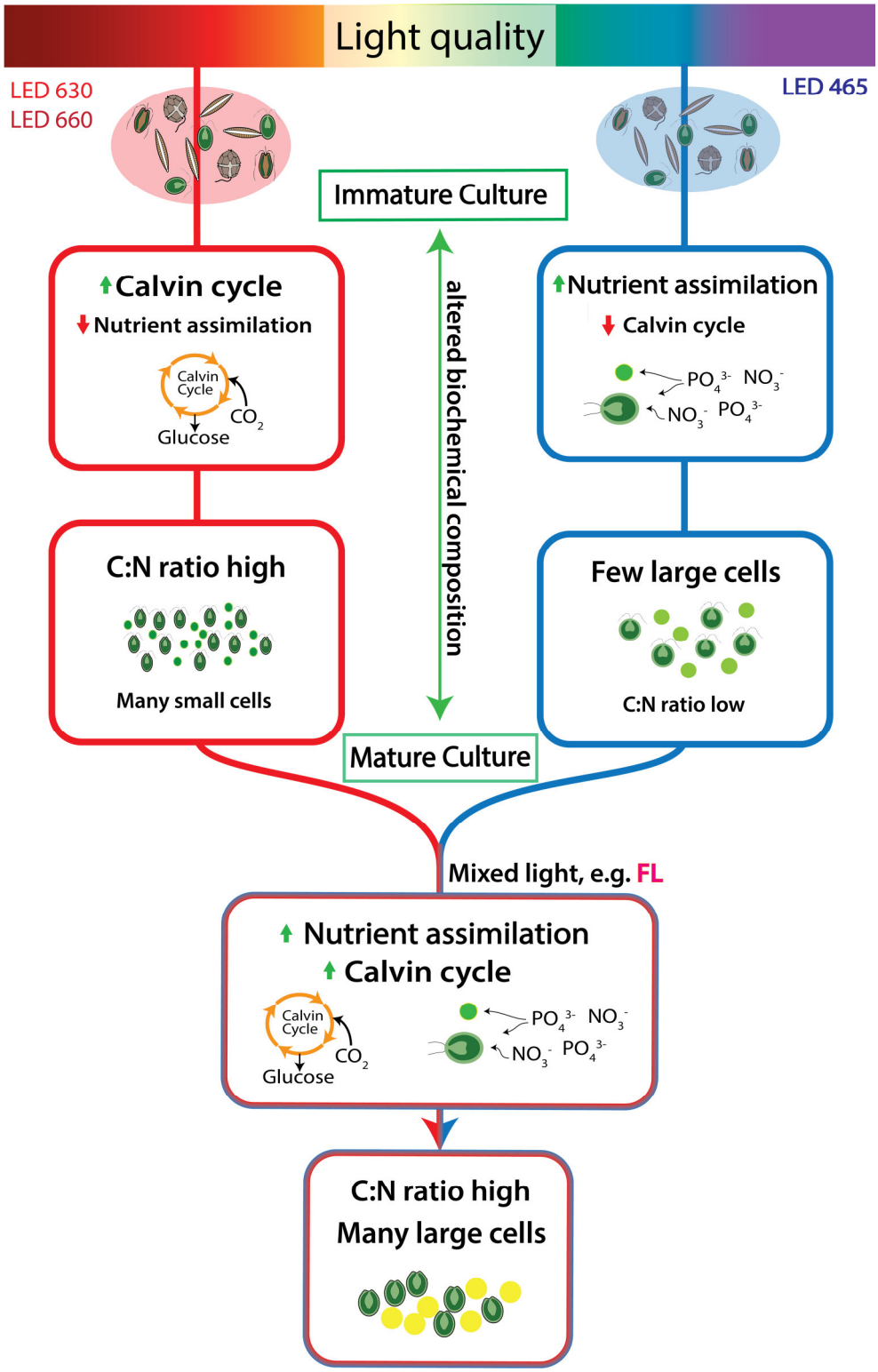

Figure 4.2-1 Suggested major interactions between light quality and cell productivity, cell size, nutrient assimilation and C:N ratios. See sections 4.1-4.6 for further discussion of the proposed model. Red light exposed algae (left pathway) show usually a high C:N ratio, indicating a reduced nutrient consumption, but a higher Calvin cycle activity. The visible effect is many small cells in the culture. Algae exposed to blue light (right pathway) show usually a low C:N ratio, indicating a high nutrient consumption (high enzyme activity related to nutrient assimilation; see 4.6). The visible effect is few big cells in the culture. Combining blue and red light (bottom) stimulates both: Calvin cycle and nutrient consumption. The result are many big cells and high C:N ratios.

hypothesis depicted in Fig. 4.2-1, because other factors may be involved, such as non-light dependent nutrient utilization (see 4.6), and the magnitude of light quality-dependent cell size variation among algae is sometimes too small, making the determination of statistically significant correlations a difficult endeavour.

In the present study microscopic observation of cell morphology, taking also into consideration cell size and lipid body formation, revealed a more detailed and thus a cell cycle (Fig. 3.2-4) different from the one suggested by Materassi *et al.* [120] for *T. suecica*. More specifically, these authors divided the cell cycle into five stages, starting with the release of daughter cells ($1_{T.\ suecica}$; "swarmers"), mature cells ($2_{T.\ suecica}$); loss of flagella and cyst formation ($3_{T.\ suecica}$); initial stage of protoplast division ($4_{T.\ suecica}$); and flagellate daughter cells within the mother cell wall ($5_{T.\ suecica}$) [57, 120]. Although some stages described therein were also found for *T. chuii*, photographic data obtained in this work suggest that *Tetraselmis* cells are not released directly with flagella from the mother cell wall, but rather cells retain the morphology of the previous stage ($6_{T.\ chuii}$). Moreover, the second cell stage ($2_{T.\ chuii}$) might remain unflagellated, as frequent observation of this cell type is always accompanied by cells smaller than those of the following stages, which does not allow for alternative reconstructions of the cell cycle. One may suggest that cells in stage $2_{T.\ chuii}$ begin to form flagella, starting from the previous elliptical cells ($1_{T.\ chuii}$) and the invagination necessary for cells to obtain their cordiform shape (stages 3-$4_{T.\ chuii}$) and where flagella usually protrude from the cell body. Cell stage $3_{T.\ chuii}$ can be considered as a small "swarmer" as described by [57, 120], being equivalent to stage $1_{T.\ suecica}$. These highly motile cells are equipped with flagella [57, 120], displaying the typical morphology of *T. chuii* cells. The fourth stage ($4_{T.\ chuii}$) is similar to the previous stage ($3_{T.\ chuii}$), but with higher cell weight, larger surface area and lower motility as described previously [57, 120] for the second stage of *T. suecica* ($2_{T.\ suecica}$). In the present study, the stages comparable to $3_{T.\ suecica}$ and $4_{T.\ suecica}$ were combined into a fifth stage ($5_{T.\ chuii}$) as the time point when cells lose their flagella. This combination is proposed because of their short duration and the impossibility of distinguishing, in a reliable way, *T. chuii* cells at stages similar to $3_{T.\ suecica}$ and $4_{T.\ suecica}$. For the last stage ($6_{T.\ chuii}$), Materassi *et al.* [120] described two flagellated rod-shaped cells within the mother cell wall, which were not found in the present study, as mentioned before (Fig. 3.2-4 (6)). The most striking observation, however, was the lipid redistribution within the cells depending upon the cell stage. While in the first stages (1-$2_{T.\ chuii}$) lipids seem to co-localise with the cytoplasm, in the motile phases (3-$4_{T.\ chuii}$) the lipid bodies co-localise with the U-shaped chloroplast. As cells form cysts (stage $5_{T.\ chuii}$), the lipids move back towards the cytoplasm before dividing

into two sets of lipid bodies, one for each daughter cell ($6_{T.\ chuii}$). This observation highlights how dynamic the lipid compartment seems to be in microalgae, which may be a consequence of the crucial role played by these molecules for the survival of these microorganisms.

4.3 Absorption spectra

With the modification of the method from Mueller and Fargion [95] by normalizing the area under the curve between 380 and 750 nm, the biomass concentration on filter-based measurements of absorption spectra of whole cells have a low effect on the obtained spectrum (see standard dilutions Annex 5). However, variations in the blue spectral range (390-490 nm) can be attributed to light properties such as increased scattering [24]. A quantitative absorption spectrum would have not been reliable as the pore size of the used filters (1 μm) was too large to guarantee an even distribution of the biomass on the filter. However, the used modification allows the observation of absorption shifts among treatments and comparison of algal strains containing different pigments. The reliability of the proposed procedural modification can be confirmed as repeated measurements of algal cultures exposed to a given light source always showed the same light absorption patterns, although the spectra differed among light treatments (e.g., *N. oculata* with LED 405 treatment).

N. oculata and *T. chuii* follow different strategies for light harvesting as can be deducted from their absorption spectra. The absorption spectrum of *N. oculata*, displaying higher absorption in the 380-450 nm and 660-700 nm regions together with the clearly visible peak at $\lambda_a \approx 630$ nm was clearly dominated by chlorophyll *a*. However, the contribution of carotenoids (λ_a = 487-490 nm) for the absorption spectra of *N. oculata* cannot be ignored. In contrast, the absorption spectrum of *T. chuii*, with higher absorption in the 450-500 nm and 550-660 nm ranges, was clearly due to the contribution of chlorophyll *b*, whereas no obvious peaks assignable to carotenoids could be observed.

Absorption spectrum shifts among treatments can be caused by complementary chromatic adaptation (CCA), leading to reconstruction of the LHPs and changes in pigment composition. These alterations may be triggered by environmental cues, such as light quality and quantity, amongst other factors [107, 121]. However, this effect is mostly known for phycobiliprotein-containing red algae or cyanobacteria, where absorption spectrum changes between treatments are clearly visible [122]. However, also SAR/Hacrobia algae undergo a CCA, as found in diatoms [123, 124], dinoflagellates [124-128], haptophytes [124] and eustigmatophytes [106], although changes are not as distinct as, for example, in cyanobacteria.

In the present study, the different absorption spectrum of *N. oculata* (an eustigmatophyte) exposed to LED 405 compared to other treatments were probably caused again by a low car:chl ratio. Solovchenko *et al.* [106] found that *Nannochloropsis* sp. with a low car:chl ratios show low absorbance between 390-490 nm but high between 500-660 nm and the opposite in cells with a high car:chl ratio. They also attributed these changes to low light conditions (75 μmol s^{-1} m^{-2}) under no limitation of nitrogen, which would strengthen the hypothesis that light quantity rather than lack of nutrients was the inhibiting factor in LED 405-treated *N. oculata* cultures.

The shift to a more greenish colour of *T. chuii* cultures exposed to WW LED and CW compared to other treatments suggests a slight chromatic adaptation due to an accumulation of chlorophyll *a*, as reported by Abiusi *et al.* [57] for *T. suecica* exposed to white light. However, the observed colour shift was not as strong as that presented by *N. oculata* exposed to LED 405. Algae may follow different CCA strategies, responding to changes in light quality by altering pigment composition in order to capture photons with an underrepresented wavelength within an emission spectrum. Alternatively, changes in pigment levels may occur due to fast nutrient utilization rates induced by light with a given wavelength, leading to extended periods of nutrient depletion. The latter hypothesis seems to be supported by the results obtained with LED 405-treated *N. oculata* cultures. However, the same cannot be stated for *T. chuii* due to the limitations of the nutrient consumption data for this alga as discussed previously (see 4.2).

Interestingly, in both algae, all changes were only evident between 390 and 660 nm, but not at 680 nm. Probably due to the constant absorption at 680 nm the linear regression among treatments and time was found and this allows the determination of biomass concentration by OD measurements at 680 nm.

4.4 Biochemical composition

N. oculata showed similar lipid contents under all LED treatments. This would suggest that light quality may not affect directly the total lipid content of this alga. However, appropriate light quality can induce changes in cell morphology and growth and a high proportion of mature cells in the culture (see 3.2), which could explain the remarkable high levels of total lipids and carbohydrates and low protein content in FL-treated cultures as compared to those lit with LEDs [7, 105]. Although nitrogen and phosphorous limitation are known to increase cellular lipid and carbohydrate contents in *Nannochloropsis* spp. [129-

132], no correlation was found between low amounts of dissolved nitrogen in the medium at the day of harvest (LED 465, CW LED, WW LED and FL; < 0.9 mg $N\text{-}NO_3^-$ L^{-1}) and lipid and carbohydrate contents. Consequently, theses cultures probably might have not been subjected to nutrient limitation. Although light stress (high light intensity) is known to affect positively the protein content of several microalgae [133], no effects were found on the lipid content in *N. gaditana* (15-2100 µmol s^{-1} m^{-2} ; [134]). Hence, one may exclude the effect of different amounts of photons traveling through a culture on lipid content as the consequence of altered light absorption properties of the algae, as it happened to LED 405-treated *N. oculata* cultures.

In *T. chuii*, the effect of nutrient limitation on the observed differences between LED light treatments is probably insignificant since all cultures showed depletion of $P\text{-}PO_4^{3-}$ and $N\text{-}NO_3^-$ at $t = 0$ and $t = 72$ h, respectively (data not shown). However, FL-lit *T. chuii* cultures grow faster and become a mature culture (see 4.2). They displayed a low protein:carbohydrate ratio and a significantly higher C:N ratio compared to algae illuminated with LEDs, which might indicate the onset of nutrient limitation [135], a situation similar to FL-treated *N. oculata* (see above).

The low carbohydrate content in *N. oculata* and *T. chuii* cultures exposed to LED 405 and CW treatments may be related to the high energetic blue photons released by these light sources, inducing an endogenous breakdown of carbohydrate reserves [74]. The accompanied increase of protein in the same cultures might be due to the accumulation of photo-protective pigments (i.e. carotenoids) in algae exposed to high energetic light irradiation [12, 16, 24, 54, 76, 77] as light-stressed algae increase their light harvesting complex proteins (LHCP) [54, 136], consisting of a protein, two carotenoids and 5 chlorophylls molecules [133, 137] to modulate light harvesting efficiency in the cell [134]. Some pigment complexes were found to contribute up to 30% of the total protein composition of algae and plants [68, 136]. Studies using discharge lamps with filters letting through a considerable portion of wavelengths below 450 nm [63, 74, 138] found similar consequences as those of the present study, i.e. blue-light related carbohydrate breakdown and an increased protein content in algae cultures. However, other studies using LEDs peaking at $\lambda_e \approx 470$ nm did not find any significant changes in the protein-carbohydrate ratio [8, 57]. Probably the breakdown of cellular carbohydrates and accumulation of proteins in algae is triggered by wavelengths lower than 450 nm. However, further research is necessary to draw a final conclusion about different blue wavelengths and their effects on biochemical composition on microalgae.

In the present study, N-prot factors were determined for the conversion from nitrogen content in DW to protein content in AFDW. The obtained values were generally slightly higher as compared to the literature for *N. oculata* (N-prot factor = 4.00 for the exponential phase and up to 5.59 for the stationary phase; [115]), whereas no previous investigated N-prot factor for *T. chuii* was found. However, *Tetraselmis gracilis* showed a lower N-prot factor (4.37-5.08; [115]) than *T. chuii* in the present study (7.2-7.8). One might advise caution for using N-prot factors to determine the protein content of experiments with different light qualities as nutrient assimilation by microalgae is strongly wavelength-dependent, influencing the N-prot factors. Incorporated intracellular nitrogen in microalgae can be fractioned to non-proteinaceous nitrogen (NPN) and proteinaceous nitrogen (PN). The former occurs mostly as inorganic intracellular nutrients (IIN), such as NO_3^-, NO_2^- and NH_3, and to a lesser extent in nucleic acids, chlorophylls or free amino acids. PN is often linked to proteinogenic amino acids [115]. Usually N-prot factors become higher with culture maturity and decreasing dissolved nitrogen concentration in the medium [115]. Especially in algae having high NPN variations among conditions and growth phases such as *N. oculata* [115], the C:N ratio needs to be taken carefully into account to detect eventual overestimations of N-prot factors under light qualities promoting nutrient assimilation. For example, *N. oculata* has usually a higher cellular total nitrogen content in cultures with low maturity, leading in turn to a lower C:N ratio as compared to ageing cultures [115]. In the present study, *N. oculata* treated with FL light showed the lowest N-prot factor, highest C:N ratio, high culture maturity and low nitrogen content in the medium, whereas LED 405 treated cultures showed the inverse trend. A correlation between low N-prot factors, high C:N ratios, high culture maturity and low nitrogen content in the medium was also found for *N. oculata* cultures exposed to LED 465, CW LED and WW LED cultures when compared to LED 630, LED 660 as well as for *T. chuii* exposed to LED 465, LED 660 and FL compared to LED 405, LED 630 and CW LED. However, in contrast to *N. oculata*, *T. chuii* did not show a linear relationship between C:N ratio and N-prot factors, which can be attributed to high culture maturity accompanied by reduced variations of N-prot factors and C:N ratios as well as the fact that *Tetraselmis* does not have a high variation of NPN content in biomass [115].

Interestingly, trends of low C:N ratios accompanied by low N-prot factors in immature cultures would also strengthen the conclusions of chapter 4.2 on the effects of light quality on the enhancement of algal culture maturity. Additionally, C:N ratios were also found to decrease with increasing light intensity in *Nannochloropsis* sp. [139], which might be also a factor in the present study due to low photon penetration into the culture as suggested in

chapter 4.1 for cells lit with LED 405. One may also consider that *N. oculata* exposed to LED 405 may accumulate a high content of growth inhibiting NO_2^- as IIN [115], which can be attributed to the low productivities found.

4.5 Fatty acids

Major fatty acids in *N. oculata* detected in this study were palmitic and mystric acids (SFAs), palmitoleic acid (MUFA) as well as AA and EPA (PUFAs), confirming earlier reports [15, 111, 139, 140]. Major fatty acids in *T. chuii* corresponded to palmitic (SFA), oleic and palmitoleic (MUFA) acids and LA and ALA (PUFA), matching those described in the literature for the genus *Tetraselmis* [25, 57]. The effects of light quality on the fatty acid composition in *Nannochloropsis* sp. has been previously reported by Das *et al.* [15]. However, although some fatty acids showed the same trends compared to the present study (e.g. no significant change of C16:0 between LED 465 and 660), most of their results do not fit to the present findings (e.g. Das *et al.* [15] found large differences of EPA levels among treatments, with white light inducing the highest contents, a result that the present study did not confirm). These discrepant observations might be due to different *Nannochloropsis* species used, different PPFDs employed by the authors or the use of inappropriate methods to measure light intensities. For *T. chuii*, the effects of light quality on fatty acid composition have not been reported previously. However, Abiusi *et al.* [57] observed a similar response pattern for *T. suecica* between blue and red LED lights, which would be equivalent to LED 465 and 630 light sources in the present study, respectively. For example, higher oleic acid accompanied by higher MUFA, lower total PUFA and similar SFA content was found under blue light ($\lambda_e \approx 465$ nm) compared to red LED light ($\lambda_e \approx 630$ nm). These similar findings suggest a similar response of fatty acids on light qualities in the genus *Tetraselmis*. In fact, some authors [105, 141, 142] mentioned higher contents of PUFAs when algae are growing actively. Considering again that culture maturity may be affected by nutrient consumption rate and depletion under FL and LED 465 treatments (as mentioned in chapter 4.2), it comes as no surprise that the PUFA content was lower compared to e.g. red LED light treatment. However, this pattern cannot be completely applied to the fatty acid profile of *N. oculata*. Culture maturation was mostly inhibited under LED 405 treatment, and thus in accordance with the aforementioned pattern. However, cells lit with FL do not support this hypothesis, since culture maturity was clearly most advanced under these conditions and PUFA content was still higher compared to the LED 630, LED 660, CW LED and WW LED treatments. The

response pattern of algae to fatty acid profiles in algae on light qualities is thus not completely understood and requires further research.

Nevertheless, disregarding the pathways of light quality effects on fatty acids in algae, but focusing on fatty acids used as high value bioproducts, such as nutraceuticals, light quality plays an important role for upgrading the biomass value. Fatty acids for human application require a high content of (*n*-3-) PUFAs and high ratios of PUFA/SFA[7] and low ratios of ∑*n*-6/∑*n*-3[8]. For further details see Pereira *et al.* [143].

Regarding *N. oculata* and taking this quality hallmark of fatty acids into account, LED 405 produced the highest quality fatty acids compared to other treatments: highest PUFA as well as *n*-3 (EPA) and *n*-6 (AA), leading to one of the lowest ∑*n*-6/∑*n*-3 ratios. *T. chuii*, showed the most favourable fatty acid profile under CW LED due to the highest total amount of PUFA (49.46±1.07 % of TFA), *n*-3 (ALA, EPA) and *n*-6 (LA) as well as highest PUFA/SFA (1.50) ratio among other treatments. Although the∑*n*-6/∑*n*-3 ratio of 0.47 was higher in CW LED treatment compared to FL treated algae (0.15) the obtained ratios are far below the recommended ratio of 10 (World Health Organization (WHO)). Therefore, the quantitative amount of the single fatty acid contributes more for the quality of fatty acids in *N. oculata* and *T. chuii* than the ∑*n*-6/∑*n*-3 ratio.

4.6 Nutrients

The consistently higher N-NO_3^- utilization of both algae grown under LED 405 and LED 465 compared to LED 630 and LED 660 light as well as the higher P-PO_4^{3-} utilization of LED 405 treated *N. oculata* cultures compared to experiments with red LEDs suggests a blue light dependent nutrient utilization. This nutrient uptake can be explained by the activation of reductases for NO_3^-, NO_2^- and PO_4^{3-} [56, 74]. Nonetheless, other studies on different *Chlorella* strains found red light as most effective for nutrient removal [14, 18, 52]. Caution must be used, however, as these studies employed inappropriate devices for measuring light intensity.

7 PUFA are highly important for human metabolism, occurring in cell membranes and cellular storage oils. PUFA have antibacterial, anti-inflammatory and antioxidant properties, among others, and can prevent cardiac diseases and tumour progression.

8 The World Health Organization (WHO) recommends a ∑*n*-6/∑*n*-3 ratio of lower than 10 as the synthesis of long chain *n*-3 and *n*-6 PUFA relies on the same enzymes. Therefore, the amount of one of these essential fatty acids comes with a decrease of the other (competition for the same metabolic enzymes). An occurring imbalance in the percentage of fatty acid can influence human health negatively.

Algae follow different strategies to assimilate NO_3^-. For instance, an obligatory autotroph such as *N. oculata* requires light (probably more blue light than other light ranges) for effective growth and nutrient utilization, whereas some green algae such as *T. chuii* can assimilate NO_3^- also in the dark (non-phototrophic conditions) [132]. Hipkin *et al.* [132] found that nutrient assimilation is in competition with carbon fixation. Thus, a photosynthetically generated electron can only be used for either nitrogen or carbon fixation. Therefore, a light quality-induced higher nutrient assimilation results in decreased carbon fixation and low C:N ratios in algal cultures showing a high NO_3^- and/or PO_4^{3-} consumption (e.g. LED 405 treatments).

High nutrient removal from growth medium might have two further aspects, being on the one hand the preferred wavelength for growth of a certain species and on the other the quantity [56] and quality of blue light. Concerning blue light quality, it is suggested that *N. oculata* is more effective in utilizing nutrients at low wavelengths (higher removal under LED 405 compared to LED 465), whereas *T. chuii* prefers longer wavelengths (higher removal under LED 465 compared to LED 405). However, the obtained data are limited as yet and do not allow a final conclusion. Thus, more studies about different species and different bluish wavelengths on nutrient removal need to be performed. This sought after wavelength for promoting highest nutrient utilisation by microalgae might be the same as the one responsible for carbohydrate breakdown as mentioned in section 4.4.

The culture medium of both algae can be classified as oxygen-rich due to photosynthetically released O_2 by the algae and the short culturing time (maximal 192 h). Under these conditions denitrification (reduction of NO_3^- over NO_2^- to N_2) is suppressed, and nitrification is supported, which would result in a transformation of NH_4^+ over NO_3^- to NO_2^- [144, 145]. The precursor NO_2^- under aerobic conditions is not stable and would be instantly transformed to NO_3^-. Because of these assumptions, only the NH_4^+concentration (not NO_2^-) was tested randomly among all treatments and algae, while a total of 6 spot tests were done at the end of the experiment (3 per algae). The organic fraction of nitrogen was expected to be negligible, as culturing time was short (max. 192 h), and nitrogen released from lysed cells and fixed into organic molecules are highly unlikely to play a significant role. Therefore the majority of the nitrogen in the system was present in form of NO_3^- and in the nitrogen incorporated in the microalgae.

4.7 CO_2 chapter and photosynthetic efficiency

The light energy supplied to the cultures together with biomass production until the time point of harvest weighed the most for calculating PE, whereas the elementary composition of the biomass played only a minor role. Therefore, LED 405 showed the lowest PE and FL the highest, because the energy supplied by LED 405 is 26 % higher while AFDW productivity was found to be 43 and 37 % lower than that of the FL treatment for *N. oculata* and *T. chuii* respectively. However, despite the lower biomass production under LED 660 compared to FL in both algae, the 15 % lower optical energy of LED 660 compensated this deficiency, resulting in no statistical differences between these treatments in both algae. The maximal observed PEs of 4.6 and 6.1 % for *N. oculata* and *T. chuii* grown under LED 660 are far from the theoretical calculated PE of 17 % for a light source emitting at 660 nm [3] and the maximal thermodynamic PE of 34 % under optimal wavelengths and conditions [24]. However, *T. chuii* showed similar PE as found by Abiusi et al (2013) for *T. suecica* (7.3% PE), growing in a flat panel reactor and exposed to red LEDs. The lower PE of *N. oculata* was caused by lower biomass productivity compared to *T. chuii* as resulted from the used salinity of ~35, whereas the optimum lays at ~25 for *N. oculata* [146]. However, PE plays also a major role for the energy required for producing biochemical components, as the same pattern became evident for the production most biochemical components per optical power input and PE (see Fig. A.10-10 in Annex 10 and Fig 3.6-1, respectively)

The CO_2 capture by algae always decreased when biomass production was low and nutrient consumption was high, being accompanied by low C:N ratios [132] (see chapter 4.6; e.g. algae exposed to LED 405 treatment). High nitrogen consumption suggests lower carbon (CO_2) fixation, whereas algae undergoing N-deficiency in the medium (i.e. mature cultures in, for example, FL treated algae) fix more carbon, storing it as carbohydrates or lipids [147].

4.8 FL vs. LEDs

The feasibility of LEDs was shown to be highly variable among manufacturers. The major reason for the choice of SMD 5050 LED strips was the easy processability and a high photon output per surface area. However, as some of the used wavelengths (e.g. 405 and 660 nm) were barely available in form of SMD 5050 strips, different LED brands had to be chosen. The different PCEs of the LED strips were dependent on the manufacturer (see Annex 3, Fig. A.3-3) and did not mirror the full properties of LEDs, making impossible a meaningful comparison of PCE between LED and FLs. However, considering only the optical output energy, it was shown that already near monochromatic LEDs with λ_e = 660 nm can

sustain similar PE than a FL specifically designed for photosynthetic growth (e.g. Silvania GroLux). A further combination of LEDs (HBLR; HRLB) was found to even exceed the efficiency in terms of biomass production at same PPFD. As with PE, energy efficiency for biochemical components production was similar between LED 660 and FL light sources. Nevertheless, the comparison between LEDs and FLs remains a difficult proposition since FL lamps release highly scattered light, whereas its LED counterpart, being a directional light source, releases photos only towards one given direction. Photons released by a FL can therefore travel towards the PBR from more than one side, elevating the total photon flux into the algal culture.

However, the choice of light quality for microalgal cultivation is dependent on the application area, space availability, and energy costs, harvesting procedures, amongst other factors. If an energy demanding extraction of a biochemical component such as protein is necessary, a high initial concentration of the biochemical component might be desired to lower the extraction costs [148] whereas costs for lighting may only play a secondary role. In this case, for *T. chuii* even LED 405 light can obtain a more satisfying protein production than FL light (see Annex 10; Fig. A.10-10B).

In wastewater treatment, where the area occupied is still the major bottleneck for a successful implementation, and flocculation is used as an energy-saving method to separate algae from the medium [146, 149], a light source promoting highly dense algal cultures, together with a high nutrient consumption rate, would have to be chosen to reduce the amount of flocculant needed [146]. For this purpose one may resort to the use of tailored light sources such as HRmix, HBmix or FL treatments used in the present study, as photons cannot penetrate deep enough into the culture, leading to low maximal concentrations. A more promising method might be the use of wavelengths beside the major pigment peaks of algae (e.g., 500-600 nm in SAR and Chlorophyta species) together with wavelength for preferred growth and/or nutrient utilization (e.g., blue light). These wavelengths penetrate deep into the culture due to low absorbance by the algae in these ranges coupled with a high cross section scattering [24] and thus nutrients are reduced to an minimum. On the other hand, for high value product production, where a fast production is required and high energy consumption can be tolerated, the choice of tailored light sources such as HRmix or HBmix in the present study might be beneficial, as the growth rate promotes high biomass production in a short time. However, this cultivation method might be less sustainable, when medium is not reused, as the amount of biomass per litre medium is low. Nevertheless, by using only two wavelengths (i.e. HRLB or HBLR), a promising compromise between both the

aforementioned cultivation techniques can be found, leading to acceptable biomass production together with the desired properties (e.g. high nutrient utilization).

Light sources designed by LEDs can supply a more precisely adjusted spectrum than any FL, making them a more reliable light source for microalgal production. However, established, renowned manufacturers should be chosen as the efficiency of LED modules strongly varies among manufacturers (see Annex 3, Fig. A.3-3).

5 Conclusion

Light quality was found to affect growth, cell morphology, total biomass and biochemical composition profile of *N. oculata* and *T. chuii*. However, it seems that only nutrient utilization and growth was directly affected by light quality, which in turn influenced the biochemical composition and induced morphologic cell changes. Light quality was also found to influence the quantity of photons traveling through an algal culture, which may lead to light inhibiting effects on the metabolism of algae and thus in turn may also alter the biochemical composition and nutrient utilization. It was shown that *N. oculata* and *T. chuii* require balanced light quality to sustain highest biomass productivities while unbalanced (monochromatic) or non-optimal white light qualities often reduced the biomass productivity. Comparisons of the present results with the literature turned out to be a difficult endeavour due to the frequent use of inappropriate measurements of the PPFDs of LEDs with sensors having highly different responses across the photosynthetic active range (400-700 nm). Research on the application of LEDs in microalgal production should use properly calibrated spectroradiometers whenever feasible. Although the price of LED-based lamps has significantly decreased, LED lighting systems are still four times more expensive than FLs on average and the quality of LED chips is still highly diverse among manufactures, affecting life time and PCEs as shown in the present study. Therefore the choice of reputed LED manufacturers is recommended to maintain the advantages of LED lighting technology. Higher initial costs can then be offset by longer lifetimes and better energy efficiency of LEDs compared to FLs. LED lighting technology is thus a feasible option for microalgal cultivation, in particular when supplemental light is needed for faster production of biomass and accumulation of specific biochemical components. Future research on LED use is promising for indoor microalgal cultivation, improving reliability of research on the light requirements of biological and molecular processes in photosynthetic organisms, which will accelerate the establishment of this novel lighting source. Furthermore, cultivation of

microalgae in a highly energy-efficient manner can be envisaged using dimmed LEDs controlled by a combination of high-frequency PWM and amplitude modulation (AM) (see Annex 1). This application would require a greater number of LEDs to maintain the PPFD needed for cultivation. Nevertheless, because LEDs are not fully exploited when dimmed, heat generation is reduced, prolonging the lifetime of LED modules and possibly rendering LED cooling unnecessary, which are two critical factors for successful application of LEDs in microalgal production.

References

1. Schulze, P.S.C., Barreira, L.A., Pereira, H.G.C., Perales, J.A., and Varela, J.C.S. (2014) Light emitting diodes (LEDs) applied to microalgal production. *Trends in Biotechnology.* **32**, 422-430
2. Chen, Y.-C. and Lee, M.-C. (2012) Double-power double-heterostructure light-emitting diodes in microalgae, *Spirulina platensis* and *Nannochloropsis oculata*, cultures. *Journal of Marine Science and Technology.* **20**, 233-236
3. Blanken, W., Cuaresma, M., Wijffels, R.H., and Janssen, M. (2013) Cultivation of microalgae on artificial light comes at a cost. *Algal Research.* **2**, 333-340
4. Carvalho, A., Silva, S., Baptista, J., and Malcata, F.X. (2011) Light requirements in microalgal photobioreactors: an overview of biophotonic aspects. *Applied Microbiology and Biotechnology.* **89**, 1275-1288
5. Wilson, R.P. (1994) Utilization of dietary carbohydrate by fish. *Aquaculture.* **124**, 67-80
6. Enright, C.T., Newkirk, G.F., Craigie, J.S., and Castell, J.D. (1986) Evaluation of phytoplankton as diets for juvenile *Ostrea edulis*. *Journal of Experimental Marine Biology and Ecology.* **96**, 1-13
7. Brown, M.R., Jeffrey, S.W., Volkman, J.K., and Dunstan, G.A. (1997) Nutritional properties of microalgae for mariculture. *Aquaculture.* **151**, 315-331
8. Baba, M., Kikuta, F., Suzuki, I., Watanabe, M.M., and Shiraiwa, Y. (2012) Wavelength specificity of growth, photosynthesis, and hydrocarbon production in the oil-producing green alga *Botryococcus braunii*. *Bioresource Technology.* **109**, 266-270
9. Otero, A., García, D., and Fábregas, J. (1997) Factors controlling eicosapentaenoic acid production in semicontinuous cultures of marine microalgae. *Journal of Applied Phycology.* **9**, 465-469

10. Castro Araújo, S. and Garcia, V.M.T. (2005) Growth and biochemical composition of the diatom *Chaetoceros cf. wighamii brightwell* under different temperature, salinity and carbon dioxide levels. I. Protein, carbohydrates and lipids. *Aquaculture.* **246**, 405-412
11. Massa, G.D., Kim, H.-H., Wheeler, R.M., and Mitchel, C.A. (2008) Plant productivity in response to LED lighting. *HortScience.* **43**, 1951–1956
12. Olle, M. and Viršile, A. (2013) The effects of light-emitting diode lighting on greenhouse plant growth and quality. *Agricultural and Food Science.* **22**, 223-234
13. US–DOE (2013) *Solid–state lighting research and development, Multi–Year Program Plan*, Secondary Solid–state lighting research and development, Multi–Year Program Plan: Office of Energy Efficiency & Renewable Energy, United States Department of Energy.
14. Zhao, Y., Wang, J., Zhang, H., Yan, C., and Zhang, Y. (2013) Effects of various LED light wavelengths and intensities on microalgae-based simultaneous biogas upgrading and digestate nutrient reduction process. *Bioresource Technology.* **136**, 461-468
15. Das, P., Lei, W., Aziz, S.S., and Obbard, J.P. (2011) Enhanced algae growth in both phototrophic and mixotrophic culture under blue light. *Bioresource Technology.* **102**, 3883-3887
16. Fu, W., Guðmundsson, Ó., Paglia, G., Herjólfsson, G., Andrésson, Ó., Palsson, B., and Brynjólfsson, S. (2013) Enhancement of carotenoid biosynthesis in the green microalga *Dunaliella salina* with light-emitting diodes and adaptive laboratory evolution. *Applied Microbiology and Biotechnology.* **97**, 2395-2403
17. Lunka, A. and Bayless, D. (2013) Effects of flashing light-emitting diodes on algal biomass productivity. *Journal of Applied Phycology.* **25**, 1679-1685
18. Yan, C., Zhang, L., Luo, X., and Zheng, Z. (2013) Effects of various LED light wavelengths and intensities on the performance of purifying synthetic domestic sewage by microalgae at different influent C/N ratios. *Ecological Engineering.* **51**, 24-32
19. Koc, C., Anderson, G.A., and Kommareddy, A. (2013) Use of red and blue light-emitting diodes (LED) and fluorescent lamps to grow microalgae in a photobioreactor. *The Israeli Journal of Aquaculture.* **65**, IJA_65.2013.797
20. Kommareddy, A.R. and Anderson, G.A., *Study of light as a parameter in the growth of algae in a photo–bioreactor (PBR)*, in *ASAE International Meeting*. 2003: Las Vegas, USA.

21. Ross, J. and Sulev, M. (2000) Sources of errors in measurements of PAR. *Agricultural and Forest Meteorology.* **100**, 103-125
22. Barnes, C., Tibbitts, T., Sager, J., Deitzer, G., Bubenheim, D., Koerner, G., and Bugbee, B. (1993) Accuracy of quantum sensors measuring yield photon flux and photosynthetic photon flux. *HortScience.* **28**, 1197-1200
23. Yam, F. and Hassan, Z. (2005) Innovative advances in LED technology. *Microelectronics Journal.* **36**, 129-137
24. Pilon, L., Berberoğlu, H., and Kandilian, R. (2011) Radiation transfer in photobiological carbon dioxide fixation and fuel production by microalgae. *Journal of Quantitative Spectroscopy and Radiative Transfer.* **112**, 2639-2660
25. Teo, C.L., Atta, M., Bukhari, A., Taisir, M., Yusuf, A.M., and Idris, A. (2014) Enhancing growth and lipid production of marine microalgae for biodiesel production via the use of different LED wavelengths. *Bioresource Technology.* **162**, 38-44
26. Jeong, H., Lee, J., and Cha, M. (2013) Energy efficient growth control of microalgae using photobiological methods. *Renewable Energy.* **54**, 161-165
27. Tsao, J.Y., Coltrin, M.E., Crawford, M.H., and Simmons, J.A. (2010) Solid-state lighting: An integrated human factors, technology, and economic perspective. *Proceedings of the IEEE.* **98**, 1162-1179
28. Mynbaev, D.K. and Scheiner, L.L., (2006) Fiber-optic communications technology. Prentice Hall.
29. Miller, D.A. (1996) Optical physics of quantum wells. *Quantum Dynamics of Simple Systems," ed. G.-L. Oppo, SM Barnett, E. Riis, and M. Wilkinson (Institute of Physics, London, 1996).* 239-266
30. Crawford, M.H. (2009) LEDs for solid-state lighting: Performance challenges and recent advances. *Selected Topics in Quantum Electronics, IEEE Journal of.* **15**, 1028-1040
31. Kane, R., Sell, H., and Sell, K., (2002) Revolution in lamps: A chronicle of 50 years of progress., ed. n. ed.: Fairmount Press.
32. Azevedo, I.L., Morgan, M.G., and Morgan, F. (2009) The transition to solid-state lighting. *Proceedings of the IEEE.* **97**, 481-510
33. Oh, J.R., Cho, S.-H., Oh, J.H., Kim, Y.-K., Lee, Y.-H., Kim, W., and Do, Y.R. (2011) The realization of a whole palette of colors in a green gap by monochromatic phosphor-converted light-emitting diodes. *Optics express.* **19**, 4188-4198

34. Mueller-Mach, R., Mueller, G.O., Krames, M.R., Shchekin, O.B., Schmidt, P.J., Bechtel, H., Chen, C.H., and Steigelmann, O. (2009) All-nitride monochromatic amber-emitting phosphor-converted light-emitting diodes. *physica status solidi (RRL)-Rapid Research Letters.* **3**, 215-217
35. Park, Y., Park, J., Hwang, S., and Jeong, B. (2012) Light source and CO2 concentration affect growth and anthocyanin content of lettuce under controlled environment. *Horticulture, Environment, and Biotechnology.* **53**, 460-466
36. Tang, H., Chen, M., Garcia, M.E.D., Abunasser, N., Ng, K.Y.S., and Salley, S.O. (2011) Culture of microalgae *Chlorella minutissima* for biodiesel feedstock production. *Biotechnology and Bioengineering.* **108**, 2280-2287
37. Xu, B., Cheng, P., Yan, C., Pei, H., and Hu, W. (2013) The effect of varying LED light sources and influent carbon/nitrogen ratios on treatment of synthetic sanitary sewage using *Chlorella vulgaris. World Journal of Microbiology and Biotechnology.* **29**, 1289-1300
38. Yan, C. and Zheng, Z. (2014) Performance of mixed LED light wavelengths on biogas upgrade and biogas fluid removal by microalga *Chlorella* sp. *Applied Energy.* **113**, 1008-1014
39. Paradiso, R., Meinen, E., Snel, J., Marcelis, L., van Ieperen, W., and Hogewoning, S. (2009) Light use efficiency at different wavelengths in rose plants. *Acta Horticulturae.* **893**, 849-855
40. Tennessen, D.J., Bula, R.J., and Sharkey, T.D. (1995) Efficiency of photosynthesis in continuous and pulsed light emitting diode irradiation. *Photosynthesis Research.* **44**, 261-269
41. Grobbelaar, J.U., Nedbal, L., and Tichý, V. (1996) Influence of high frequency light/dark fluctuations on photosynthetic characteristics of microalgae photoacclimated to different light intensities and implications for mass algal cultivation. *Journal of Applied Phycology.* **8**, 335-343
42. Matthijs, H.C., Balke, H., Van Hes, U.M., Kroon, B., Mur, L.R., and Binot, R.A. (1996) Application of light-emitting diodes in bioreactors: Flashing light effects and energy economy in algal culture (*Chlorella pyrenoidosa*). *Biotechnology and Bioengineering.* **50**, 98-107
43. Keeling, P.J. (2013) The number, speed, and impact of plastid endosymbioses in eukaryotic evolution. *Annual Review of Plant Biology.* **64**, 583-607

44. Takaichi, S. (2011) Carotenoids in algae: distributions, biosyntheses and functions. *Marine Drugs.* **9**, 1101-1118
45. Itoh, K.-i., Nakamura, K., Aoyama, T., Kakimoto, T., Murakami, M., and Takido, T. (2014) The influence of wavelength of light on cyanobacterial asymmetric reduction of ketone. *Tetrahedron Letters.* **55**, 435-437
46. Chen, H.-B., Wu, J.-Y., Wang, C.-F., Fu, C.-C., Shieh, C.-J., Chen, C., Wang, C.-Y., and Liu, Y.-C. (2010) Modeling on chlorophyll *a* and phycocyanin production by *Spirulina platensis* under various light-emitting diodes. *Biochemical Engineering Journal.* **53**, 52-56
47. Wang, C.-Y., Fu, C.-C., and Liu, Y.-C. (2007) Effects of using light-emitting diodes on the cultivation of *Spirulina platensis. Biochemical Engineering Journal.* **37**, 21-25
48. Ho, S.-H., Chan, M.-C., Liu, C.-C., Chen, C.-Y., Lee, W.-L., Lee, D.-J., and Chang, J.-S. (2014) Enhancing lutein productivity of an indigenous microalga *Scenedesmus obliquus* FSP-3 using light-related strategies. *Bioresource Technology.* **152**, 275-282
49. Shu, C.H., Tsai, C.C., Liao, W.H., Chen, K.Y., and Huang, H.C. (2012) Effects of light quality on the accumulation of oil in a mixed culture of *Chlorella* sp. and *Saccharomyces cerevisiae. Journal of Chemical Technology and Biotechnology.* **87**, 601-607
50. Choi, B., Lim, J.-H., Lee, J., and Lee, T. (2013) Optimum conditions for cultivation of *Chlorella* sp. FC-21 using light emitting diodes. *Korean Journal of Chemical Engineering.* **30**, 1614-1619
51. Atta, M., Idris, A., Bukhari, A., and Wahidin, S. (2013) Intensity of blue LED light: A potential stimulus for biomass and lipid content in fresh water microalgae *Chlorella vulgaris. Bioresource Technology.* **148**, 373-378
52. Yan, C., Zhao, Y., Zheng, Z., and Luo, X. (2013) Effects of various LED light wavelengths and light intensity supply strategies on synthetic high-strength wastewater purification by *Chlorella vulgaris. Biodegradation.* **24**, 721-732
53. Rendon, S.M., Roldan, G.J.C., and Voroney, R.P. (2013) Effect of Carbon Dioxide Concentration on the Growth Response of Chlorella vulgaris Under Four Different Led Illumination. *International Journal of Biotechnology for Wellness Industries.* **2**, 125-131
54. Katsuda, T., Lababpour, A., Shimahara, K., and Katoh, S. (2004) Astaxanthin production by *Haematococcus pluvialis* under illumination with LEDs. *Enzyme and Microbial Technology.* **35**, 81-86

55. Beltran, L., Garzon-Castro, C., Valencia, D., and Uribe, V. (2013) Web control and monitoring system: Experimentation with *Haematococcus Pluvialis*. *International Journal of Engineering.* **26**, 1025-2495
56. Kim, T.-H., Lee, Y., Han, S.-H., and Hwang, S.-J. (2013) The effects of wavelength and wavelength mixing ratios on microalgae growth and nitrogen, phosphorus removal using *Scenedesmus* sp. for wastewater treatment. *Bioresource Technology.* **130**, 75-80
57. Abiusi, F., Sampietro, G., Marturano, G., Biondi, N., Rodolfi, L., D'Ottavio, M., and Tredici, M.R. (2013) Growth, photosynthetic efficiency, and biochemical composition of *Tetraselmis suecica* F&M-M33 grown with LEDs of different colors. *Biotechnology and Bioengineering.* **111**, 956-964
58. Chen, C.-Y., Chen, Y.-C., Huang, H.-C., Huang, C.-C., Lee, W.-L., and Chang, J.-S. (2013) Engineering strategies for enhancing the production of eicosapentaenoic acid (EPA) from an isolated microalga *Nannochloropsis oceanica* CY2. *Bioresource Technology.* **147**, 160-167
59. Costa, B.S., Jungandreas, A., Jakob, T., Weisheit, W., Mittag, M., and Wilhelm, C. (2013) Blue light is essential for high light acclimation and photoprotection in the diatom *Phaeodactylum tricornutum. Journal of Experimental Botany.* **64**, 483-493
60. Miao, H., Sun, L., Tian, Q., Wang, S., and Wang, J. (2012) Study on the effect of monochromatic light on the growth of the red tide diatom *Skeletonema costatum. Optics and Photonics Journal.* **2**, 152
61. Kwon, H.K., Oh, S.J., Yang, H.S., Kim, D.M., Kang, I.J., and Oshima, Y. (2013) Laboratory study for the phytoremediation of eutrophic coastal sediment using benthic microalgae and light emitting diode (LED). *Journal of the Faculty of Agriculture, Kyushu University.* **58**, 417-425
62. Yoshioka, M., Yago, T., Yoshie-Stark, Y., Arakawa, H., and Morinaga, T. (2012) Effect of high frequency of intermittent light on the growth and fatty acid profile of *Isochrysis galbana. Aquaculture.* **338**, 111-117
63. Marchetti, J., Bougaran, G., Jauffrais, T., Lefebvre, S., Rouxel, C., Saint-Jean, B., Lukomska, E., Robert, R., and Cadoret, J.P. (2013) Effects of blue light on the biochemical composition and photosynthetic activity of *Isochrysis* sp.(T-iso). *Journal of Applied Phycology.* **25**, 109-119
64. Hohmann-Marriott, M.F. and Blankenship, R.E. (2011) Evolution of photosynthesis. *Annual Review of Plant Biology.* **62**, 515-548

65. Tomitani, A., Okada, K., Miyashita, H., Matthijs, H.C., Ohno, T., and Tanaka, A. (1999) Chlorophyll *b* and phycobilins in the common ancestor of cyanobacteria and chloroplasts. *Nature.* **400**, 159-162
66. Grimm, B., (2007) Chlorophylls and bacteriochlorophylls: biochemistry, biophysics, functions and applications. Vol. 25. Springer.
67. Lee, C.-G. and Palsson, B.Ø. (1996) Photoacclimation of *Chlorella vulgaris* to red light from light-emitting diodes leads to autospore release following each cellular division. *Biotechnology Progress.* **12**, 249-256
68. Stadnichuk, I.N., Bulychev, A.A., Lukashev, E.P., Sinetova, M.P., Khristin, M.S., Johnson, M.P., and Ruban, A.V. (2011) Far-red light-regulated efficient energy transfer from phycobilisomes to photosystem I in the red microalga *Galdieria sulphuraria* and photosystems-related heterogeneity of phycobilisome population. *Biochimica et Biophysica Acta (BBA)-Bioenergetics.* **1807**, 227-235
69. Sánchez-Saavedra, M., Jiménez, C., and Figueroa, F. (1996) Far-red light inhibits growth but promotes carotenoid accumulation in the green microalga *Dunaliella bardawil. Physiologia Plantarum.* **98**, 419-423
70. Bussell, A.N. and Kehoe, D.M. (2013) Control of a four-color sensing photoreceptor by a two-color sensing photoreceptor reveals complex light regulation in cyanobacteria. *Proceedings of the National Academy of Sciences.* **110**, 12834-12839
71. Kianianmomeni, A. and Hallmann, A. (2014) Algal photoreceptors: in vivo functions and potential applications. *Planta.* **239**, 1-26
72. Beel, B., Prager, K., Spexard, M., Sasso, S., Weiss, D., Müller, N., Heinnickel, M., Dewez, D., Ikoma, D., and Grossman, A.R. (2012) A flavin binding cryptochrome photoreceptor responds to both blue and red light in *Chlamydomonas reinhardtii. The Plant Cell Online.* **24**, 2992-3008
73. Lin, C. (2002) Blue light receptors and signal transduction. *The Plant Cell Online.* **14**, 207-225
74. Kamiya, A. and Saitoh, T. (2002) Blue-light-control of the uptake of amino acids and of ammonia in *Chlorella* mutants. *Physiologia Plantarum.* **116**, 248-254
75. Pazos, J.V.P. and Izquierdo, P.F. (2011) Synthesis of neutral lipids in *Chlorella* sp. under different light and carbonate conditions. *CT&F-Ciencia, Tecnología y Futuro.* **4**, 47-58

76. Jahns, P. and Holzwarth, A.R. (2012) The role of the xanthophyll cycle and of lutein in photoprotection of photosystem II. *Biochimica et Biophysica Acta (BBA)-Bioenergetics.* **1817**, 182-193
77. Depauw, F.A., Rogato, A., d'Alcalá, M.R., and Falciatore, A. (2012) Exploring the molecular basis of responses to light in marine diatoms. *Journal of Experimental Botany.* **63**, 1575-1591
78. Mohsenpour, S.F. and Willoughby, N. (2013) Luminescent photobioreactor design for improved algal growth and photosynthetic pigment production through spectral conversion of light. *Bioresource Technology.* **142**, 147-153
79. Zeinalov, Y. and Maslenkova, L. (2000) On the action spectra of photosynthesis and spectral dependence of the quantum efficiency. *Bulgarian Journal of Plant Physiology.* **26**, 58-69
80. Redwood, M.D., Dhillon, R., Orozco, R.L., Zhang, X., Binks, D.J., Dickinson, M., and Macaskie, L.E. (2012) Enhanced photosynthetic output via dichroic beam-sharing. *Biotechnology Letters.* **34**, 2229-2234
81. Wu, D., Chen, M., Wang, Q., and Gao, W. (2013) Algae (*Microcystis* and *Scenedesmus*) absorption spectra and its application on Chlorophyll *a* retrieval. *Frontiers of Earth Science.* **7**, 522-530
82. Coltelli, P., Barsanti, L., Evangelista, V., Frassanito, A.M., Passarelli, V., and Gualtieri, P. (2013) Automatic and real time recognition of microalgae by means of pigment signature and shape. *Environmental Science: Processes & Impacts.* **15**, 1397-1410
83. Nhut, D.T. and Nam, N.B. (2010) Light-emitting diodes (LEDs): An artificial lighting source for biological studies. in *The Third International Conference on the Development of Biomedical Engineering in Vietnam*. Springer.
84. Elmoraghy, M. and Farag, I.H. (2012) Bio-jet fuel from microalgae: reducing water and energy requirements for algae growth. *Res Inventy.* **1**, 22-30
85. Khozin-Goldberg, I. and Boussiba, S. (2011) Concerns over the reporting of inconsistent data on fatty acid composition for microalgae of the genus *Nannochloropsis* (Eustigmatophyceae). *Journal of Applied Phycology.* **23**, 933-934
86. O'Connor, S., Moltschaniwskyj, N., Bolch, C.J., and O'Connor, W. (2012) Dietary influence on growth and development of flat oyster, *Ostrea angasi* (Sowerby, 1871), larvae. *Aquaculture Research.* **43**, 1317-1327

87. Lowry, O.H., Rosebrough, N.J., Farr, A.L., and Randall, R.J. (1951) Protein measurement with the Folin phenol reagent. *Journal of Biological Chemistry.* **193**, 265-275
88. Pomory, C.M. (2008) Color development time of the Lowry protein assay. *Analytical Biochemistry.* **378**, 216-217
89. Bligh, E.G. and Dyer, W.J. (1959) A rapid method of total lipid extraction and purification. *Canadian journal of biochemistry and physiology.* **37**, 911-917
90. Zhu, C. and Lee, Y. (1997) Determination of biomass dry weight of marine microalgae. *Journal of Applied Phycology.* **9**, 189-194
91. Clescerl, L.S., Greenberg, A.E., and Eaton, A.D., (1999) Standard Methods for the Examination of Water and Wastewater. Vol. 20. American Public Health Association (APHA).
92. Müller, R. and Wiedemann, F., *Die Bestimmung des Nitrats in Wasser*, in *Vom Wasser. Ein Jahrbuch für Wasserchemie und Wasserreinigungstechnik.* 1955, Verlag Chemie. p. 247-271.
93. Pereira, H., Barreira, L., Mozes, A., Florindo, C., Polo, C., Duarte, C.V., Custódio, L., and Varela, J. (2011) Microplate-based high throughput screening procedure for the isolation of lipid-rich marine microalgae. *Biotechnology for biofuels.* **4**, 1-12
94. Cooper, M.S., Hardin, W.R., Petersen, T.W., and Cattolico, R.A. (2010) Visualizing" green oil" in live algal cells. *Journal of Bioscience and Bioengineering.* **109**, 198-201
95. Mueller, J.L., Fargion, G.S., McClain, C.R., Mueller, J., Brown, S., Clark, D., Johnson, B., Yoon, H., Lykke, K., and Flora, S. (2003) Ocean optics protocols for satellite ocean color sensor validation, Revision 5, Volume VI: Special Topics in Ocean Optics Protocols, Part 2. *NASA Tech. Memo.* **211621**
96. Cleveland, J. and Weidemann, A.D., *Quantifying absorption by aquatic particles: A multiply scattering correction for glass-fiber filters*. 1993, DTIC Document.
97. Verhulst, P.-F. (1838) Notice sur la loi que la population suit dans son accroissement. *Correspondance Mathématique et Physique Publiée.* **10**, 113-121
98. Ruiz, J., Arbib, Z., Álvarez-Díaz, P., Garrido-Pérez, C., Barragán, J., and Perales, J. (2013) Photobiotreatment model (PhBT): a kinetic model for microalgae biomass growth and nutrient removal in wastewater. *Environmental Technology.* **34**, 979-991
99. Lasdon, L.S., Waren, A.D., Jain, A., and Ratner, M. (1978) Design and testing of a generalized reduced gradient code for nonlinear programming. *ACM Transactions on Mathematical Software (TOMS).* **4**, 34-50

100. Ruiz, J., Álvarez-Díaz, P., Arbib, Z., Garrido-Pérez, C., Barragán, J., and Perales, J. (2013) Performance of a flat panel reactor in the continuous culture of microalgae in urban wastewater: prediction from a batch experiment. *Bioresource Technology*. **127**, 456-463

101. Syrett, P. (1981) Nitrogen metabolism of microalgae. *Canadian Bulletin of Fisheries and Aquatic Sciences*. **210**, 182-210

102. Callejón-Ferre, A., Velázquez-Martí, B., López-Martínez, J., and Manzano-Agugliaro, F. (2011) Greenhouse crop residues: Energy potential and models for the prediction of their higher heating value. *Renewable and Sustainable Energy Reviews*. **15**, 948-955

103. Menden-Deuer, S., Lessard, E.J., and Satterberg, J. (2001) Effect of preservation on dinoflagellate and diatom cell volume and consequences for carbon biomass predictions. *Marine Ecology Progress Series*. **222**, 41-50

104. Oldenhof, H., Zachleder, V., and Van Den Ende, H. (2006) Blue-and red-light regulation of the cell cycle in *Chlamydomonas reinhardtii* (Chlorophyta). *European Journal of Phycology*. **41**, 313-320

105. Hodgson, P.A., Henderson, R.J., Sargent, J.R., and Leftley, J.W. (1991) Patterns of variation in the lipid class and fatty acid composition of *Nannochloropsis oculata* (Eustigmatophyceae) during batch culture. *Journal of Applied Phycology*. **3**, 169-181

106. Solovchenko, A., Khozin-Goldberg, I., Recht, L., and Boussiba, S. (2011) Stress-induced changes in optical properties, pigment and fatty acid content of *Nannochloropsis* sp.: Implications for non-destructive assay of total fatty acids. *Marine Biotechnology*. **13**, 527-535

107. Kandilian, R., Lee, E., and Pilon, L. (2013) Radiation and optical properties of *Nannochloropsis oculata* grown under different irradiances and spectra. *Bioresource Technology*. **137**, 63-73

108. Owens, T.G., Gallagher, J.C., and Alberte, R.S. (1987) Photosynthetic light-harvesting function of violaxanthin in *Nannochloropsis* spp. (Eustigmatophyceae). *Journal of Phycology*. **23**, 79-85

109. Yan, C., Luo, X., and Zheng, Z. (2013) Performance of purifying anaerobic fermentation slurry using microalgae in response to various LED light wavelengths and intensities. *Journal of Chemical Technology and Biotechnology*. **88**, 1622-1630

110. Bohren, C.F. and Huffman, D.R., (2008) Absorption and scattering of light by small particles. John Wiley & Sons.

111. Forján, E., Garbayo, I., Henriques, M., Rocha, J., Vega, J.M., and Vílchez, C. (2011) UV-A mediated modulation of photosynthetic efficiency, xanthophyll cycle and fatty acid production of *Nannochloropsis. Marine Biotechnology.* **13**, 366-375
112. Sánchez-Saavedra, M.d.P. and Voltolina, D. (2006) The growth rate, biomass production and composition of *Chaetoceros* sp. grown with different light sources. *Aquacultural Engineering.* **35**, 161-165
113. Palanichamy, S. and Rani, V. (2004) Observations on the long term preservation and culture of the marine microalga, *Nannochloropsis oculata. Journal of the Marine Biological Association of India.* **46**, 98-103
114. Lubián, L.M., Montero, O., Moreno-Garrido, I., Huertas, I.E., Sobrino, C., González-del Valle, M., and Parés, G. (2000) *Nannochloropsis* (Eustigmatophyceae) as source of commercially valuable pigments. *Journal of Applied Phycology.* **12**, 249-255
115. Lourenço, S.O., Barbarino, E., Lavín, P.L., Lanfer Marquez, U.M., and Aidar, E. (2004) Distribution of intracellular nitrogen in marine microalgae: calculation of new nitrogen-to-protein conversion factors. *European Journal of Phycology.* **39**, 17-32
116. Brown, M.R., Garland, C.D., Jeffrey, S.W., Jameson, I.D., and Leroi, J.M. (1993) The gross and amino acid compositions of batch and semi-continuous cultures of *Isochrysis* sp. (clone T.ISO), *Pavlova lutheri* and *Nannochloropsis oculata. Journal of Applied Phycology.* **5**, 285-296
117. Alsull, M. and Omar, W.M.W. (2012) Responses of *Tetraselmis sp.* and *Nannochloropsis* sp. isolated from Penang National Park coastal waters, Malaysia, to the combined influences of salinity, light and nitrogen limitation. in *Proceedings of the International Conference on Chemical, Ecology and Environmental Sciences (ICEES)*.
118. Lee, M.-Y., Min, B.-S., Chang, C.-S., and Jin, E. (2006) Isolation and characterization of a xanthophyll aberrant mutant of the green alga *Nannochloropsis oculata. Marine Biotechnology.* **8**, 238-245
119. Hein, M., Pedersen, M.F., and Sand-Jensen, K. (1995) Size-dependent nitrogen uptake in micro-and macroalgae. *Marine ecology progress series. Oldendorf.* **118**, 247-253
120. Materassi, R., Tredici MR, M.F., Sili C, Pelosi E, Vincenzini M, Torzillo G, Balloni W, Florenzano G, and K., W., *Development of a production size system for the mass culture of marine microalgae*, in *Energy from biomass*, P. W and D, P., Editors. 1983, D. Reidel Publishing Company: Dordrecht. p. 150-158.
121. Kehoe, D.M. and Gutu, A. (2006) Responding to color: the regulation of complementary chromatic adaptation. *Annual Review of Plant Biology.* **57**, 127-150

122. Terauchi, K., Montgomery, B.L., Grossman, A.R., Lagarias, J.C., and Kehoe, D.M. (2004) RcaE is a complementary chromatic adaptation photoreceptor required for green and red light responsiveness. *Molecular Microbiology.* **51**, 567-577
123. Mouget, J.-L., Rosa, P., and Tremblin, G. (2004) Acclimation of *Haslea ostrearia* to light of different spectral qualities–confirmation ofchromatic adaptation in diatoms. *Journal of Photochemistry and Photobiology B: Biology.* **75**, 1-11
124. Schofield, O., Bidigare, R.R., and Prézelin, B.B. (1990) Spectral photosynthesis, quantum yield and blue-green light enhancement of productivity rates in the diatom *Chaetoceros gracileand* the prymnesiophyte *Emiliania huxleyi. Marine Ecology Progress Series.* **64**, 175-186
125. Faust, M.A., Sager, J.C., and Meeson, B.W. (1982) Response of *prorocentrum mariae-lebouriae* (Dinophyceae) to light of different spectral qualities and irradiances: Growth and Pigmentation. *Journal of Phycology.* **18**, 349-356
126. Nelson, N.B. and Prezelin, B.B. (1990) Chromatic light effects of physiological modeling of absorption properties of heterocapsa pygmaea equals *glenodinium* sp. *Ine Ecology Progress Series.* **63**, 37-46
127. Kroon, B., Prézelin, B.B., and Schofield, O. (1993) Chromatic regulation of quantum yields for photosystem || charge seperation, oxygen evolution, and carbon fixation in *Heterocapsa pygmaea* (Pyrrophyta). *Journal of Phycology.* **29**, 453-462
128. Schofield, O., Prézelin, B., and Johnsen, G. (1996) wavelenght dependency of the maximum quantum yield of carbon fixation for two red tide Dinoflagellates, *Heterocapsa pygmaea* and *Prorocentrum minimum* (Pyrrophyta): Implication for measuring photosynthetic rates. *Journal of Phycology.* **32**, 574-583
129. Pal, D., Khozin-Goldberg, I., Cohen, Z., and Boussiba, S. (2011) The effect of light, salinity, and nitrogen availability on lipid production by *Nannochloropsis* sp. *Applied Microbiology and Biotechnology.* **90**, 1429-1441
130. Hu, H. and Gao, K. (2006) Response of growth and fatty acid compositions of *Nannochloropsis* sp. to environmental factors under elevated CO_2 concentration. *Biotechnology Letters.* **28**, 987-992
131. Bondioli, P., Della Bella, L., Rivolta, G., Chini Zittelli, G., Bassi, N., Rodolfi, L., Casini, D., Prussi, M., Chiaramonti, D., and Tredici, M.R. (2012) Oil production by the marine microalgae *Nannochloropsis* sp. F&M-M24 and *Tetraselmis suecica* F&M-M33. *Bioresource Technology.* **114**, 567-572

132. Hipkin, C., Thomas, R., and Syrett, P. (1983) Effects of nitrogen deficiency on nitrate reductase, nitrate assimilation and photosynthesis in unicellular marine algae. *Marine Biology*. **77**, 101-105
133. Cade-Menun, B.J. and Paytan, A. (2010) Nutrient temperature and light stress alter phosphorus and carbon forms in culture-grown algae. *Marine Chemistry*. **121**, 27-36
134. Simionato, D., Sforza, E., Corteggiani Carpinelli, E., Bertucco, A., Giacometti, G.M., and Morosinotto, T. (2011) Acclimation of *Nannochloropsis gaditana* to different illumination regimes: Effects on lipids accumulation. *Bioresource Technology*. **102**, 6026-6032
135. Fábregas, J., Patiño, M., Vecino, E., Cházaro, F., and Otero, A. (1995) Productivity and biochemical composition of cyclostat cultures of the marine microalga *Tetraselmis suecica. Applied Microbiology and Biotechnology*. **43**, 617-621
136. Bennett, J. (1983) Regulation of photosynthesis by reversible phosphorylation of the light-harvesting chlorophyll *a*/*b* protein. *Biochemical Journal*. **212**, 1-13
137. Carbonera, D., Agostini, A., Di Valentin, M., Gerotto, C., Basso, S., Giacometti, G.M., and Morosinotto, T. (2014) Photoprotective sites in the violaxanthin–chlorophyll *a* binding Protein (VCP) from *Nannochloropsis gaditana. Biochimica et Biophysica Acta (BBA)-Bioenergetics*. **1837**, 1235-1246
138. Kamiya, A. (1985) Light-induced changes in the molecular size of starch in colorless *Chlorella* cells. *Plant and cell physiology*. **26**, 759-763
139. Fábregas, J., Maseda, A., Domínguez, A., and Otero, A. (2004) The cell composition of *Nannochloropsis* sp. changes under different irradiances in semicontinuous culture. *World Journal of Microbiology and Biotechnology*. **20**, 31-35
140. Renaud, S., Parry, D., Thinh, L.-V., Kuo, C., Padovan, A., and Sammy, N. (1991) Effect of light intensity on the proximate biochemical and fatty acid composition of Isochrysis sp. and *Nannochloropsis oculata* for use in tropical aquaculture. *Journal of Applied Phycology*. **3**, 43-53
141. Guzmán, H.M., de la Jara Valido, A., Duarte, L.C., and Presmanes, K.F. (2010) Estimate by means of flow cytometry of variation in composition of fatty acids from *Tetraselmis suecica* in response to culture conditions. *Aquaculture International*. **18**, 189-199
142. Dunstan, G., Volkman, J., Barrett, S., and Garland, C. (1993) Changes in the lipid composition and maximisation of the polyunsaturated fatty acid content of three microalgae grown in mass culture. *Journal of Applied Phycology*. **5**, 71-83

143. Pereira, H., Barreira, L., Figueiredo, F., Custódio, L., Vizetto-Duarte, C., Polo, C., Rešek, E., Engelen, A., and Varela, J. (2012) Polyunsaturated fatty acids of marine macroalgae: potential for nutritional and pharmaceutical applications. *Marine Drugs.* **10**, 1920-1935
144. Satoh, H., Nakamura, Y., Ono, H., and Okabe, S. (2003) Effect of oxygen concentration on nitrification and denitrification in single activated sludge flocs. *Biotechnology and Bioengineering.* **83**, 604-607
145. Cabello, P., Roldán, M.D., and Moreno-Vivián, C. (2004) Nitrate reduction and the nitrogen cycle in archaea. *Microbiology.* **150**, 3527-3546
146. Araujo, G.S., Matos, L.J.B.L., Gonçalves, L.R.B., Fernandes, F.A.N., and Farias, W.R.L. (2011) Bioprospecting for oil producing microalgal strains: Evaluation of oil and biomass production for ten microalgal strains. *Bioresource Technology.* **102**, 5248-5250
147. Adams, C. and Bugbee, B. (2014) Nitrogen retention and partitioning at the initiation of lipid accumulation in nitrogen-deficient algae. *Journal of Phycology.* **50**, 356-365
148. Milledge, J.J. (2011) Commercial application of microalgae other than as biofuels: a brief review. *Reviews in Environmental Science and Biotechnology.* **10**, 31-41
149. Arbib, Z., Ruiz, J., Álvarez-Díaz, P., Garrido-Pérez, C., Barragan, J., and Perales, J.A. (2013) Long term outdoor operation of a tubular airlift pilot photobioreactor and a high rate algal pond as tertiary treatment of urban wastewater. *Ecological Engineering.* **52**, 143-153
150. Williamson, S.J. and Cummins, H.Z., (1983) Light and color in nature and art. Vol. 1. New York, USA,: Wiley.

Annexes

Annex 1

Author´s publication

Review

CellPress

Light emitting diodes (LEDs) applied to microalgal production

Peter S.C. Schulze[1,2], Luísa A. Barreira[1], Hugo G.C. Pereira[1], José A. Perales[2], and João C.S. Varela[1]

[1] Centre of Marine Sciences, University of Algarve, Campus de Gambelas, 8005-139 Faro, Portugal
[2] Centro Andaluz de Ciencia y Tecnología Marinas, University of Cadiz, Campus Universitario de Puerto Real, Cádiz, Spain

Light-emitting diodes (LEDs) will become one of the world's most important light sources and their integration in microalgal production systems (photobioreactors) needs to be considered. LEDs can improve the quality and quantity of microalgal biomass when applied during specific growth phases. However, microalgae need a balanced mix of wavelengths for normal growth, and respond to light differently according to the pigments acquired or lost during their evolutionary history. This review highlights recently published results on the effect of LEDs on microalgal physiology and biochemistry and how this knowledge can be applied in selecting different LEDs with specific technical properties for regulating biomass production by microalgae belonging to diverse taxonomic groups.

Light in microalgal production

Microalgal biomass is used as feed in aquaculture, bulk food, and as feedstock for food or feed supplements, nutraceuticals, and cosmetics, and has been considered as a promising feedstock for biofuel production [1,2]. Photoautotrophic growth of microalgae requires CO_2, a growth medium containing nutrients, such as nitrogen and phosphorus, and a light source. Under heterotrophic and mixotrophic conditions, many microalgal species are able to use organic matter as a source of carbon and other nutrients. Photosynthesis in photoautotrophic and mixotrophic microalgae can be driven by sunlight or artificial light. Although sunlight is the most cost-effective energy source for microalgal production, artificial light is still economically feasible when biomass is used as a feedstock for high-value products, such as food or feed supplements (e.g., carotenoids and n-3 polyunsaturated fatty acids) or nutraceuticals [1]. Artificial light also provides better regulation of the photosynthetic photon flux density (PPFD; see Glossary), photoperiod, and light spectra in microalgal production, which can result in gains in biomass productivity and quality, two key factors for the success of any agricultural or industrial product [2]. However, the use of artificial light sources comes at a cost, so their improvement in terms of photosynthetic and electronic efficiency can provide a wider and cheaper array of products obtained from microalgal biomass [2]. This strategy has already been recognized as useful for horticulture [3].

Artificial lighting in microalgal research and production usually involves fluorescence lamps (FLs), which have wide emission spectra, including wavelengths with low photosynthetic activity for certain microalgae [2]. Alternatively, light-emitting diodes (LEDs) can be used [1,3,4]. LEDs are long-lasting (~50 000 h), mercury-free, and fast-responding (nanosecond scale) artificial light sources emitting nearly monochromatic light at various wavelengths by virtue of solid-state electronics [3,4]. Hence, LEDs can also be applied to adjust the biochemical composition of the biomass produced by microalgae via single wavelengths at

Glossary

Color rendering index (CRI): indicates how true the color of an irradiated object is revealed by a particular light source to human eyes.
Color temperature (K): denotes the trend of a light spectrum towards bluish or reddish wavelengths and is related to the irradiation spectrum of a heated Planck's black body at a given temperature (K). The human eye perceives a black body heated to 2000 K as having a reddish tint, whereas at 10 000 K a black body has a more bluish appearance.
Luminous efficacy (lm/W): efficiency of electrical power transformation to optical energy as perceived by the human eye. This measure is commonly used to compare light sources. The absorption spectrum of light-harvesting complexes of photosynthetic organisms [11] may differ from that of the human eye [4], and thus luminous efficacy is not a suitable indicator of the quality of a light source for photoautotrophic cultivation. Light sources with the same wattage and the same PCE can have very different luminous efficacy, depending on their spectrum. For conversion of luminous efficacy to μmol photons s^{-1} W^{-1}, see [1].
Photosynthetically active photon flux density (PPFD): amount of photosynthetic active photons in μmol striking a surface of 1 m^2 in 1 s. The photosynthetically active wavelength range is 400–700 nm. However, algae and plants can be photosynthetically active between 380 and 750 nm. Measurement of the PPFD of light sources with narrow spectra using quantum sensors often causes significant over- or underestimation at certain wavelengths, and correction factors are essential [70,71].
Power conversion efficiency (PCE): ratio between the electrical optical output and input energy ($W_{output(optical)}/W_{input}$) of a illuminant as a percentage. When the absolute spectral irradiance (W m^{-2} nm^{-1}; obtained by radiometric measurements, for example) of an illuminant is known, PCE can be used to estimate the photon flux and photosynthetic efficiency.
White light: light composed of photons of different wavelengths among a broadband spectrum. It is usually evaluated in the human vision context via parameters such as the color temperature, color rendering index, or luminous efficacy.
λ_a and λ_e: maximum absorption and emission wavelengths, respectively. λ_{a_red} and λ_{a_blue} are absorption peaks within the red and blue light ranges, respectively. λ_{max} denotes the preferred wavelength for optimal growth (see Table S1 in the supplementary material online) or preferred wavelength for a metabolic effect (see Table 1 in the main text), whereas λ_{min} denotes an alternative preferred wavelength that may be suboptimal.

Corresponding author: Varela, J.C.S. (jvarela@ualg.pt).
Keywords: microalgae; light-emitting diodes (LEDs); light requirements; energy efficiency; microalgal biomass; microalgal biochemicals.

0167-7799/
 http://dx.doi.org/10.1016/j.tibtech.2014.06.001

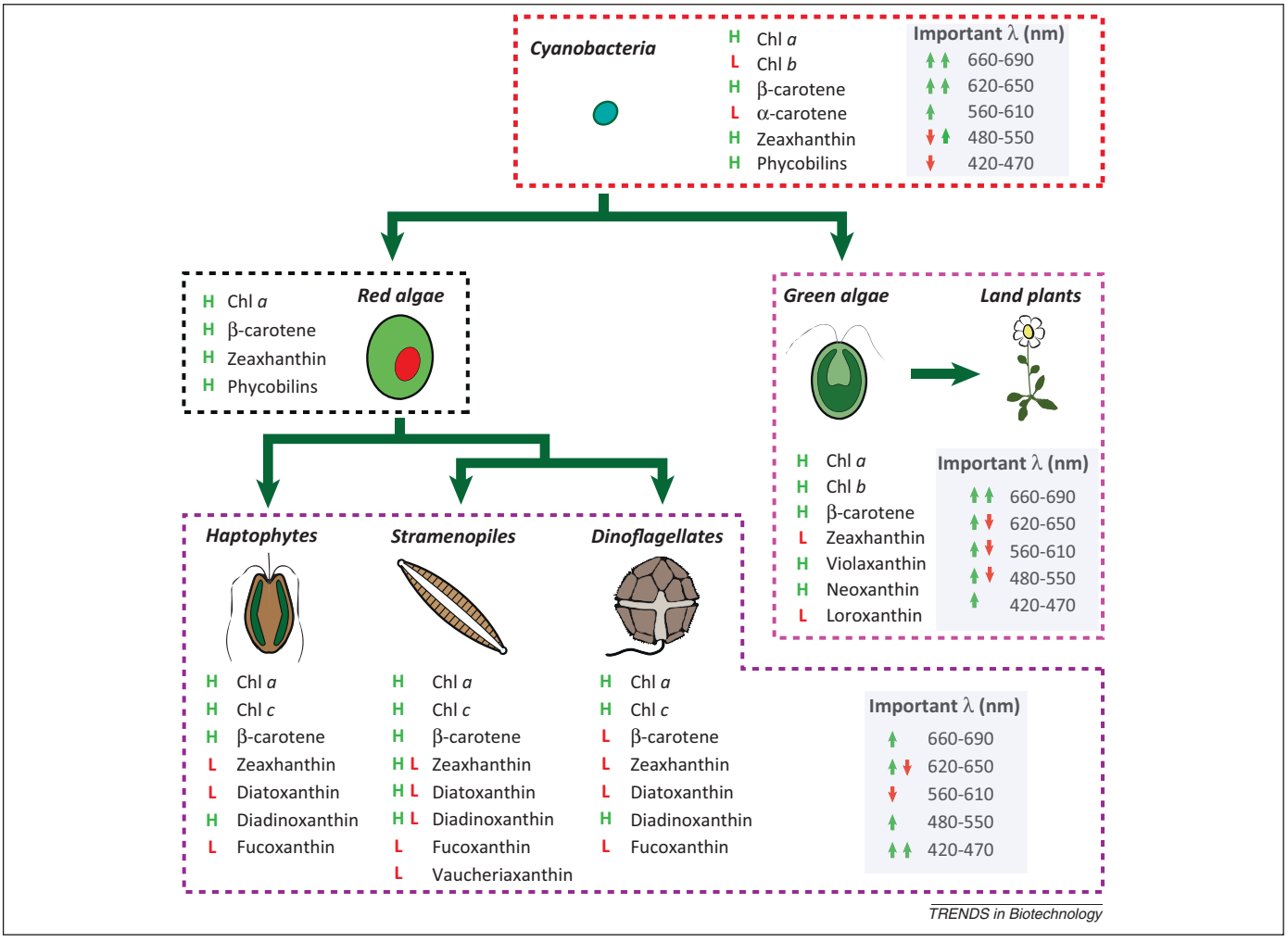

Figure 1. Approximate light requirements of microalgae according to results in Table S1 in the supplementary material, main pigments, and the evolutionary relationships among major microalgal megagroups [12–14]. Abbreviations: Chl, chlorophyll; H, high pigment content; L, low pigment content; H L, variation between high and low pigment contents among species.

different light intensities or pulse light frequencies [5–9]. Exposure of microalgae growing in photobioreactors to different light sources and the economic feasibility of this approach have been discussed previously [1,2,10,11]. However, the use of LEDs to supply specific light ranges for microalgal growth and to obtain high-value biochemical traits has not been reviewed extensively. LEDs will certainly become one of the world's most important light sources [4], so this review provides an overview of the application of various LED types to microalgal production.

Effects of light quality on algal growth

The number of photons at blue or red wavelengths that can be captured by a molecule of chlorophyll in an alga depends on the cellular architecture, pigment composition, and chloroplast arrangement. Interestingly, the evolutionary history of microalgae as purported by Keeling [12] seems to account for the preference of microalgae to grow under either blue ($\lambda \approx 420$–470 nm) or red ($\lambda \approx 660$ nm) light (Table S1 in the supplementary material online). This preference correlates well with the evolutionary megagroup of each microalga, which in turn seems to reflect the pigment composition of the light-harvesting complexes in their chloroplasts (Table S1 in the supplementary material online) [13]. As discussed by Keeling [12], a primary endosymbiotic event between a eukaryote and a chlorophyll-*b*-containing ancestor of cyanobacteria gave rise directly or indirectly to most photoautotrophic eukaryotes (Figure 1). Cyanobacteria, especially those lacking chlorophyll *b*, use chlorophyll *a* ($\lambda_a \approx 430$ and 680 nm) and accessory phycobiliproteins such as phycoerythrin ($\lambda_a \approx 550$ nm) and phycocyanin ($\lambda_a \approx 620$ nm), in light-harvesting protein–pigment (LHP) complexes [14]. As a result, cyanobacteria are able to utilize mostly red, yellow, and green light and, to a significantly lesser extent, blue light [12,15,16].

The first endosymbiotic event with the ancestor of cyanobacteria as the endosymbiont led to the appearance of chlorophytes (green algae) and rhodophytes (red algae) [17]. Red light is crucial for the growth of chlorophytes (and land plants) [13]. However, these organisms are able to utilize blue light more efficiently than cyanobacteria are, probably because of the loss of chlorophyll *b* by many cyanobacterial species [14] and a higher diversity of carotenoids in photosynthetic eukaryotes (Figure 1). As a trade-off, chlorophytes lack the ability to utilize yellow and green light extensively because they lost phycobilins during evolution [14]. Therefore, for chlorophyll-*a*-containing microalgae, major wavelengths are within the range 420–470 nm and/or 660–680 nm, and accessory

wavelengths are located below, between, or above these ranges. Exposure of microalgae to accessory wavelengths ($\lambda_e \approx$ 500–630 nm) alone consistently leads to lower biomass production compared to growth under either blue ($\lambda_e \approx$ 430–470 nm) or red ($\lambda_e \approx$ 660 nm) LEDs [6,12,15,18–24]. Green ($\lambda_e \approx$ 525–550 nm) LEDs were often found to be highly unsuitable for microalgae if used without additional light sources (Table S1 in the supplementary material online) [1,22,23,25,26].

Secondary endosymbiotic events involving heterotrophic eukaryotes and green algae gave rise to mixotrophic euglenids and chlorarachniophytes with a pigment composition and most probably light requirements similar to those of the ancestors of their plastids. Conversely, microalgae such as rhodophytes and glaucophytes are probably better adapted to shorter wavelengths (blue, green, yellow) than chlorophytes are because they retained phycobilins during evolution [12].

Cryptomonads and haptophytes (e.g., *Isochrysis*), belonging to the Hacrobia megagroup, and heterokontophytes (e.g., diatoms) and dinoflagellates, belonging to the Stramenopiles–Alveolata–Rhizaria (SAR) megagroup, are assumed to have evolved from secondary endosymbiosis of a heterotrophic eukaryote engulfing a rhodophyte, whereupon most species lost phycobilins. Instead, they developed a higher diversity of carotenoids and acquired chlorophyll *c*, a type of chlorophyll that absorbs strongly in the blue light range [27]. As a result, Hacrobia and SAR algae are usually better equipped for using bluish light compared to cyanobacteria and chlorophytes (Table S1 in the supplementary material online). Serial and tertiary endosymbiosis resulted in other eukaryotic photoheterotrophs (mostly dinoflagellates) with preferred wavelengths probably similar to those of the ancestors of their endosymbionts, although no studies on the light requirements of these microalgae have been found. Therefore, a shared evolutionary history of microalgae as suggested by Keeling's tree of endosymbiotic events [12] may provide information about the light requirements of algae within groups (Figure 1). For further information about pigments and their role in light harvesting for photosynthesis, see work by Cheng and Fleming [28] and Scholes *et al.* [29].

Effects of light quality on microalgal traits

In general, photons with a wavelength of 660–680 nm yield the highest quantum efficiencies in most plants and algae containing chlorophyll *a* (λ_{a_red} = 680 nm) and/or *b* (λ_{a_red} = 660 nm) [1,11]. The efficiency sharply decreases at longer wavelengths [30,31]. Interestingly, red to far-red light ($\lambda \approx$ 630-750 nm) induces high growth rates and smaller cells by accelerating the cell cycle in many microalgae of diverse evolutionary lines [1,16,19,32–35]. However, far-red light can suppress volumetric biomass production when supplementing a broadband light source [34] because it regulates light-harvesting mechanisms in microalgae [35]. In terrestrial plants, far-red light promotes flowering, fruit development, and biomass production, but it can also cause growth arrest due to a complete breakdown of photosynthesis if not applied properly [36].

Red to far-red light can be detected by photoreceptors such as phytochromes in land plants and charophytes, as well as multiple light-sensing photoreceptors in cyanobacteria [37,38]. In free-swimming chlorophytes, no obvious genes encoding phytochromes have been found. Instead, an "animal-like" cryptochrome seems to be the long-sought-after red receptor in chlorophytes, although it is unable to detect far-red light [39]. This multitude of red/far-red photoreceptors in different evolutionary lines strongly indicates that caution must be used when extrapolating how the red or far-red light range is detected and how it regulates growth. Clearly, further research is needed to understand how different photosynthetic organisms detect and respond to this range of the electromagnetic spectrum.

For shorter wavelengths, blue light influences gene expression and several metabolic pathways in algae and plants via photoreceptors such as cryptochromes, phototropins, aureochromes, and neochromes [38–42]. Blue light is, for example, responsible for endogenous breakdown of carbohydrate reserves [43], which may explain why the haptophyte *Isochrysis* sp. T-ISO exposed to blue light and grown in a chemostat displayed lower carbohydrate content than when grown under other wavelengths [44]. However, the opposite or no significant effect has been obtained in green algae grown in batch culture [23,24]. Kim *et al.* found that changing the ratio between red and blue light affected nutrient utilization more than biomass production [22] because of increased enzyme activity such as carbonic anhydrase activation for hydrogen carbonate (HCO_3^-) uptake [45] or nutrient uptake due to activation of reductases for nitrite, nitrate, and phosphorus utilization [21,43,45,46]. Blue light, most probably via photoreceptors such as phototropins, seems to induce pigment accumulation in several species (Table 1) [7,26,39,46]. Moreover, because the energy of blue photons is higher than that required for photosynthesis [10], blue light might result in nonphotosynthetic quenching (NPQ), generating reactive oxygen species (ROS) [7]. Therefore, to protect the photosynthetic apparatus against ROS, algae and plants accumulate photoprotective pigments (e.g., xanthophylls) [3,7,11,47,48].

Lastly, increased green light content within a broadband light source can increase leaf photosynthesis and biomass production in land plants [3,49,50] because these photons can penetrate through the canopy and promote photosynthesis in leaves located below [12,16,51]. Mohsenpour and Willoughby demonstrated that green light could induce pigmentation in algae [51]. However, further research is needed before drawing a definitive conclusion about the effect of green light on algae.

LEDs for microalgal production

Light quality influences the growth and biochemistry of microalgae, so artificial lighting can be used to manipulate the final biomass for specific uses, particularly for high-end markets. To design an artificial lighting system for microalgal growth, the electronic and photosynthetic efficiency of FLs and LEDs must be considered. On conversion of an electric current to light in LEDs (Box 1) and FLs (Box 2), energy losses occur because of thermal dissipation and inward light reflection and reabsorption, among other factors. Reduction of such inefficiency has resulted in higher power conversion efficiency (PCE) for LEDs

Table 1. Light quality effects on microalgal biochemical composition at specific wavelengths

Light	λ_{max} (nm)	Alga	Effects	Refs
Blue	460–475	*Arthrospira platensis* (syn. *Spirulina platensis*)	Lowest chl and phycocyanin content in biomass compared to yellow, green, red, and white LEDs	[16]
	440–470	*Chlorella* sp.	Higher lipid content in biomass compared to red (650–680 nm) LEDs	[19]
	500	*Chlorella sp.*	Blue light induces slightly higher lipid production compared to red light	[46]
	470	*Dunaliella salina*	β-Carotene and lutein accumulation when blue light was supplemented with red (660 nm)	[7]
	470	*Haematococcus pluvialis*	Accumulation of red pigments	[20]
	380–470	*Haematococcus pluvialis*	Astaxanthin accumulation	[26]
	NA	*Isochrysis* T-ISO	Higher protein content and lower carbohydrate and chl content per cell compared to white FLs	[44]
	NA	*Isochrysis galbana*	Higher DHA and phospholipid content compared to red LEDs under intermittent light (f = 10 kHz)	[72]
	475	*Nannochloropsis oceanica* CY2f	Blue and red (λ_e ~630 nm) LEDs showed highest EPA content in biomass compared to FLs and white and yellow LEDs	[73]
	470	*Nannochloropsis* sp.	Highest palmitoleic acid and lowest EPA content compared to red, green, and white LEDs under phototrophic conditions; highest total FAMEs per dry weight under blue, green, and white light, lowest under red when grown mixotrophically; similar FAME contents under phototrophic conditions	[6]
	450	*Nitzschia* sp.	Highest chl content compared to red (650 nm) and yellow (590 nm) LEDs	[74]
	NA	*Phaeodactylum tricornutum*	Lager pool of xanthophyll cycle pigments and higher chl *a* content compared to red and white LEDs (low light conditions)	[42]
	470	*Tetraselmis suecica* F&M-M33	Higher chl accumulation compared to cool white FLs and red, green, and blue LEDs; higher carbohydrate content for cells grown under blue compared to red LEDs	[23]
Green	NA	*Chlorella vulgaris*	Higher chl accumulation compared to blue, yellow, orange, and red broadband light spectra	[51]
	550	*Nannochloropsis* sp.	Higher AA content under phototrophic conditions compared to FLs and red and white LEDs	[6]
Red	660	*Botryococcus braun*ii Bot-144	Evidence of higher carotenoid/chlorophyll ratio compared to blue and green LEDs	[25]
	660	*Chlorella* sp.	Highest biogas production compared to yellow, blue, and white LEDs	[5]
	660	*Mychonastes homosphaera* (syn. *Chlorella minutissima*)	Increased C18:2 and decreased C18:3 content in FAME; no fatty acid changes between FLs and white LEDs; total FAMEs unaffected among all light sources	[57]
	680	*Nannochloropsis* sp.	Higher oleic acid content compared to blue, green, and white LEDs under phototrophic conditions	[6]
	NA	*Tetraselmis suecica* F&M-M33	EPA content increased under red light compared to blue, green, and white LEDs	[23]
Far-red	NA	*Dunaliella salina* (syn. *D. bardawil*)	Higher carotenoid levels compared to cells grown under FLs	[34]

Abbreviations: AA, arachidonic acid; chl, chlorophyll; EPA, eicosapentaenoic acid; FAME, fatty acid methyl ester; FL, fluorescent lamp; NA, spectrum not available or broadband spectrum.

(up to 50%) [4] compared to gas-discharge lighting technologies such as FLs (~30%) (Table S2 in the supplementary material online) [52,53].

At present, cool white phosphor-converted-LEDs (pc-LEDs) yield the highest PPFD per input wattage (PPFD/W) among white LEDs and can be highly photosynthetically active because of their blue emission peak ($\lambda_e \approx$ 440-460 nm) [54], which almost perfectly fits the blue absorption spectrum of LHP in many plants and algae [11,55,56]. Both FLs and pc-LEDs emit light within the range of photosynthetically important long wavelengths ($\lambda_e > 650$ nm), whereas most color-mixed-LEDs (cm-LEDs) display a sharp decrease in light emission at shorter wavelengths [4]. Furthermore, white pc-LEDs and FLs emit a broad spectrum of light with high photon release in the blue and green spectral ranges that decreases at $\lambda_e > 650$ nm. pc-LEDs and FLs have similar emission spectra, so pc-LEDs might be well suited for FL replacement within the same color temperature range without causing significant changes in algal growth rates and biochemical properties. This replacement would lead to more competitive energy usage for biomass production (Table S2 in the supplementary material online) [1,55,57]. Nevertheless, unlike FLs or pc-LEDs, single-color LEDs usually have higher PCE because they can emit at specific wavelengths without the use of phosphor layers and thus avoid losses (>30%) for conversion of higher- to lower-energy photons [4]. However, single-color LEDs emitting within the green–amber light range often have very low PCE, a problem known as the green gap or green–yellow gap [58].

In addition, more photons are usually released by LEDs emitting at longer wavelengths (e.g., red), resulting in higher PPFD/W ratios than for LEDs emitting at shorter wavelengths (e.g., blue) [1], because blue photons are more energetic than red photons. Specifically, red (λ_e = 660 nm) LEDs can emit double the number of photons that blue LEDs emit, whereas green LEDs emit approximately three times fewer photons than red LEDs do [5,18,58–60]. At face value, these results suggest that 660-nm red LEDs are able to sustain biomass growth with the highest energy

Box 1. How LEDs work

LEDs are semiconductor devices consisting of a positive (P doped) layer and a negative (N doped) layer (Figure IA). The P layer has an excess of electron holes in the valence band because of the presence of acceptor dopant atoms; the N layer has excess electrons in the conduction band owing to the presence of donor dopant atoms. When N and P semiconductors are brought together, excess carriers diffuse to the opposite side, resulting in a depletion region without free carriers. Application of an opposite voltage allows electrons from the N side and holes from the P side to enter the depletion region and recombine. This recombination corresponds to de-excitation of an electron from the conduction band to the valence band, and a photon with the corresponding difference in energy (energy gap between the bands) can be released. A blue–green (365–550 nm) InGaN semiconductor has a wider energy gap than an orange–red (560–650 nm) emitting AlGaInP diode or a red–infrared (630–940 nm) GaAlAs chip (Figure IB). Thus, recombination of semiconductor materials controls the wavelengths (color and energy of emitted light). To increase the efficiency, most (high-power) LED chips are built up in heterostructures with a more complex internal structure comprising more than one semiconductor material, which can also include multiple quantum wells. Further information on the theoretical background and application of these techniques is available in the literature [52,54,75,76]. White LEDs can be obtained by combining different LED chips in color-mixed LEDs (cm-LEDs) or by coating single blue chips with a photon-converting layer in phosphor-converted LEDs (pc-LEDs) [4].

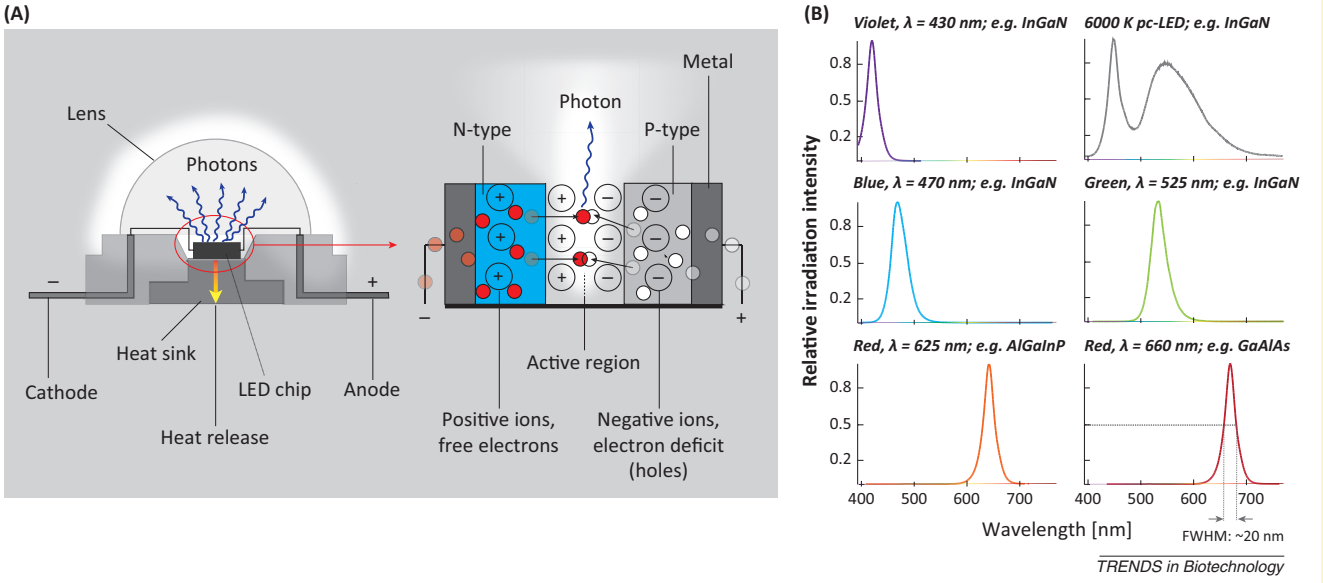

Figure I. **(A)** Simplified diagram showing how low-power (homostructured) LEDs work. **(B)** Emission spectra for different LEDs. The full width at half-maximum (FWHM) corresponds to the wavelength difference (usually 20 nm) for which the LED attains 50% of its maximum intensity.

efficiency [1]. However, LEDs with $\lambda_e > 680$ nm also release photons with photosynthetically inefficient wavelengths ($\lambda_e > 695$ nm) [31,61], leading to lower photon utilization by the algae and thus less biomass production per input wattage. Nevertheless, caution is needed because PPFD/W ratios and PCE may vary with the LED manufacturer. Finally, the fast response time of LEDs compared to that of FLs can also be beneficial, because LEDs can be used to grow algae under customized flashing light via pulse width modulation (PWM; Box 3), which increases biomass production [8,62,63] and might allow algae to exceed the proposed maximum photosynthetic efficiency of 17% [1].

Tailored light sources

Spectral matching

To maximize photosynthetic efficiency, all photons released from a light source should be captured by the photosynthetic apparatus of microalgae. A strategy to achieve a high level of light utilization is complete spectral matching of a light source to the photosynthetically active spectrum (PAS). However, this strategy can only yield an approximation because PAS measurement for microalgae is still difficult [30]. Determination of a general PAS for single taxonomic groups or megagroups, as done for green algae [64], may help to estimate the light quality required for a species belonging to a specific taxon. Absorption spectra of intact cells, however, are easier to obtain and may give a rough idea of the light quality needed for optimal growth. Comparison of the wavelengths of absorption peaks [65,66] and the preferred wavelengths (λ_{max} and λ_{min}) for growth (Table S1 in the supplementary material online) of algae within a given megagroup reveals a relatively good spectral match. However, the wavelength of the highest absorption peak seldom matches the preferred wavelength for optimal growth (either 420–470 or 660–670 nm) of cyanobacteria and green algae. These species usually show better growth and biomass production under 660-nm LEDs (Table S1 in the supplementary material online), whereas maximum absorption often occurs in the blue range of the electromagnetic spectrum [65,66]. This is because the absorption spectra of cells include the contributions of all cellular components able to absorb or scatter light, which may not necessarily contribute to the light-harvesting processes needed for photosynthesis and thus may mask the true light requirements for growth of a specific microalga.

Box 2. How fluorescent lights work

Electrodes located at each side of an FL are heated to induce emission of electrons into the space in front of the electrodes in a process called thermionic emission (Figure IA) [53]. An electric field is thereby built up and accelerates the electrons until their energy is high enough to excite gaseous mercury atoms, distributed in the space between the electrodes, from the ground stage to a higher energetic level. An excited mercury atom falls back to its ground stage and releases the energy difference by emitting a photon with energy of ~5.5 eV (8.83×10^{-19} J). This high-energy UV photon can then be absorbed by the phosphor coating on the inside of the tube and is transformed into less energetic visible and photosynthetically active light (380–750 nm or 1.7–3.2 eV). The energy difference (40–70%) is dissipated as heat, which drastically limits the FL efficiency [53]. Figure IB shows emission spectra for different FL types. The spectra of grow-light FLs have high levels of red light (630–680 nm) matching the chlorophyll *a* and *b* absorption peaks within the red spectral range. Therefore, these FLs can be used in growing photosynthetic organisms, although they are more expensive and less energetically efficient than FLs with major emission at shorter wavelengths (e.g., cool daylight FLs) [10]. The spectra of warm white FLs may not be suitable for growing algae in an energy-efficient manner because a significant proportion of their emission lies outside the major photosynthetic ranges (420–450 and 630–690 nm).

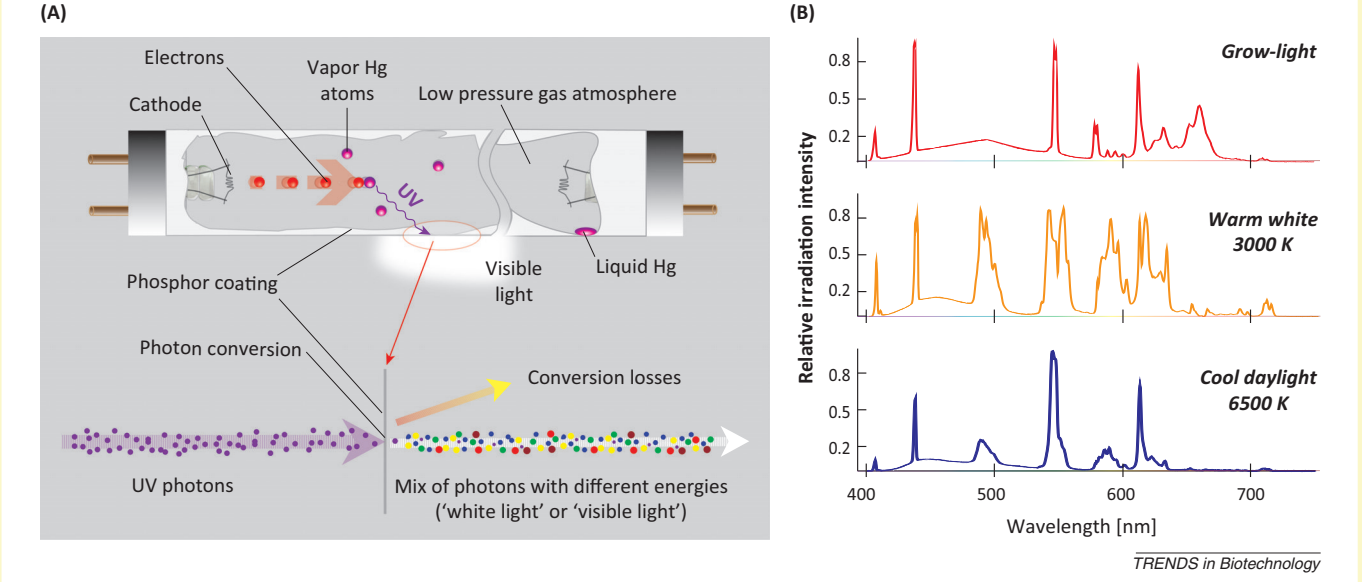

Figure I. **(A)** Simplified diagram showing how fluorescent lamps (FLs) work. **(B)** Emission spectra for different FL types, including grow-lights, warm white FL, and cold daylight FLs.

Light quality and design of LED usage

A tailored LED-based light source for high-volume production at the present state of the art might include pc-LEDs as a good starting point because their broadband phosphor emission at $\lambda_e \approx 560$ nm (Box 1) covers the green, yellow, and amber (500–610 nm) wavelength ranges. Violet–blue (preferably 420–450 nm) and red (660–670 nm) wavelengths can then be further adjusted to the species selected for cultivation. However, white pc-LEDs, especially those with cooler color temperatures, also emit photons with $\lambda_{e\_blue} \approx$ 440–460 nm (Box 1), so the levels of blue light available are higher. Moreover, as previously discussed, the taxonomy of the selected microalga may be used to predict the most important LEDs for growth (Figure 1 and Table S1 in the supplementary material online) or production of specific biochemicals (Table 1). Concerning red-to-blue ratios, land plants showed optimal biomass production when red LED light was supplemented with 10–30% blue light [67]. This suggests that similar red and blue ratios may also be suitable for green algae, because their plastids are closely related to those of terrestrial plants in terms of structure, metabolism, and biochemical composition. This assumption seems to be correct, because mixing of red and blue photons in this proportion has often increased biomass production compared to red light alone [7,21,60,68]. Regarding other taxa such as cyanobacteria and SAR microalgae, higher blue light content may be needed. However, a relative dearth of studies on red-to-blue ratios for these species means that no final conclusion is possible.

The success of increasing biomass productivity via tailored supplemental artificial light depends on environmental parameters for photosynthesis such as PPFD, light path length, CO_2 concentration, pH, macro- and micronutrient availability, and temperature, among other factors [2,35]. For example, nitrogen starvation can cause chromatic adaptation of cyanobacteria and red algae, resulting in degradation of phycobilisomes (phycobilin-containing light-harvesting complexes) and leading to diminished green light absorption [35]. Furthermore, the light path length of the bioreactor can influence the choice of wavelengths coming from a light source. A higher proportion of green–amber wavelengths might be beneficial for green and SAR algae grown in photobioreactors with a long light path or high-density cultures because photon absorption is lower, so they can travel deeper into the culture. In turn, the same light quality might be unsuitable for algae growing in flat panel photobioreactors with shorter light paths or low-density cultures. Lastly, Miao *et al.* concluded that the light saturation point for *Skeletonema costatum* is lower for a suitable than for an unsuitable light source [69]. If this result is confirmed in other species, growth of

Box 3. Dimming of LEDs

The PPFD of LEDs can be controlled by PWM or AM, also referred to as continuous current reduction (CCR) [77,78]. PWM entails the use of alternating states in which the current is completely turned either on or off. At a fixed frequency, the relative duration of the on-period (duty cycle) can be regulated. A low duty cycle of 10% means that the LED is on for 10% of the on-and-off cycle. Alternatively, AM is achieved by reducing the current intensity, which in turn leads to decreased light output [77,78]. The luminous efficacy of the two dimming methods varies, though AM can reach 200% of the nominal efficacy of an LED provided by the supplier when dimmed to 10% of its nominal current. Conversely, at the same dimming level, PWM provides only 70% of the nominal efficacy [77]. AM dimming can be used to prevent photoinhibition during early growth stages because photons are emitted continuously over time at low PPFD. By contrast, PWM-dimmed LEDs emit almost all photons within the LED capacity in a short duty cycle of flashing light, during which microalgae can be exposed to the fully available PPFD [8]. Because photosynthesis does not require continuous lighting [8,62] and microalgae can display satisfactory photosynthetic rates even if the duration of the dark cycle is increased [62], PWM may be used as an effective tool for controlling microalgal growth. In addition, an increase in the instantaneous maximum PPFD within the duty cycle of flashing LEDs by increasing the voltage (overloading) and/or the amount of LEDs will probably not result in photoinhibition and the released photons may penetrate deeper into highly concentrated algal cultures, increasing biomass productivity with lower electrical power consumption [8]. However, both dimming methods can shift λ_e by ~10 nm [77,78] and may change the photon capture when these peaks move towards or away from the optimal LHP absorption range, thus affecting microalgal growth. It is questionable which dimming method produces the highest biomass per input energy, because both have the aforementioned advantages and disadvantages. High-frequency PWM with AM-controlled LEDs may be implemented to reduce wavelength shifts and combine the advantages of both methods [78].

microalgae at lower PPFD with lower energy consumption could be possible if tailored light sources are selected for specific microalgal strains, growth phases, or photobioreactors.

Concluding remarks and future perspectives

Over the last few years, the prices of LED-based lamps have significantly decreased; nevertheless, LED lighting systems are still four times more expensive than FLs on average. However, this higher initial cost can be offset by the longer lifetimes and often better energy efficiency of LEDs compared to FLs. LED lighting technology is thus a feasible option for microalgal cultivation, in particular when supplemental light is needed for faster production of biomass and accumulation of specific biochemical components. As a result, research on microalgae grown under LEDs of different colors has strongly increased over the last 2–3 years. However, the combined application of different LEDs has seldom been studied, especially for LEDs emitting between 500 and 630 nm or above 700 nm (far-red region). Unfortunately, in many studies that used white LEDs, information about the emission spectra used is rarely mentioned, so meaningful comparisons are not possible. Moreover, optical density measurements for biomass determination in experiments with microalgae under different light qualities might be prone to error because the cell size and pigment composition can strongly change with light quality. Measurements of the PPFD of LEDs with narrow bandwidths using quantum sensors may also lead to errors because the responses of these sensors vary across the photosynthetically active range (400–700 nm). Thus, research on the application of LEDs in microalgal production should use properly calibrated spectroradiometers whenever feasible. Despite these problems, future research on LED use is promising and may lead to higher energy efficiency for indoor microalgal cultivation and improved reliability of research on the light requirements of biological and molecular processes in photosynthetic organisms. Furthermore, cultivation of microalgae in a highly energy-efficient manner can be envisaged using dimmed LEDs controlled by a combination of high-frequency PWM and amplitude modulation (AM) (Box 3). This application would require a greater number of LEDs to maintain the PPFD needed for cultivation. Nevertheless, because LEDs are not fully exploited when dimmed, heat generation is reduced, prolonging the lifetime of LED modules and possibly rendering LED cooling unnecessary, which are two critical factors for successful application of LEDs in microalgal production.

Acknowledgments

We wish to thank Prof. Rui Guerra from the Physics Department of the University of Algarve for his support in providing information and reviewing the manuscript.

Appendix A. Supplementary data

Supplementary data associated with this article can be found, in the online version, at http://dx.doi.org/10.1016/j.tibtech.2014.06.001.

References

1 Blanken, W. *et al.* (2013) Cultivation of microalgae on artificial light comes at a cost. *Algal Res.* 2, 333–340
2 Carvalho, A.P. *et al.* (2011) Light requirements in microalgal photobioreactors: an overview of biophotonic aspects. *Appl. Microbiol. Biotechnol.* 89, 1275–1288
3 Olle, M. and Virsile, A. (2013) The effects of light-emitting diode lighting on greenhouse plant growth and quality. *Agric. Food Sci.* 22, 223–234
4 US DOE (2013) *Solid-State Lighting Research and Development. Multi-Year Program Plan*, Office of Energy Efficiency & Renewable Energy, United States Department of Energy
5 Zhao, Y. *et al.* (2013) Effects of various LED light wavelengths and intensities on microalgae-based simultaneous biogas upgrading and digestate nutrient reduction process. *Bioresour. Technol.* 136, 461–468
6 Das, P. *et al.* (2011) Enhanced algae growth in both phototrophic and mixotrophic culture under blue light. *Bioresour. Technol.* 102, 3883–3887
7 Fu, W. *et al.* (2013) Enhancement of carotenoid biosynthesis in the green microalga *Dunaliella salina* with light-emitting diodes and adaptive laboratory evolution. *Appl. Microbiol. Biotechnol.* 97, 2395–2403
8 Lunka, A.A. and Bayless, D.J. (2013) Effects of flashing light-emitting diodes on algal biomass productivity. *J. Appl. Phycol.* 25, 1679–1685
9 Yan, C. *et al.* (2013) Effects of various LED light wavelengths and intensities on the performance of purifying synthetic domestic sewage by microalgae at different influent C/N ratios. *Ecol. Eng.* 51, 24–32
10 Kommareddy, A.R. and Anderson, G.A. (2003) Study of light as a parameter in the growth of algae in a photo-bioreactor (PBR). In *ASAE International Meeting*. ASAE Paper No. 034057
11 Pilon, L. *et al.* (2011) Radiation transfer in photobiological carbon dioxide fixation and fuel production by microalgae. *J. Quant. Spectrosc. Radiat.* 112, 2639–2660
12 Keeling, P.J. (2013) The number, speed, and impact of plastid endosymbioses in eukaryotic evolution. *Annu. Rev. Plant Biol.* 64, 583–607
13 Takaichi, S. (2011) Carotenoids in algae distribution, biosyntheses and functions. *Mar. Drugs* 9, 1101–1118

14 Marriott, M.F.H. and Blankenship, R.E. (2011) Evolution of photosynthesis. *Annu. Rev. Plant Biol.* 62, 515–548
15 Itoh, K-I. *et al.* (2014) The influence of wavelength of light on cyanobacterial asymmetric reduction of ketone. *Tetrahedron Lett.* 55, 435–437
16 Chen, H.B. *et al.* (2010) Modelling on chlorophyll *a* and phycocyanin production by *Spirulina platensis* under various light-emitting diodes. *Biochem. Eng. J.* 53, 52–56
17 Tomitani, A. *et al.* (1999) Chlorophyll *b* and phycobilins in the common ancestor of cyanobacteria and chloroplasts. *Nature* 400, 159–162
18 Xu, B. *et al.* (2013) The effect of varying LED light sources and influent carbon/nitrogen ratios on treatment of synthetic sanitary sewage using *Chlorella vulgaris*. *World J. Microbiol. Biotechnol.* 29, 1289–1300
19 Shu, C.H. *et al.* (2012) Effects of light on the accumulation of oil in a mixed culture of *Chlorella* sp. and *Saccharomyces cerevisiae*. *J. Chem. Technol. Biotechnol.* 87, 601–607
20 Beltran, L.M. *et al.* (2013) Web control and monitoring system: experimentation with *Haematococcus pluvialis*. *Int. J. Eng.* 26, 219–228
21 Ho, S-H. *et al.* (2014) Enhancing lutein productivity of an indigenous microalga *Scenedesmus obliquus* FSP-3 using light-related strategies. *Bioresour. Technol.* 152, 275–282
22 Kim, T.H. *et al.* (2013) The effects of wavelength and wavelength mixing ratios on microalgae growth and nitrogen, phosphorus removal using *Scenedesmus* sp. for wastewater treatment. *Bioresour. Technol.* 130, 75–80
23 Abiusi, F. *et al.* (2014) Growth, photosynthetic efficiency, and biochemical composition of *Tetraselmis suecica* F&M-M33 grown with LEDs of different colors. *Biotechnol. Bioeng.* 111, 956–964
24 Rendón, S.M. *et al.* (2013) Effect of carbon dioxide concentration on the growth response of *Chlorella vulgaris* under four different LED illumination. *Int. J. Biotechnol. Wellness Ind.* 2, 125–131
25 Baba, M. *et al.* (2012) Wavelength specificity of growth, photosynthesis, and hydrocarbon production in the oil-producing green alga *Botryococcus braunii*. *Bioresour. Technol.* 109, 266–270
26 Katsuda, T. *et al.* (2004) Astaxanthin production by *Haematococcus pluvialis* under illumination with LEDs. *Enzyme Microb. Technol.* 35, 81–86
27 Grimm, B. *et al.*, eds (2006) *Chlorophylls and Bacteriochlorophylls: Biochemistry, Biophysics, Functions and Applications* (Advances in Photosynthesis and Respiration, Vol. 25), Springer
28 Cheng, Y.C. and Fleming, G.R. (2009) Dynamics of light harvesting in photosynthesis. *Annu. Rev. Phys. Chem.* 60, 241–262
29 Scholes, G.D. *et al.* (2011) Lessons from nature about solar light harvesting. *Nat. Chem.* 3, 763–774
30 Zeinalov, Y. and Maslenkova, L. (2000) On the action spectra of photosynthesis and spectral dependence of the quantum efficiency. *Bulg. J. Plant Physiol.* 26, 58–69
31 Tennessen, D.J. *et al.* (1995) Efficiency of photosynthesis in continuous and pulsed light emitting diode irradiation. *Photosynth. Res.* 44, 261–269
32 Koc, C. *et al.* (2013) Use of red and blue light-emitting diodes (LED) and fluorescent lamps to grow microalgae in a photobioreactor. *Isr. J. Aquac.* 65, 797 IJA_65 2013
33 Lee, C.G. and Palsson, B.Ø. (1996) Photoacclimation of *Chlorella vulgaris* to red light from light-emitting diodes leads to autospore release following each cellular division. *Biotechnol. Prog.* 12, 249–256
34 Saavedra, M.P.S. *et al.* (1996) Far-red light inhibits growth but promotes carotenoid accumulation in the green microalga *Dunaliella bardawil*. *Physiol. Plant* 98, 419–423
35 Stadnichuk, I.N. *et al.* (2011) Far-red light-regulated efficient energy transfer from phycobilisomes to photosystem I in the red microalga Galdieria suphuraria and photosystems-related heterogeneity of phycobilisome population. *Biochim. Biophys. Acta* 1807, 227–235
36 Tamulaitis, G. *et al.* (2005) High-power light-emitting diode based facility for plant cultivation. *J. Phys. D: Appl. Phys.* 38, 3182–3187
37 Bussell, A.N. and Kehoe, D.M. (2013) Hierarchical regulation between four-color and two-color cyanobacteriochromes. *Proc. Natl. Acad. Sci. U.S.A.* 110, 12834–12839
38 Kianianmomeni, A. and Hallmann, A. (2014) Algal photoreceptors *in vivo* functions and potential applications. *Planta* 239, 1–46
39 Beel, B. *et al.* (2012) A flavin binding cryptochrome photoreceptor responds to both blue and red light in *Chlamydomonas reinhardtii*. *Plant Cell* 24, 2992–3008
40 Lin, C. (2002) Blue light receptors and signal transduction. *Plant Cell* 14, 207–225
41 Ruyters, G. (1984) Effects of blue light on enzymes. In *Blue Light Effects in Biological Systems* (Senger, H., ed.), pp. 283–301, Springer
42 Costa, B.S. *et al.* (2013) Blue light is essential for high light acclimation and photoprotection in the diatom *Phaeodactylum tricornutum*. *J. Exp. Bot.* 64, 483–493
43 Kamiya, A. and Saitoh, T. (2002) Blue-light-control of the uptake of amino acids and of ammonia in *Chlorella* mutants. *Physiol. Plant* 116, 248–254
44 Marchetti, J. *et al.* (2013) Effects of blue light on the biochemical composition and photosynthetic activity of *Isochrysis* sp. (T-iso). *J. Appl. Phycol.* 25, 109–119
45 Giráldez, N. *et al.* (2000) Limiting CO_2 levels induce a blue light-dependent HCO_3^- uptake system in *Monoraphidium braunii*. *J. Exp. Bot.* 51, 807–815
46 Pazos, J.V.P. and Izquierdo, P.F. (2011) Synthesis of neutral lipids in *Chlorella* sp. under different light and carbonate conditions. *Cien. Tecnol. Fut.* 4, 47–58
47 Jahns, P. and Holzwarth, A.R. (2012) The role of the xanthophyll cycle and of lutein in photoprotection of photosystem II. *Biochim. Biophys. Acta* 1817, 182–193
48 Depauw, F.A. *et al.* (2012) Exploring the molecular basis of responses to light in marine diatoms. *J. Exp. Bot.* 63, 1575–1592
49 Kim, H.H. *et al.* (2004) Green-light supplementation for enhanced lettuce growth under red- and blue-light-emitting diodes. *Hortscience* 39, 1617–1622
50 Terashima, I. *et al.* (2009) Green light drives leaf photosynthesis more efficiently than red light in strong white light revisiting the enigmatic question of why leaves are green. *Plant Cell Physiol.* 50, 684–697
51 Mohsenpour, S.F. and Willoughby, N. (2013) Luminescent photobioreactor design for improved algal growth and photosynthetic pigment production through spectral conversion of light. *Bioresour. Technol.* 142, 147–153
52 Tsao, J.Y. *et al.* (2009) Solid-state lighting an integrated human factors, technology and economic perspective. *Proc. IEEE* 98, 1–17
53 Kane, R. *et al.*, eds (2002) *Revolution in Lamps: A Chronicle of 50 Years of Progress* (2nd edn), Fairmount Press
54 Crawford, M.H. (2009) LEDs for solid-state lighting performance: challenges and recent advances. *IEEE J. Sel. Top. Quant. Electron.* 15, 1028–1040
55 Chen, Y.C. and Lee, M.C. (2012) Double-power double heterostructure light-emitting diodes in microalgae *Spirulina platensis* and *Nannochloropsis oculata*, cultures. *J. Mar. Sci. Technol.* 20, 233–236
56 Park, Y.G. *et al.* (2012) Light source and CO_2 concentration affect growth and anthocyanin content of lettuce under controlled environment. *Hortic. Environ. Biotechnol.* 53, 460–466
57 Tang, H. *et al.* (2011) Culture of microalgae *Chlorella minutissima* for biodiesel feedstock production. *Biotechnol. Bioeng.* 108, 2280–2287
58 Müller-Mach, R. *et al.* (2009) All-nitride monochromatic amber-emitting phosphor-converted light-emitting diodes. *Phys. Status Solidi* 3, 215–217
59 Yan, C. *et al.* (2013) Effects of various LED light wavelengths and light intensity supply strategies on synthetic high-strength wastewater purification by *Chlorella vulgaris*. *Biodegradation* 24, 721–732
60 Yan, C. and Zheng, Z. (2014) Performance of mixed LED light wavelengths on biogas upgrade and biogas fluid removal by microalga *Chlorella* sp. *Appl. Energy* 113, 1008–1014
61 Paradiso, R. *et al.* (2011) Light use efficiency at different wavelengths in rose plants. *Acta Hortic.* 893, 849–856
62 Grobbelaar, J.U. *et al.* (1996) Influence of high frequency light/dark fluctuations on photosynthetic characteristics of microalgae photoacclimated to different light intensities and implications for mass algal cultivation. *J. Appl. Phycol.* 8, 335–343
63 Matthijs, H.C.P. *et al.* (1996) Application of light-emitting diodes in bioreactors: flashing light effects and energy economy in algal culture (*Chlorella pyrenoidosa*). *Biotechnol. Bioeng.* 50, 98–107
64 Redwood, M.D. *et al.* (2012) Enhanced photosynthetic output via dichroic beam-sharing. *Biotechnol. Lett.* 34, 2229–2234
65 Wu, D. *et al.* (2013) Algae (*Microcystis* and *Scenedesmus*) absorption spectra and its application on chlorophyll *a* retrieval. *Front. Earth Sci.* 7, 522–530

66 Coltelli, P. *et al.* (2013) Automatic and real time recognition of microalgae by means of pigment signature and shapes. *Environ. Sci. Process. Impacts* 15, 1397–1410
67 Nhut, D.T. and Nam, N.B. (2010) Light-emitting diodes (LEDs): an artificial lighting source for biological studies. *IFMBE Proc.* 27, 134–139
68 Elmoraghy, M. and Farag, I.H. (2012) Bio-jet fuel from microalgae reducing water and energy requirements for algae growth. *Int. J. Eng. Sci.* 1, 22–30
69 Miao, H. *et al.* (2012) Study on the effect of monochromatic light on the growth of the red tide diatom *Skeletonema costatum*. *Opt. Photonics J.* 2, 152–156
70 Ross, J. and Sulev, M. (2000) Sources of errors in measurements of PAR. *Agric. For. Meteorol.* 100, 103–125
71 Barnes, C. *et al.* (1993) Accuracy of quantum sensors measuring yield photon flux and photosynthetic photon flux. *Hortic. Sci.* 28, 1197–1200
72 Yoshioka, M. *et al.* (2012) Effects of high frequency of intermittent light on the growth and fatty acid profile of Isochrysis galbana. *Aquaculture* 338–341, 111–117
73 Chen, C-Y. *et al.* (2013) Engineering strategies for enhancing the production of eicosapentaenoic acid (EPA) from an isolated microalga *Nannochloropsis oceanica* CY2. *Bioresour. Technol.* 147, 160–167
74 Kwon, H.K. *et al.* (2013) Laboratory study for the phytoremediation of eutrophic coastal sediment using benthic microalgae and light emitting diode (LED). *J. Fac. Agric. Kyushu Univ.* 58, 417–425
75 Mynbaev, D.K. and Scheiner, L.L., eds (2006) *Fiber-Optic Communications Technology*, Prentice Hall
76 Miller, D.A.B. *et al.* (1996) Optical physics of quantum wells. In *Quantum Dynamics of Simple Systems* (Oppo, G.-L. *et al.*, eds), pp. 239–266, Institute of Physics
77 Gu, Y. *et al.* (2006) Spectral and luminous efficacy change of high-power LEDs under different dimming methods. *Proc. SPIE* 6337, 63370J
78 Beczkowski, S. and Nielsen, S.M. (2010) LED spectral and power characteristics under hybrid PWM/AM dimming strategy. In *Proceedings of the 2010 Energy Conversion Congress and Exposition*. pp. 731–735, IEEE Press

Annex 2

Calculation Lux to PPFD

Deduction of an approximate variation factor between measurements of illuminance (Si: Lux; lm m^{-2}) of near monochromatic light (FWHM: ~20-30 nm) measured by an optimal luxmeter and PPFD is described step by step. This calculation assumes a Gaussian normal distribution of photons peaking at λ_e (this includes most single colour LEDs and may thus be imprecise for most pc-LEDs). A more precise calculation for more complex spectra can only be obtained if detailed data about photon distribution (radiospectrometric measurements) and response spectrum of the used luxmeter are given, as proposed by Blanken *et al.* [3]. In this case, all equations mentioned below require an integration of light with wavelengths from 400 to 700 nm. However, in most studies these data are not provided to the readers. An example of LEDs with λ_e = 470 and 680 nm and the correct application of the relevant equations is given below.

The spectral irradiance ($\Phi_{\lambda,\Phi v}$; J m^{-2} s^{-1}) of a certain monochromatic light measured by a luxmeter can be determined as:

$$\Phi_{\lambda,\Phi v} = \frac{\Phi v}{V\lambda * \left(683 \frac{lm}{W}\right)} \quad (17)$$

where V_λ is the Photopic Luminous Efficacy at a given wavelength (i.e. 680 nm = 0.017000; 470 nm = 0.090980; listed in a table in Ref. [150]); and Φ_v, measured luminous emittance via luxmeter (lux; lm m^{-2}). The conversion factor 683 indicates that 683 Lumen (lm) correspond to one Watt (W) at a wavelength of 555 nm. The obtained spectral irradiance can also be directly measured via radiospectrometric measurements obtained in absolute spectral irradiance per area and wavelength (W m^{-2} nm^{-1}) or powermetric measurements at a defined wavelength (W m^{-2}).

The energy calculation of 1 µmol of a monochromatic light is defined as:

$$E_{\lambda,\mu mol} = \frac{h * c * N_A}{\lambda_{max} * 10^6} \quad (18)$$

h = Max Planck constant (6.626 x 10^{-34} J s^{-1})

c = speed of light (299,792,458 m s^{-1})

λ = wavelength of light (m).

N_A= Avogadro's number (6.02×10^{23} mol^{-1});

The averaged energy for LED with λ_{max} = 680 and 470 nm would thus be:

$E_{1umol\ photon\ \lambda(470)}$= 0,254515963966714 J µmol $photons^{-1}$

$E_{1umol\ photon\ \lambda(680)=}$ 0,175915445682876 J µmol $photons^{-1}$

Dividing the spectral irradiance (eq. 17) by the energy of 1 µmol of photons (eq. 18) at same λ_e gives the PPFD at a given λ_e and measured illuminance (eq. 19).

$$PPFD_{\lambda,\Phi v} = \frac{\Phi_\lambda}{E_{\lambda,\mu mol}} \tag{19}$$

Substituting Φ_v and $E_{\lambda,\mu mol}$ by eq. 17 and eq.18 gives eq. 20 being dependent on wavelength and illuninance.

$$PPFD_{\lambda,\Phi v} = \frac{\lambda_{max} * 10^6 * \Phi v}{V\lambda * \left(683 \frac{lm}{W}\right) * h * c * N_A} \tag{20}$$

The relation or rather variation factor $F_{\lambda 1,2}$ is the ratio between the PPFD of one wavelength (i.e. $PPFD_{\lambda 1}$ = 470 nm) and the PPFD of a second wavelength ($PPFD_{\lambda 2}$= 680 nm) measured via luxmeter.

$$F_{\lambda 1,2} = \frac{PPFD_{\lambda 1,\Phi v1}}{PPFD_{\lambda 2,\Phi v2}} \tag{21}$$

Substituting $PPFD_{\lambda 1,\Phi v1}$ and $PPFD_{\lambda 2,\Phi v2}$ by equation 20 for two different wavelengths allows the following simplification:

$$F_{\lambda 1,2} = \frac{\lambda_{max1} * \Phi v1 * V\lambda 2}{\lambda_{max2} * \Phi v2 * V\lambda 1} \tag{22}$$

When the given illuminance Φv is equal among tested treatments as is the case in most published studies as a ´similar light quantity´ is desired, Φv can be considered as constant:

$$F_{\lambda 1,2} = \frac{\lambda_1 * V_{\lambda 2}}{\lambda_2 * V_{\lambda 1}} \quad (23)$$

Substituting λ_1 $V_{\lambda 1}$ in equation 1 with the data of LED 470 ($V_{\lambda 470} = 0.0910$ and $\lambda_1 = 470$ nm) and λ_2 $V_{\lambda 2}$ with the data for LED 680 ($V_{\lambda 680} = 0.0170$ and $\lambda_2 \approx 680$ nm), the variation factor F can be estimated ($F_{(\lambda max\ 1\&2\ (470\ \&\ 680\ nm))} \approx 7.7$).

Annex 3

Quantum sensor response

As each quantum sensor has a different response at different wavelengths, a correction factor needs to be applied to the measured values in order to obtain the real PPFD. The spectral response of the used quantum sensor (Apogee MQ 100) was corrected by applying factors calculated by the relative spectral light distribution according to [21]. The obtained correction values were further validated my measuring the light energy of each LED type via an optical power meter (Thor Labs Inc.).

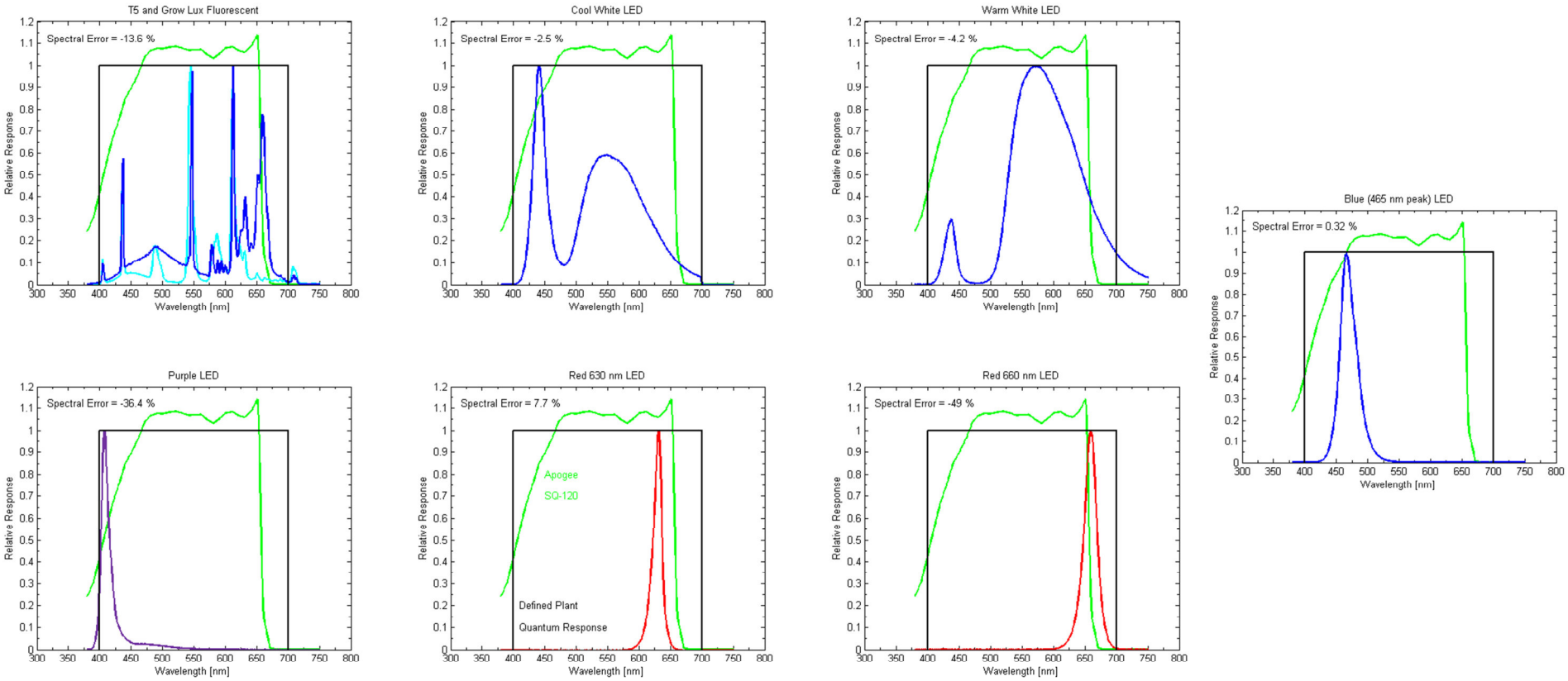

Figure A.3-1 Spectral response curve of the used apogee MQ 100 quantum sensor (green line) with calibration light source (T5; cyan spectrum), optimum quantum response curve (black line; equal response among all wavelengths between 400 and 700 nm). Errors of correction values were for LED 405, LED 465, LED 630, LED 660, CW LED, WW LED as well as FL 1.364, 1.032, 0.923, 1.490, 1.025, 1.042, and 1.135, respectively. T5 spectrum (top-left) was used to calibrate the quantum sensor data were kindly provided by Apogee Instruments **Inc.**

To determine the approximate relative efficiency between input wattage and output wattage per m^2 and input wattage and output PPFD, which also served the purpose to validate the correction factors provided by Apogee Instruments Inc., (Fig. A.3-1) an additional experiment was setup. At certain distances the optical power (Optical power meter, Thor Labs Inc.) and the PPFD (Apogee MQ 100) was measured in a dark room (Fig. A.3-2). The results are given in Fig. A.3-3.

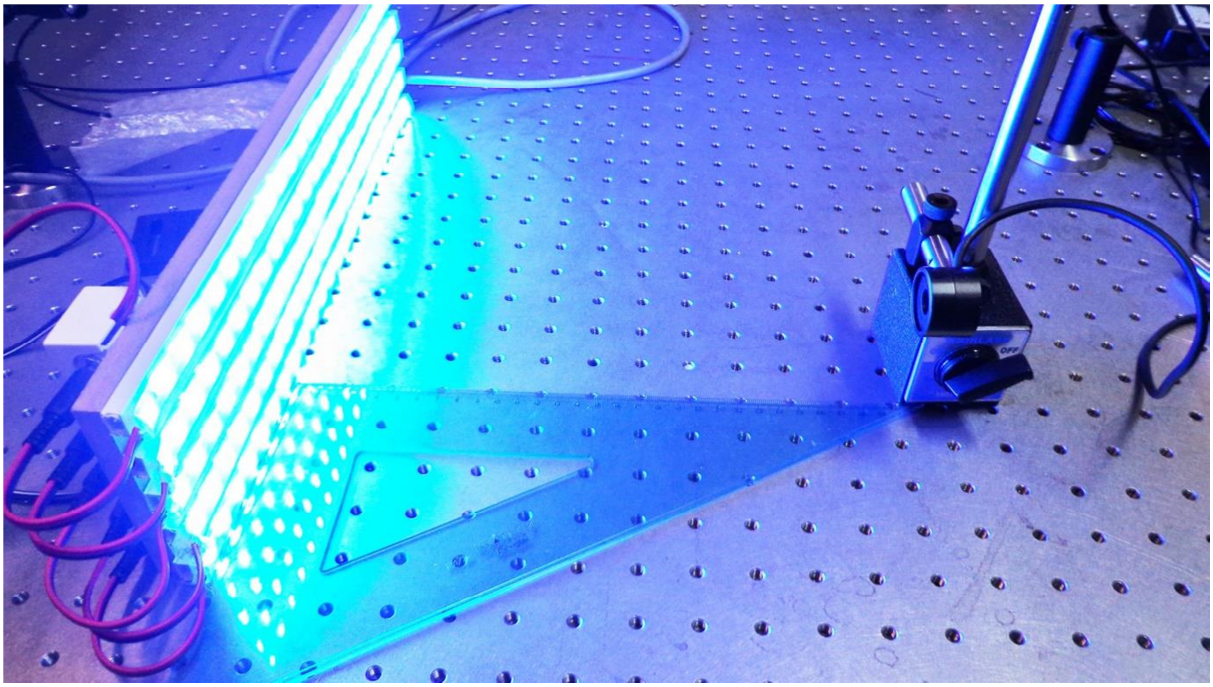

Figure A.3-2 Experimental setup for the estimation of approximate relative efficiency parameter (PPFD/W and $_{Wout\_optic}$ m^{-2} / W_{input}) of light sources under study.

However, obtained data can only be considered as approximate and relative values, since photons are scattering through space, being dependent on the reflector angle incorporated in the LEDs, geometry of the light source, amongst other factors. For example, a FL releases large amounts of photons upwards, which are not detected by the sensors [20]. Furthermore, the power meter was equipped with a flat sensor, detecting only photons that are traveling from the light source towards the sensor in a straight path, whereas the quantum sensor had a diffuse sensor, collecting also photons hitting the sensor at an angle. Therefore, at short distances, where light is more diffuse, higher PPFDs were measured via quantum sensor compared to the PPFD calculated via optical energy output measured by a power meter (data not shown). However, for validating purposes of the correction factors for the quantum sensor this experimental setup can be considered as sufficient. For further information about measuring light sources see also Kommareddy and Anderson [20].

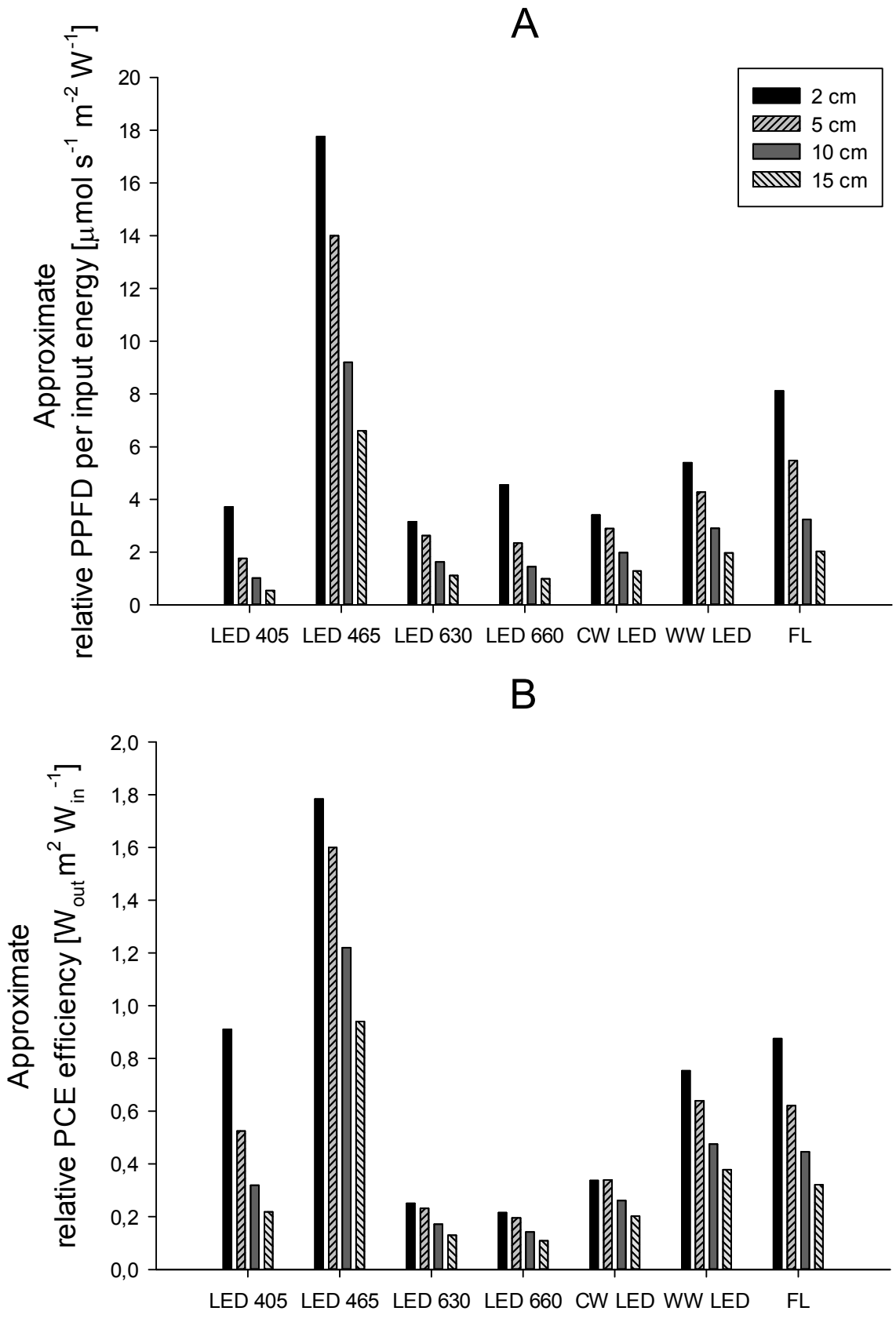

Figure A.3-3 Approximate efficiency parameter PPFD/W (A) and W_{out_optic} m^{-2}/W_{input} (B) of light sources at different distances.

For the experiments, all light sources were operated under nominal currents while power ranged between 20 and 28 watts (measured via electric meter), depending on the light source. LED 465 was clearly the highest effective light source in terms of PPFD/W and PCE/m^2, followed by FL. Low efficiencies were obtained by LED 660 and 630.

Annex 4

Standard curve protein determination

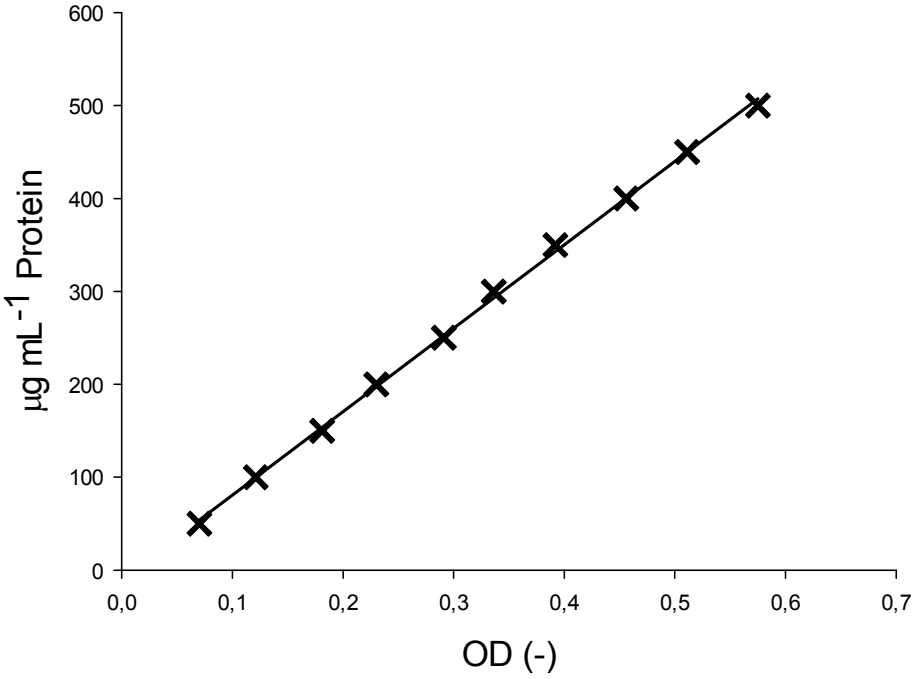

Figure A.2-4 Calibration curve for Lowry [87] protein analysis. Concentration of bovine serum albumin (BSA) standard is plotted against optical density (OD) determined at 750 nm. Equation was: Y=897.76x- 8.964 (R^2 = 0.9991; r = 0.9995; p < 0.01).

Annex 5

Absorption spectra

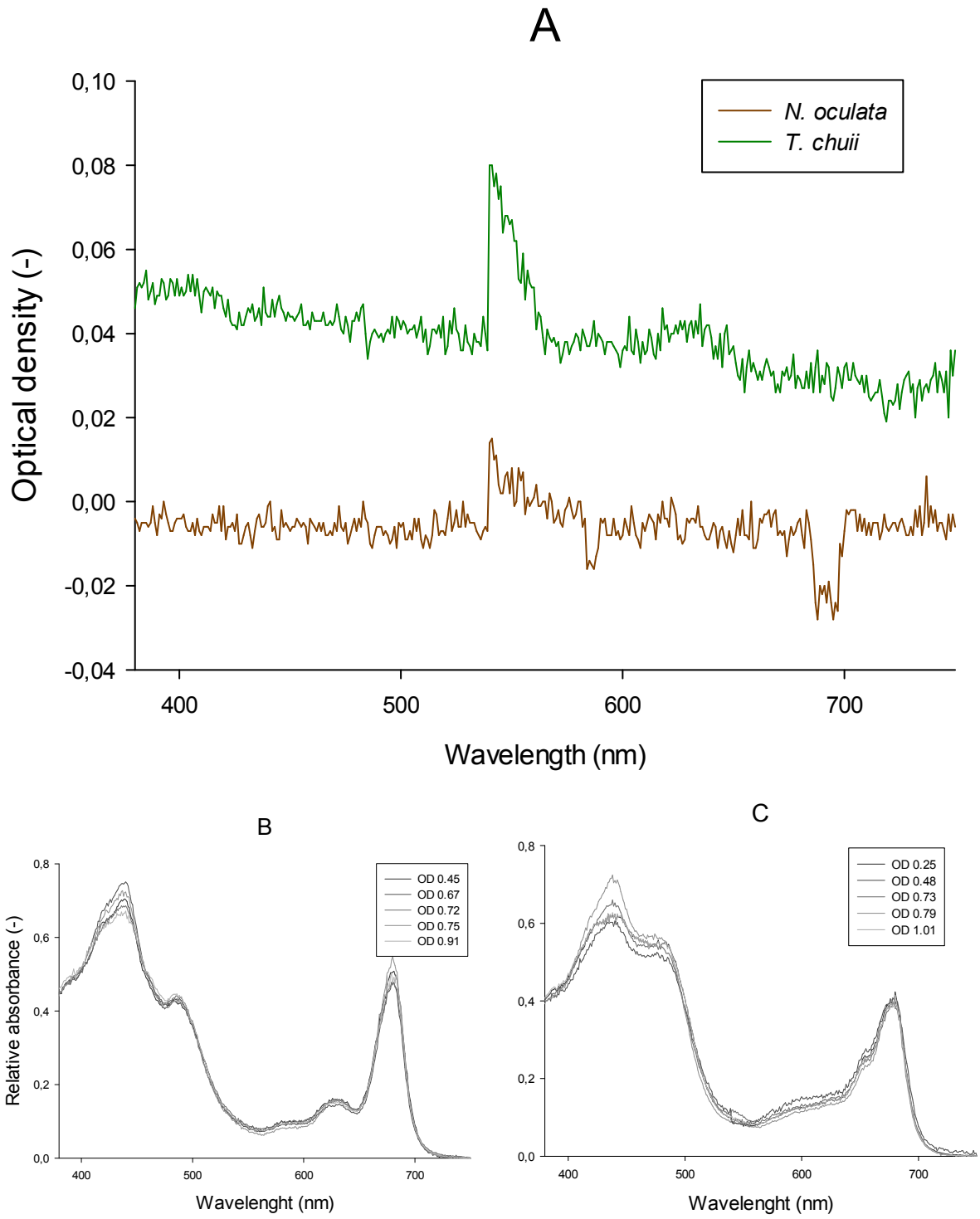

Figure A.5-5 (A) represents the baseline noise of filter containing only filtered seawater for *N. oculata* and *T. chuii* absorption spectra analyses. (B) and (C) represent the deviations of absorption spectra due to changing biomass concentration on the filter and filter variations for *N. oculata* and *T. chuii*, respectively. Each curve represents the average of two absorption spectra of the same sample. Optical density (OD) shows the absorption of the original sample before data treatment at 680 nm.

Annex 6

Quantitative growth parameters of *N. oculata* and *T. chuii*

Table A.6-1 *N. oculata* and *T.* chuii growth parameters based on ash free dry weight (AFDW) determinations (n = 3). Statistical differences are indicated by different letters among each experiment and growth parameter.

AFDW		P_{AFDW}[b] ± SD	μ_{AFDW}[c] ± SD	X_{AFDW}[d] ± SD
N. oculata	Treatment[a]	mg AFDW L^{-1} d^{-1}	d^{-1}	g AFDW L^{-1}
	LED 405	60.9 ± 3.3 c	0.42 ± 0.01 c	537 ± 33 c
	LED 465	91.3 ± 3.1 b	0.51 ± 0.01 b	803 ± 31 a
	LED 630	80.8 ± 3.3 b	0.47 ± 0.01 b	721 ± 26 a,b
Exp. 1	LED 660	83.9 ± 3.3 b	0.51 ± 0.01 b	678 ± 29 b
	CW LED	90.5 ± 2.9 b	0.49 ± 0.02 b	829 ± 36 a
	WW LED	88.3 ± 2.7 b	0.49 ± 0.02 b	804 ± 38 a
	FL (1)	107.0 ± 3.8 a	0.59 ± 0.02 a	799 ± 36 a
	HRLB	97.6 ± 3.9 a	0.56 ± 0.01 a	685 ± 27 a,b
Exp. 2	HBmix	91.9 ± 6.2 a	0.59 ± 0.01 a	615 ± 21 b
	FL (2)	95.1 ± 3.6 a	0.52 ± 0.01 b	751 ± 36 a
	HBLR	122.2 ± 5.0 a	0.53 ± 0.01 b	1000 ± 20 a
Exp. 3	HRmix	118.6 ± 4.8 a	0.58 ± 0.00 a	866 ± 28 b
	FL (3)	119.7 ± 4.5 a	0.54 ± 0.00 b	971 ± 27 a

AFDW		P_{AFDW}[b] ± SD	μ_{AFDW}[c] ± SD	X_{AFDW}[d] ± SD
T. chuii	Treatment[a]	mg AFDW L^{-1} d^{-1}	d^{-1}	g AFDW L^{-1}
	LED 405	136.7 ± 4.9 b,c	0,90 ± 0,04 b	712 ± 8 b
	LED 465	174.0 ± 4.3 b	1.17 ± 0,02 a,b	713 ± 12 b
	LED 630	141.9 ± 7.5 b,c	0.86 ± 0.07 b	806 ± 7 a
Exp. 1	LED 660	155.0 ± 12.9 b,c	0.89 ± 0.07 b	828 ± 44 a
	CW LED	135.8 ± 1.1 c	0.88 ± 0.04 b	721 ± 17 b
	WW LED	161.0 ± 5.1 b,c	1.02 ± 0.05 a,b	788 ± 19 a
	FL (1)	220.4 ± 23.9 a	1.34 ± 0.21 a	806 ± 17 a
	HRLB	122.2 ± 2.5 b	0.75 ± 0.03 b	741 ± 6 a
Exp. 2	HBmix	124.4 ± 2.2 b	0.77 ± 0.03 b	720 ± 5 b
	FL (2)	145.3 ± 4.6 a	0.93 ± 0.07 a	721 ± 3 b
	HBLR	200.8 ± 5.6 a	0.88 ± 0.02 a	1013 ± 9 b
Exp. 3	HRmix	185.6 ± 11.3 a	0.90 ± 0.08 a	953 ± 8 c
	FL (3)	202.b4 ± 5.8 a	0.84 ± 0.02 a	1064 ± 18 a

a. LED *nnn* correspond to the treatment with LED light with an emission band centered at the wavelength *nnn* nm; CW LED represents cool white; WW LED warm white; FL, fluorescent light; HRLB, high red low blue; HBLR, high blue low red; HRmix, High red mixed with other wavelengths; and HBmix, high blue content mixed with other wavelength;
b. $\mathbf{P_{AFDW}}$**:** AFDW productivity (mg L^{-1} d^{-1});
c. $\boldsymbol{\mu_{AFDW}}$: Maximal growth rate based on AFDW (d^{-1});
d. $\mathbf{X_{AFDW}}$: Maximal AFDW concentration (mg L^{-1}).

Table A.6-2 *N. oculata* and *T. chuii* growth parameter based on cell counts. Statistical differences are indicated by different letters among each experiment and growth parameter.

Cell counts		P_{cell}[b] ± SD		μ_{cell}[c] ± SD		X_{cell}[d] ± SD	
N. oculata	Treatment	× cell × 10^7 L^{-1} d^{-1}		d^{-1}		× cell × 10^7 L^{-1}	
	LED 405	0.99 ± 0.08	c	0.68 ± 0.04	b	5.70 ± 0.74	b
	LED 465	1.09 ± 0.08	b,c	0.74 ± 0.01	b	6.97 ± 0.43	a
	LED 630	1.24 ± 0.11	b,c	0.80 ± 0.01	b	6.68 ± 0.50	a
Exp. 1	LED 660	1.58 ± 0.09	a	1.22 ± 0.09	a	6.18 ± 0.57	b
	CW LED	1.21 ± 0.11	b	0.62 ± 0.02	b	8.93 ± 1.07	a
	WW LED	1.28 ± 0.13	a,b	0.82 ± 0.06	b	7.28 ± 0.48	a
	FL (1)	1.34 ± 0.06	a,b	0.84 ± 0.13	b	7.63 ± 1.11	a
	HRLB	1.73 ± 0.02	a	1.03 ± 0.17	a	6.69 ± 0.73	a
Exp. 2	HBmix	1.32 ± 0.11	b	0.89 ± 0.03	a,b	5.57 ± 0.37	a
	FL (2)	1.07 ± 0.04	c	0.59 ± 0.06	b	7.11 ± 0.89	a
	HBLR	1.98 ± 0.16	a	0.87 ± 0.05	a	11.84 ± 1.11	a
Exp. 3	HRmix	1.95 ± 0.22	a	0.84 ± 0.07	a	11.31 ± 0.56	a
	FL (3)	1.80 ± 0.11	a	0.85 ± 0.06	a	10.65 ± 1.22	a

Cell counts		P_{cell}[b] ± SD		μ_{cell}[c] ± SD		X_{cell}[d] ± SD	
T. chuii	Treatment	× cell × 10^5 L^{-1} d^{-1}		d^{-1}		× cell × 10^6 L^{-1}	
	LED 405	3.08 ± 0.12	b	0.81 ± 0.11	a,b,c	1.44 ± 0.16	d
	LED 465	3.96 ± 0.15	b	0.64 ± 0.08	c	2.52 ± 0.40	b
	LED 630	4.33 ± 0.32	a,b	0.73 ± 0.01	b	2.66 ± 0.18	b
Exp. 1	LED 660	5.20 ± 0.34	a	0.91 ± 0.05	a,b	2.58 ± 0.28	b
	CW LED	4.17 ± 0.28	a,b	0.98 ± 0.04	a	1.93 ± 0.19	b,c,d
	WW LED	4.75 ± 0.43	a	0.88 ± 0.06	a,b	2.45 ± 0.07	b
	FL (1)	5.41 ± 0.70	a	0.81 ± 0.09	a	2.88 ± 0.18	a,b
	HRLB	3.38 ± 0.32	a	0.97 ± 0.04	b	1.59 ± 0.18	a
Exp. 2	HBmix	3.46 ± 0.24	a	1.09 ± 0.04	a,b	1.45 ± 0.09	a
	FL (2)	3.82 ± 0.24	a	1.17 ± 0.06	a	1.61 ± 0.14	a
	HBLR	4.71 ± 0.15	a	0.94 ± 0.11	a	2.22 ± 0.22	a
Exp. 3	HRmix	4.93 ± 0.31	a	1.15 ± 0.09	a	2.14 ± 0.22	a
	FL (3)	5.47 ± 0.61	a	1.11 ± 0.08	a	2.31 ± 0.23	a

a. LED *nnn* correspond to the treatment with LED light with an emission band centered at the wavelength *nnn* nm; CW LED represents cool white; WW LED warm white; FL, fluorescent light; HRLB, high red low blue; HBLR, high blue low red; HRmix, High red mixed with other wavelengths; and HBmix, high blue content mixed with other wavelength;
b. $\mathbf{P_{cell}}$**:** cell productivity (cell L^{-1} d^{-1});
c. $\boldsymbol{\mu_{cell}}$: Maximal growth rate based on AFDW or cell determinations (d^{-1});
d. $\mathbf{X_{cell}}$: Maximal AFDW or cell concentration in the culture (cell mL^{-1}).

If absolute growth AFDW-based parameters from the first experiment are compared (Table A.6-1 in Annex 6), FL light treatment was found to be the most efficient light source in terms of AFDW productivity and specific growth rate for *N. oculata* and *T. chuii* cultures ($P_{AFDW} \approx$ 107 and 220 mg d^{-1} L^{-1}, $\mu_{AFDW} \approx$ 0.59 and 1.34 d^{-1}, respectively). The maximal biomass concentration reached in the reactors (X_{AFDW}) was highest for *N. oculata* under LED 465, LED 630, CW LED, WW LED and FL(1), while the lowest were found for LED 405. For *T. chuii* LED 630, LED 660, WW LED and FL(1) treatment showed the highest X_{AFDW}.

In the second and third experiment, no statistical differences ($p > 0.05$) were found in P_{AFDW} of *N. oculata* between LED mixed light sources and FL treatments. *T. chuii* showed in the second experiment highest productivity under FL(2), but in the third experiment no differences could be observed. For *N. oculata* and *T. chuii* X_{AFDW} was always lowest under HBmix and HRmix treatments.

Absolute cell-based growth parameters from the first experiment (Table A.6-2 in Annex 6), indicate that LED 660 promoted always one of the highest cell productivities in *N. oculata* and *T. chuii* cultures ($P_{cell} \approx 1.58 \times 10^7$ and 5.20; $\times 10^5$ $Cell^{-1}$ L^{-1} d^{-1}, respectively). LED 405 treatment showed always one of the lowest P_{cell} values among both algae and all treatments (Fig 3.1-4, Table A.6-2). Maximal cell concentrations (X_{cell}) in the culture were obtained under CW LED for *N. oculata* and under FL for *T. chuii* ($8.93 \pm 1.07 \times 10^7$ and $2.88 \pm 0.18 \times 10^6$ cells mL^{-1}, respectively). LED 405 treatment showed always lowest X_{cell} values among both algae and treatments. The growth rate was of *N. oculata* clearly highest under LED 660 treatment ($\mu_{cell} \approx 1.22$ d^{-1}). *T. chuii* showed high growth rates under LED 405, LED 660 CW LED, WW LED and FL(1) treatments (Average: 0.87 ± 0.1 d^{-1}) and the lowest under LED 465 treatment ($\mu_{cell} \approx 0.64$ d^{-1}). In the second experiment of *N. oculata* HRLB gained highest and HRmix lowest cell production. The growth rate was also highest under HRLB and lowest under FL(2) treatment. The highest maximal concentration was obtained under FL (2) treatment (not statistically different to HRLB and HBmix treatments). The third experiment showed no differences of any growth parameter between the treatments. In the second and third experiment, *T. chuii* cultures showed similar growth parameters between the treatments, respectively.

Annex 7

Growth curves of *N. oculata* and *T. chuii*

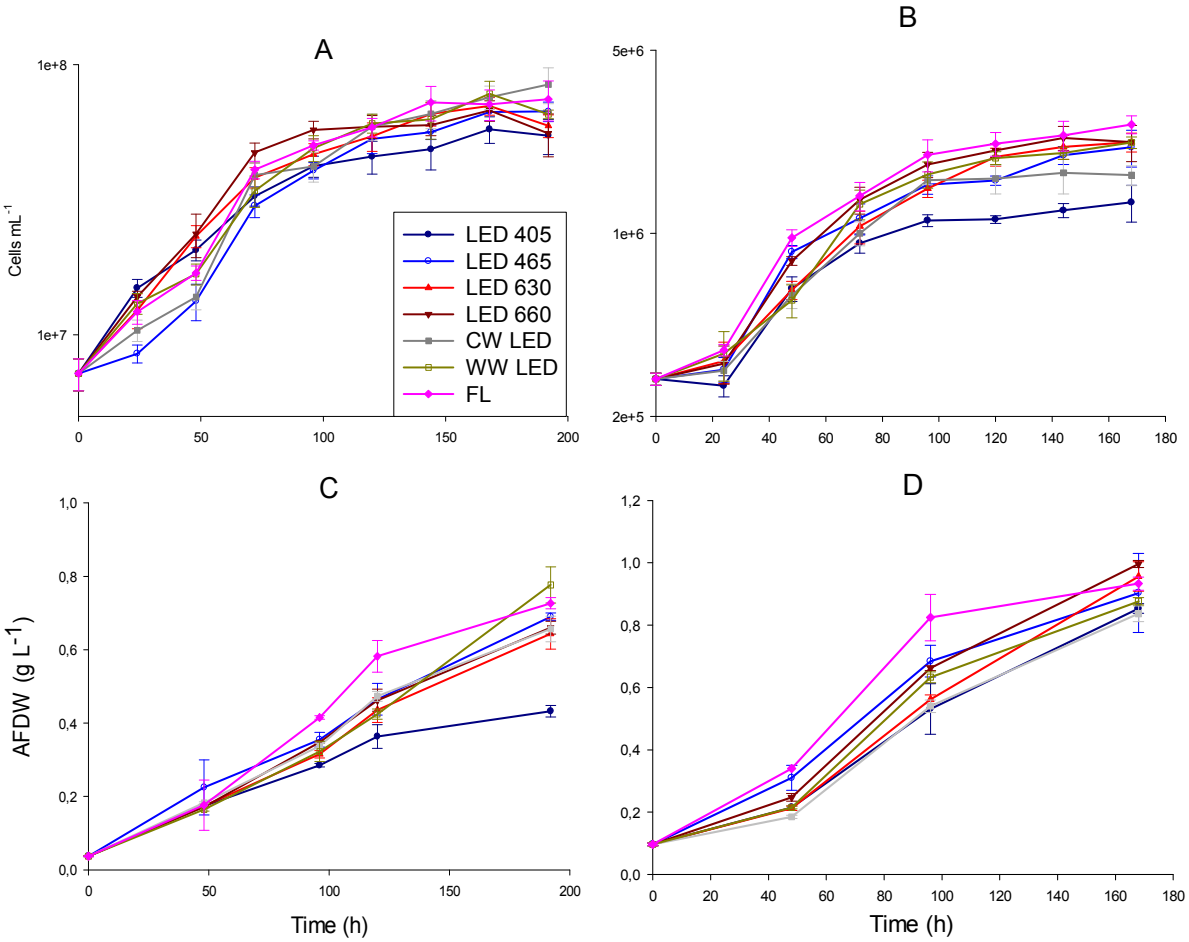

Figure A.7-6 Original growth curves based on cell counts (top; daily counts with $n = 6$) and AFDW determinations (bottom) of *N. oculata* (A and C, respectively) as well as *T. chuii* (B and D, respectively).

Annex 8

Productivity under continuous conditions (calculated)

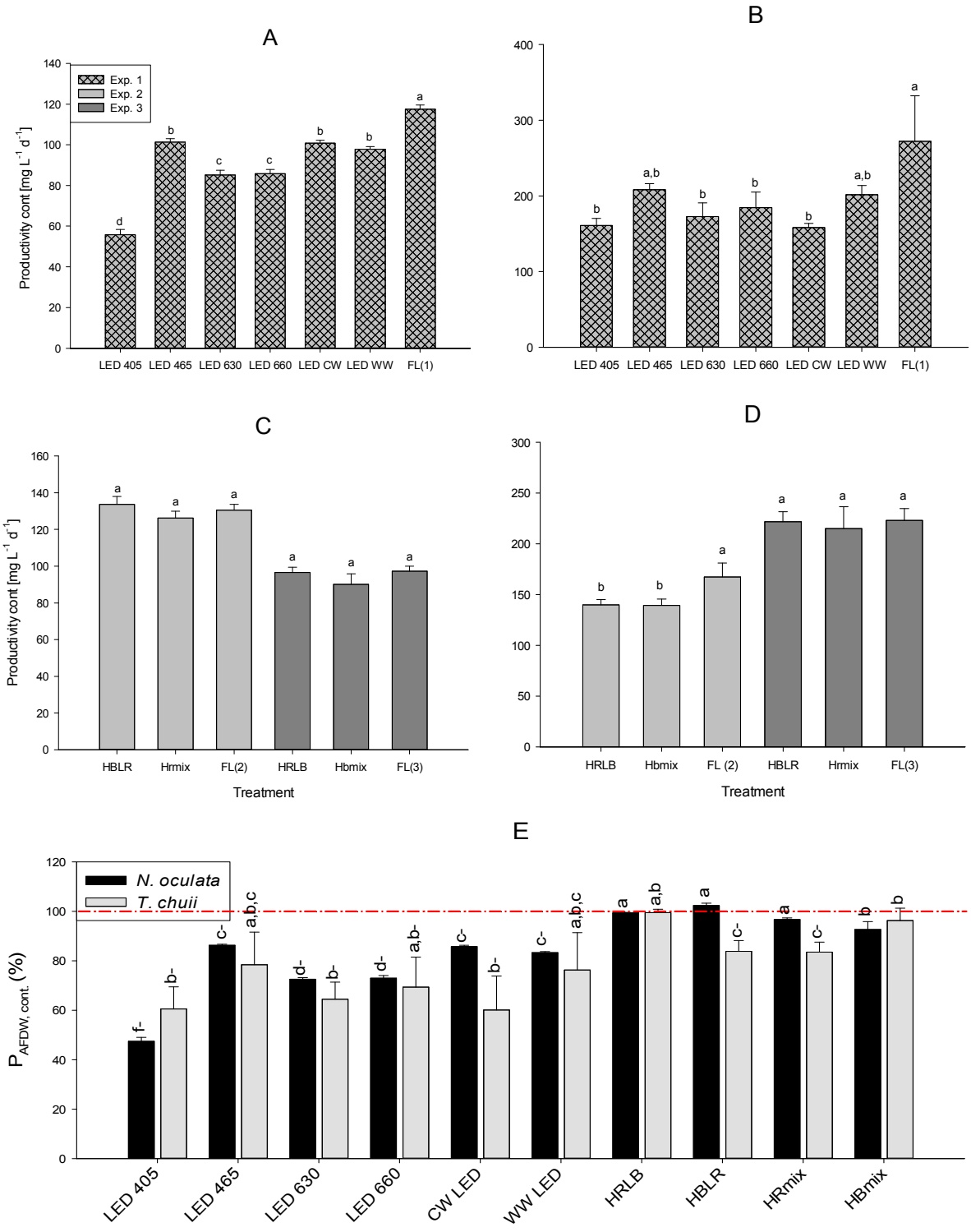

Figure A.8-7 Absolut productivity of *N. oculata* in the first, second and third experiment (A and C) and *T. chuii* (B and D) under continuous conditions when μ is maximal, calculated according to eq. 7. (E) shows the data from A-D normalized (relative) for both algae. The reference data (red dashed line) was obtained with cells growing under FL. Statistical differences ($p < 0.05$) within *N. oculata* (black bar) and *T. chuii* (grey bar) among treatments are indicated by different letters. Statistical higher or lower values as compared to those of the reference (FL) cultures are given as + and - signed letters, respectively. Unsigned letters indicate no statistical differences were found between cells under a given light treatment and under also FL (See and A.6-2 in Annex 6).

By applying the maximal growth rate μ and maximal concentration X_{AFDW} from table A.6-1 and A.6-2 to eq. 7 the maximal biomass productivity under continuous operation was estimated. *N. oculata* showed highest production rate under FL treatment followed by cells under LED 465, CW LED and WW LED. LED 630 and 660 showed lower rates as compared to LED 465. Lowest productivity was obtained under LED 405.

T. chuii showed highest production rate under FL(1) treatment, being not statistically different from LED 465 and WW LED. Lowest productivities were obtained under LED 405, LED 630, LED 660 and CW LED.

The productivities under adapted light in experiment 2 (HBLR, HRmix, FL(2)) and experiment 3 (HRLB, HBmix, FL (2)) were not statistically different.

Annex 9

Colouration of *N. oculata* cultures

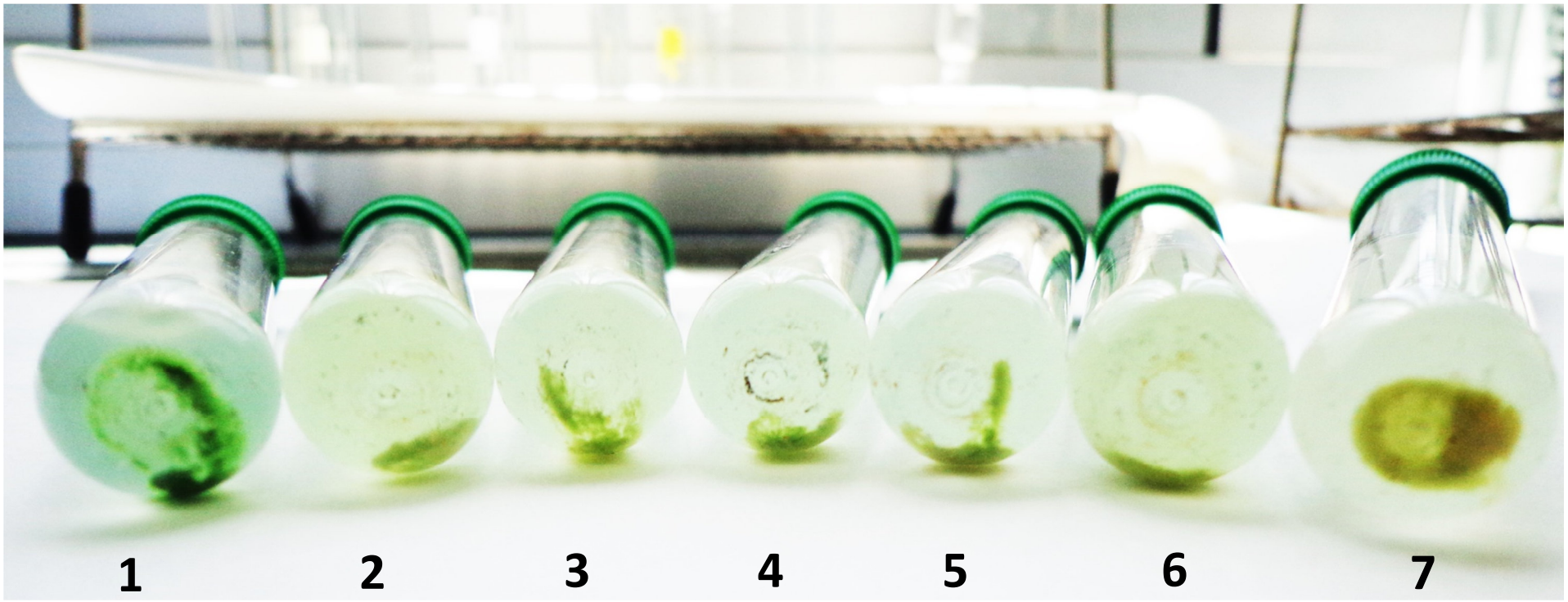

Figure A.9-8 Photograph of preserved *N. oculata* cultures from the end of the experiment (t = 192 h), showing different colours among the treatments. Tube 1, containing LED 405-treated algae, shows a clear green colour; tubes 2, 3, 4, 5 and 6, containing LED 465, LED 630, LED 660, CW LED and WW LED-treated algae, respectively, are more yellowish and less greenish; and finally tube 7, containing FL-treated algae, showed a clear yellow colour.

Annex 10

Biochemical production rate

The production of total lipids per litre and day was highest in *N. oculata* cultures treated with FL (55.7±3.8 mg L^{-1} d^{-1}; Fig. A.3-3) and lowest under LED 405 treatment (27.6±2.4 mg L^{-1} d^{-1}). In contrast, protein production was highest under LED 405 and CW LED treatment (41.0±4.3 and 37.9±1.7 mg L^{-1} d^{-1}, respectively) and lowest under LED 630 treatment (27.1±1.7 mg L^{-1} d^{-1}). Carbohydrates production was highest under LED 465, LED 630, LED 660 and FL treatment (average 24.1±1.1 mg L^{-1} d^{-1}) and clearly lowest under LED 405 treatment (5.4±0.9 mg L^{-1} d^{-1}). Summarizing, in *N. oculata* the production of total lipids, proteins and carbohydrates was highest under FL, LED 405 and LED 660 treatment, respectively.

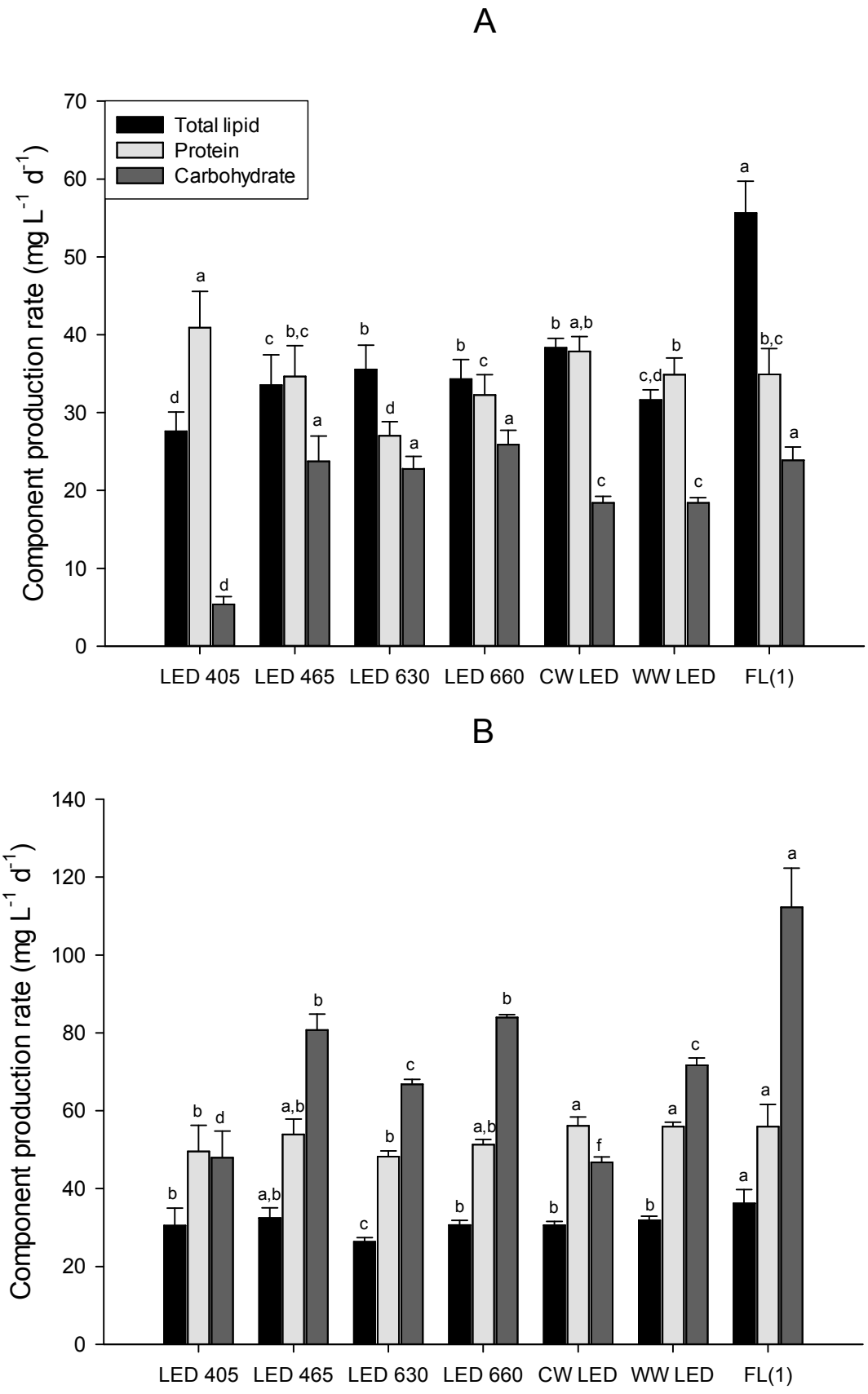

Figure A.10-9 Productivity of total lipids (black bar left), proteins (light grey bar middle) and carbohydrates (dark grey bar right) for *N. oculata* (A) and *T. chuii* (B) among light treatments. Different letters within each biochemical and among treatments indicate statistical differences.

T. chuii showed highest lipid production under FL and LED 465 treatment (36.3±3.1and 32.5±2.3 mg L^{-1} d^{-1}, respectively), but no statistical differences were found between LED 465 and LED 660, CW LED and WW LED (average: 31.5±0.8 mg L^{-1} d^{-1}). Lowest total lipid production was found under LED 630 treatment (26.4±0.9 mg L^{-1} d^{-1}). Regarding proteins, the highest productivity was found under CW LED, WW LED and FL showing no statistical differences amongst each other (average 56.1±0.1 mg L^{-1} d^{-1}). Lowest protein production rates were found under LED 405 and LED 630 treatments (49.0±0.7 mg L^{-1} d^{-1}). Protein production under LED 465 and LED 660 treatments was not statistically different from the aforementioned treatments. Carbohydrate production was clearly highest under FL treatments (112.4±9.2 mg L^{-1} d^{-1}). Lowest carbohydrate production was found under CW LED treatment (46.8±1.2 mg L^{-1} d^{-1}) followed by LED 405 (48.0±6.3 mg L^{-1} d^{-1}).

Taking together, these results indicate that *T. chuii* cultures exposed to FL treatments showed, consistently, highest production rates in terms of total lipids, protein, and carbohydrates.

However, the input optical energy (KJ) demand per litre of reactor and per mg of total lipids, proteins and carbohydrates can be more important for some algae production, if, e.g., expensive extraction processes are used to isolate high value products. Therefore in Fig. A.3-3 the productivity of biomass in relation to the optical energy supplied to the culture is also given.

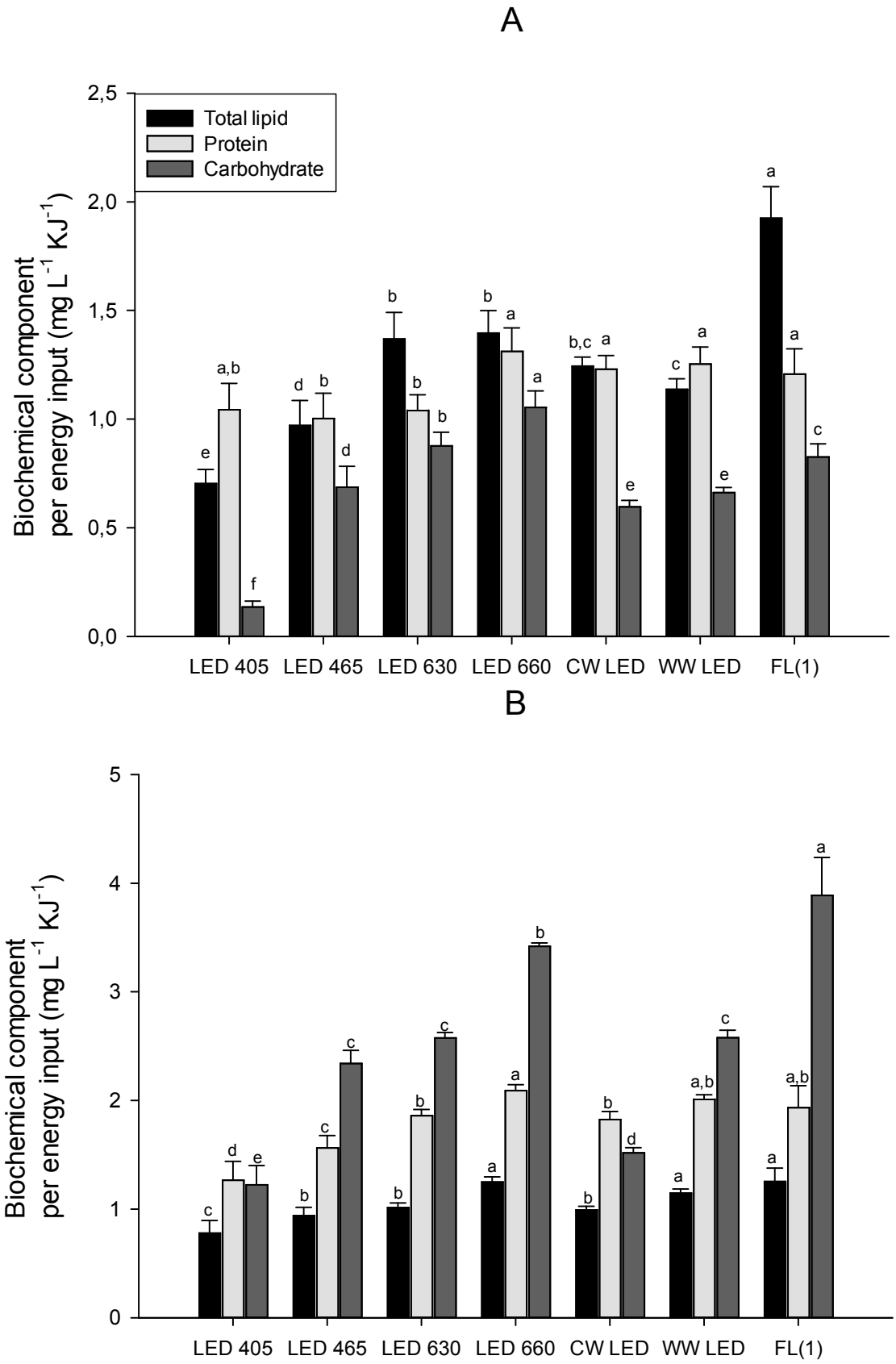

Figure A.10-10 Energy demand for producing total lipids (black bar), proteins (light grey bar) and carbohydrates (dark grey bar) per litre of culture from *N. oculata* (A) and *T. chuii* (B). Different letters within each biochemical and among treatments indicate statistical differences.

N. oculata exposed to LED 405 showed consistently one of the highest demands of energy for the production of total lipids, proteins and carbohydrates, whereas cultures exposed to LED 660 and FL showed always the most energy efficient production. Especially FL was the most effective light source to produce lipids, while LED 660 was best for protein and carbohydrate production.

T. chuii showed always highest demand of energy per produced total lipid, protein and carbohydrate per litre. Also LED 660 and FL treatments were able to produce total lipids, proteins and carbohydrates in the most energy efficient manner among all treatments. *T. chuii* exposed to LED 465, LED 630 and CW LED displayed adequate energy demand per biochemical component at all time points.

However, it may be concluded that light sources with high PE were also always more energetically efficient for the production of every biochemical component than light sources with low PE.